INFLAMMATION AND OXIDATIVE STRESS IN AN ANIMAL MODEL OF INFECTION-INDUCED LIMBIC EPILEPSY

by

Dipankumar C. Patel

A dissertation submitted to the faculty of
The University of Utah
in partial fulfillment of the requirements for the degree of

Doctor of Philosophy

Department of Pharmacology and Toxicology

The University of Utah

December 2016

The University of Utah Graduate School

STATEMENT OF DISSERTATION APPROVAL

The dissertation of **Dipankumar C. Patel**

has been approved by the following supervisory committee members:

Karen S. Wilcox	, Chair	**08/08/2016** Date Approved
Donald K. Blumenthal II	, Member	**08/08/2016** Date Approved
H. Steve White	, Member	**08/08/2016** Date Approved
Robert S. Fujinami	, Member	**08/08/2016** Date Approved
Thomas E. Lane	, Member	**08/08/2016** Date Approved

and by **Karen S. Wilcox** , Chair/Dean of

the Department/College/School of **Pharmacology and Toxicology**

and by David B. Kieda, Dean of The Graduate School.

ABSTRACT

Central nervous system (CNS) infection can induce epilepsy that is often refractory to established antiseizure drugs. The Theiler's murine encephalomyelitis virus (TMEV)-induced mouse model of limbic epilepsy is an important model in which to study the mechanisms underlying epileptogenesis and to identify novel therapeutics. Previous studies have demonstrated the importance of inflammation, especially mediated by tumor necrosis factor-α (TNFα), in the development of TMEV-induced acute seizures. TNFα is known to modulate glutamate receptor trafficking via TNF receptor 1 (TNFR1) to cause increased excitatory synaptic transmission. Therefore, we hypothesized that an increase in hippocampal TNFα following TMEV infection might contribute to hyperexcitability and seizures by increasing excitatory postsynaptic strength through TNFR1. Furthermore, inflammation is known to contribute to oxidative stress that in turn can precipitate seizures. Therefore, we also investigated the occurrence of oxidative stress in TMEV-infected mice.

We found a significant increase in the levels of oxidative stress markers and TNFα in the hippocampus, a brain region known to be involved in seizure generation, following TMEV infection. In addition, a significant increase in the protein expression ratio of TNF receptors (TNFR1:TNFR2) in hippocampus suggests that TNFα signaling, predominantly through TNFR1, may contribute to limbic hyperexcitability. Consistent with increased TNFR1 signaling, increases in hippocampal cell surface glutamate

receptor expression was also observed during the acute period. While pharmacological inhibition of TNFR1-mediated signaling had no effect on acute seizures, several lines of transgenic animals deficient in either TNFα or its receptors were found to have robust changes in seizure incidence and severity following TMEV infection. $TNFR2^{-/-}$ mice were highly susceptible to developing TMEV-induced acute seizures, suggesting that signaling through the TNFR2 pathway may provide beneficial effects during the acute seizure period. Moreover, cannabidiol (180 mg/kg), which exhibits antiinflammatory and antiseizure properties, dramatically inhibited TMEV-induced acute seizures.

Taken together the present results suggest that oxidative stress and inflammation in the hippocampus contribute to hyperexcitability and increase the probability of seizures following TMEV infection and that the TNFα signaling pathway is involved in this process. Pharmacotherapies designed to suppress inflammation and oxidative stress may provide antiseizure and disease modifying effects following CNS infection.

TABLE OF CONTENTS

LIST OF FIGURES

Figures

LIST OF TABLES

Tables

LIST OF ABBREVIATIONS

3NT, 3-nitrotyrosine

AMPAR, α-amino-3-hydroxy-5-methyl-4-isoxazole propionic acid

ANOVA, analysis of variance

ASD, antiseizure drug

CBD, cannabidiol

DG, dentate gyrus

DGCs, dentate granule cells

DI, during injection

dpi, days postinfection

GABA, gamma-aminobutyric acid

GSH, glutathione

GSSG, glutathione disulfide

HSV, herpes simplex virus

i.c.v., intracerebroventricular

i.p., intraperitoneal

IFNγ, interferon-γ

IL, interleukin

JEV, Japanese encephalitis virus

LTα3, lymphotoxin α3

mEPSC, miniature excitatory postsynaptic current

mIPSC, miniature inhibitory postsynaptic current

NCC, neurocysticercosis

OD, optical density

PAG, phosphate-activated glutaminase

PFU, plaque forming units

RNS, reactive nitrogen species

ROS, reactive oxygen species

s.c., subcutaneous

SCI, spinal cord injury

SD, standard deviation

SEM, standard error of the mean

sTNFα, soluble TNFα

TGFβ, transforming growth factor-β

TLE, temporal lobe epilepsy

TMEV, Theiler's murine encephalomyelitis virus

tmTNFα, transmembrane TNFα

TNFR, tumor necrosis factor receptor

TNFα, tumor necrosis factor-α

TPE, time to the peak effect

vEEG, video electroencephalography

WNV, West Nile virus

CHAPTER 1

POSTINFECTIOUS EPILEPSY[1]

Abstract

Central nervous system (CNS) infections are common risk factors for seizures and the development of epilepsy. Various infectious agents including viruses, parasites, bacteria, and fungi are clinically associated with seizures and epilepsy. The detailed cellular and molecular mechanisms of pathological and physiological changes in the brain due to acute infection are not clearly understood. Infection induces inflammation in the brain which could contribute to the process of epileptogenesis in which normal neuronal circuits transform into epileptic circuits which increase the probability of the development of epilepsy. A detailed understanding of epileptogenesis following infection is of utmost importance for the development of advanced therapies to treat the seizures as well as to prevent the progression of disease. Several infection-induced animal models of seizure and epilepsy have been described mainly using viral infection and parasitoses in rodents. This chapter describes several of them, including those models using herpes simplex virus-1, West Nile virus, neurocysticercosis, and Theiler's virus. We will discuss the methods of seizure generation, pathological and physiological changes in the brain,

[1] This article was published in Models of Seizure and Epilepsy, Second Edition, in press, Dipan C. Patel, Karen S. Wilcox, Postinfectious epilepsy, Copyright Elsevier (2017). Reproduced with permission from Elsevier.

clinical relevance, advantages, and limitations of the models.

Introduction

Infections of the central nervous system are common risk factors for seizures and the development of epilepsy. Infections can potentially cause encephalitis (inflammation of the brain parenchyma) and encephalopathy (diffuse CNS disease manifested by altered consciousness, a range of cognitive and motor neurological symptoms, and systemic metabolic disturbances) by directly or indirectly damaging the brain. A broad range of infectious agents including viruses (e.g., herpes viruses, enteroviruses, flaviviruses, paramyxoviruses), parasites (e.g., *Taenia solium*, *Plasmodium falciparum*, *Toxoplasma gondii*), bacteria (e.g., *Haemophilus*, *Streptococcus*, *Neisseria*, *Mycobacterium*), and fungi (e.g., *Candida*, *Cryptococcus*) are clinically associated with seizures and epilepsy (Vezzani et al., 2016). Among them, viral encephalitis and parasitic infections are the most widely reported causes of infection-induced epilepsies in patients.

Over 100 neurotrophic viruses are known to cause encephalitis in humans and many of them may subsequently contribute to seizures and epilepsy. The prevalence of viral encephalitis which can be either sporadic or epidemic has been calculated ~7.5 persons per 100,000 people in the general population (Misra et al., 2008). Herpes simplex virus type 1 (HSV-1) is the most common cause of sporadic encephalitis (Theodore, 2014). Early (acute) seizures can occur in 40-60% of cases of HSV-1 encephalitis which is probably due to tropism of HSV-1 for mesial temporal lobe structures, especially hippocampus, that are strongly involved in seizure generation and epileptogenesis. A prospective study of the consequences of prolonged febrile seizures (FEBSTAT)

determined primary or prior human herpes virus-6B (HHV-6B) and HHV-7 viremia in 32% and 7% of pediatric patients with febrile status epilepticus, respectively, which is associated with increased risk for hippocampal injury and temporal lobe epilepsy (Epstein et al., 2012). Japanese encephalitis is the most common form of epidemic encephalitis associated with acute seizures, which occur in 7-46% of patients (Misra et al., 2008). Viral encephalitis also increases the risk for the development of late (chronic) unprovoked/spontaneous seizures. As in acute symptomatic seizures, the development of chronic seizures also varies among the types of viral encephalitis; for example, late unprovoked seizures occur in 40-65% of patients following HSV encephalitis, while only 10-12% of La Crosse encephalitis patients go on to develop epilepsy (Misra et al., 2008). Other noteworthy viral infections implicated in seizures and epilepsy are human immunodeficiency virus (HIV), enterovirus, West Nile virus, measles, cytomegaloviruses, influenza viruses, dengue, and chikungunya (Vezzani et al., 2016).

CNS infection due to parasites can also cause seizures. Major parasitoses associated with increased incidence of seizures and epilepsy are neurocysticercosis (NCC) and cerebral malaria (CM) notably in low income countries. Up to 10% of African children suffering from CM develop epilepsy (Birbeck et al., 2010). CM-associated seizures are often focal which may occasionally generalize and ~20% of children present with subclinical seizures (Birbeck et al., 2010). 28% of CM patients may develop status epilepticus, which is often resistant to antiseizure medications and associated with increased neurological disability and mortality rate. NCC is caused by CNS infection of the larval stage of tapeworm *Taenia solium* and it is the most common preventable risk factor for adult-acquired epilepsy worldwide. About 80% of patients with symptomatic

NCC develop recurrent seizures and NCC accounts for up to 29% of all epilepsy cases in some endemic regions (Ndimubanzi et al., 2010).

There are fewer clinical cases of epilepsies associated with bacterial infection compared to viral infection and parasitoses. However, any bacterial infection of the CNS can cause acute seizures and chronic epilepsy. Infections with *Haemophilus influenzae* are more commonly associated with seizures compared to other bacterial infections (Stringer, 2006). Acute infection of meninges by *Neisseria meningitidis* can result in acute seizures. After a latent period ranging from several weeks to few years, chronic spontaneous seizures, often drug resistant, develop in about 5-10% of survivors of meningitis (Oostenbrink et al., 2002). Bacterial infections may induce formation of intracranial empyemas and abscesses, and seizures occur in about 35% of patients with brain cerebral abscesses and in >50% of patients with dural empyemas (Labar and Harden, 1998). Although the cases of fungal infection-induced epilepsy are relatively uncommon, many species of fungi including *Candida*, *Cryptococcus*, *Aspergillus*, *Blastomyces*, and *Histoplasma* have been found to cause seizures, especially in immunocompromised people (Vezzani et al., 2016).

Infection can cause damage to the brain parenchyma by directly infecting the cells or by unleashing uncontrolled inflammatory reactions to surrounding tissue. CNS damage and excessive inflammation may engender acute seizures and persistent neurological abnormalities can result in epilepsy. The detailed mechanisms of neuropathological and inflammatory changes due to acute infection and the mechanisms of epileptogenesis as a consequence (a process of structural and physiological changes in brain parenchyma following insult which transform normal neuronal circuits into epileptic circuits) are

unknown and it is an active area of research. A detailed understanding of epileptogenesis following infection is of utmost importance as it will open the door for novel therapeutic approaches to prevent the progression of disease.

Several infection-induced animal models of seizure and epilepsy have been described mainly using viral infection and parasitoses in rodents. This chapter describes several of them, including those models using HSV-1, West Nile virus, NCC, and Theiler's virus. The Theiler's virus model of limbic epilepsy is the most extensively studied among all the models with numerous studies published in the last few years validating its usefulness for translational studies. We will discuss the method of seizure generation, structural and functional changes in the brain, clinical relevance, advantages, and limitations of the models.

Herpes simplex virus (HSV)-induced model of limbic seizures

HSV-1 is a neurotrophic virus capable of penetrating into brain from intranasal route via retrograde axonal pathway and replicating into brain parenchymal cells. It is the most common virus clinically associated with seizures and epilepsy. Attempts have been made to develop animal models for HSV-1 encephalitis-induced seizures in rabbit (Stroop and Schaefer, 1989), rat (Beers et al., 1993; Solbrig et al., 2006), mouse (Wu et al., 2003; Wu et al., 2004), and an *in vitro* system (Chen et al., 2004).

Methods of generation

Intranasal or corneal inoculation methods have been used for generating HSV-induced model of seizures. Animals are briefly anesthetized before infecting them.

Female New Zealand white (NZW) rabbits weighing 2-3 kg are inoculated in each nostril with 0.1 ml solution containing 10^6 $TCID_{50}$ (50% tissue culture infectious dose) of neurovirulent +GC substrain of HSV-1. Similarly, female Lewis rats (around 225 g) are infected intranasally with $1.4x10^6$ $TCID_{50}$ (50% tissue culture infectious dose) of +GC. In another rat study, 9 week-old male Lewis rats are infected with $3x10^6$ PFU (plaque forming units) of McKrae HSV-1 administered as eye drops in the right eye and conjunctival sac followed by closing and opening the eye. For the mouse model, 5-6 weeks old male BALB/c mice are inoculated with RE strain of HSV-1 ranging from $2x10^5$ to $2x10^6$ PFU into the right eye by corneal scarification. For *in vitro* system, organotypic cultures of hippocampal slices from Sprague-Dawley rat pups (P10-12) are infected with $1x10^5$ PFU of RE at 14 days *in vitro* for 1 h.

Characteristics and defining features

Seizures

NZW rabbits infected with +GC resulted in severe motor seizures in about 59% of rabbits (10/17) during 5-12 days postinfection (dpi) (Stroop and Schaefer, 1989). The rabbits had the Jacksonial type of seizures lasting for several minutes during each occurrence, beginning with muscle movements around nose and mouth which sequentially spread to neck, forelimbs and hindlimbs followed by unnatural upright posture with nose pointed almost vertically. Electroencephalographic (EEG) abnormalities were observed during the first week of infection in two of three rabbits. Of the 22 rabbits used overall, all except two rabbits eventually either died or had to be euthanized due to moribund condition and chronic studies could not be conducted.

Lewis rats infected with +GC developed complex partial seizures which secondarily generalized between 7-10 dpi (Beers et al., 1993). Compared to the rabbit study, 39% of the rats (9/23) had acute seizures of 30-60 s in duration and only 12% (3/26) of the rats died during acute infection. It was not determined if epilepsy developed in those rats that survived the infection. Lewis rats infected with McKrae HSV-1 exhibited Racine stage 1 and 2 limbic focal seizures that did not generalize, although long-term EEG recordings were not performed (Solbrig et al., 2006).

BALB/c mice infected with the RE strain developed progressively worsening physical symptoms from ruffled fur, hunched posture, and loss of appetite to limb weakness, ataxia, and seizures between 4 and 14 dpi (Wu et al., 2003). Neurological deficits, seizures, and mortality varied among infected mice and were correlated with viral titer. All the mice with severe encephalitis developed behavioral and EEG seizures originating from hippocampus and died by 10 dpi. Only 21% of mice with moderate encephalitis had seizures, whereas the mice with mild symptoms of infection did not develop seizures. Behavioral seizures started with staring and chewing, and progressed to forelimb clonus with/without rearing and generalized tonic-clonic extension. The duration of EEG seizures varied from several to tens of seconds.

Neuropathology

HSV-1 invaded and replicated in the rabbit brain as viral antigens were detected in cortical layers IV-VI, trigeminal and olfactory system, amygdala, nucleus accumbens, locus ceruleus, and brainstem. The shedding of virus was also detected in ocular and nasal secretions in the first 2 weeks of infection. The neuropathological changes such as

mild leptomeningitis, lymphocytic infiltration in medulla, and death of hippocampal neurons were found at 6 dpi. The virulence of the virus correlated with its expression levels in the brain.

In Lewis rats infected with +GC, the bilateral inflammatory and hemorrhagic lesions and astrogliosis were colocalized with the presence of viral antigens and nucleic acids in trigeminal ganglia, olfactory bulbs, piriform and entorhinal cortices, hippocampus, and amygdala during the first week of infection. As in the rabbit study, shedding of virus in ocular and nasal secretions was also observed. On the other hand, inflammatory lesions, gliosis, and viral antigens were not detected in any brain structure at 76 and 160 dpi. However, viral nucleic acids were present in the hippocampus and the piriform and entorhinal cortices at 76 and 160 dpi suggesting that HSV-1 can establish CNS latency in the rat.

In BALB/c mice infected with RE-HSV-1, the severity of neurological damage was highest in the limbic region particularly CA3 of hippocampus, amygdala, entorhinal and pyriform cortex, and correlated with the high expression level of viral antigens. Infiltration of neutrophils and lymphocytes was detected in hippocampus, pyriform cortex, and meninges. Patch-clamp recordings from the CA3 hippocampal neurons during 7-12 dpi showed more depolarized resting membrane potential, increased membrane input resistance, and decreased threshold for bursting activity suggesting that hyperexcitability in CA3 neuronal circuitry could facilitate the development of seizures. These electrophysiological changes in CA3 neurons were also reported in RE-HSV-1-infected organotypic hippocampal slice culture. HSV-1-infected mice had an increased susceptibility to kainic acid-induced seizures (Wu et al., 2003) and HSV-1 infection also

caused neuronal death and a marked increase in mossy fiber sprouting in the supragranular area in slice cultures (Chen et al., 2004). Neuronal loss was ameliorated by treating the infected slices with antiviral agent, acyclovir (Chen et al., 2004). Similarly, valacyclovir decreased pentylenetetrazole-induced seizure susceptibility in HSV-1-infected mice (Wu et al., 2004). These results suggest that HSV-1 infection can cause hyperexcitability in the hippocampal neuronal circuit leading to seizures and such changes can be prevented by restricting the infection.

Limitations

These models are limited by high mortality during the acute infection, although the rat model should be investigated for the development of unprovoked chronic seizures and epilepsy. HSV-1 also poses other problems with respect to ease of use, as it is known to cause diseases in humans and is classified under biosafety level 2 (BSL2) requiring regulatory approvals for study.

Insight into human disorders

Both rat and mouse models could be useful to study herpes infection-induced epilepsies in human as the rodents infected with HSV-1 develop behavioral seizures and show clinically relevant neurological lesions and histological changes, especially in the temporal region. Therefore, they could be valuable to investigate mechanisms of HSV-1-mediated seizures. For example, the study investigating the mechanism of seizure generation using male Lewis rats infected with McKrae HSV-1 found a decrease in the expression of dynorphin A, an endogenous opioid molecule which can contribute to

anticonvulsant activity, in the hippocampus (Solbrig et al., 2006). A kappa opioid receptor agonist, U50488, effectively blocked ictal activity confirming the antiseizure functions of dynorphin. The slice culture model could also be important as it allows high-throughput screening of potential antiseizure and antiepileptogenic compounds for future detailed investigation in animal models (Dyhrfjeld-Johnsen et al., 2010). However, a thorough validation of the *in vitro* system is essential given its drawbacks.

West Nile virus (WNV)-induced limbic seizures

WNV is a neurotrophic virus causing epidemic encephalitis often manifested with seizures. One mouse model of WNV-induced limbic seizures is reported (Getts et al., 2007).

Methods of generation

Adult female C57BL/6 mice aged 8-14 weeks are briefly anesthetized and intranasally inoculated with 10 µl of WNV solution in sterile phosphate-buffered saline containing $6x10^4$ PFU of virus.

Characteristics and defining features

Acute seizures

Mice are monitored for seizures twice daily until 4 dpi and then every four hours. Seizure intensity is recorded based on a summative scoring system ranging from 0 to 12. Limbic seizures first appeared on 5 dpi and started with piloerection, tail stiffening, hunching, excessive face washing, extreme wet dog shaking, and developed into

handling-induced seizures followed by rearing and falling. Seizure intensity gradually increased and all the mice developed limbic seizures. The highest seizure scores were coincided with advanced stages of disease on 7 dpi.

Neuropathology

Viral antigens first appeared in the olfactory bulb by 3 dpi and subsequently spread into cortex and pyramidal neurons of CA1-3 regions of hippocampus on 5 dpi. By 6 dpi, virus was detected throughout the hippocampus. Thus, the extent of viral infiltration and replication in the brain appear to correlate with the induction of seizures and gradual increase in the seizure intensity. No histopathological abnormalities were detected in the first 3 days of infection. Adhesion of leukocytes to vascular endothelium, leukocyte infiltration into the brain parenchyma, and microgliosis were observed at 6 dpi.

The expression of tumor necrosis factor-α (TNFα) and interleukin-6 (IL-6) in the brain were significantly elevated at 7 dpi. However, $TNF\alpha^{-/-}$ mice intranasally infected with WNV had limbic seizures comparable to WT mice. The role of interferon-γ (IFNγ) was evaluated in detail in this model (Getts et al., 2007). $IFN\gamma^{-/-}$ mice infected with WNV had a significant reduction in seizure intensity and did not have severe limbic seizures, indicating that the presence of IFNγ may contribute to seizure progression. The pattern of viral infiltration and replication in the brain, neuropathological and inflammatory changes including the levels of TNFα and IL-6 were not different between WT and $IFN\gamma^{-/-}$ mice, suggesting that additional factors might be implicated in causing different seizure outcomes in the two strains.

Limitations

All the mice succumb to infection around 7-8 dpi, thus restricting the use of this model to infection-induced acute seizures.

Neurocysticercosis (NCC) model of limbic seizures

General description

NCC is a common helminthic infection of the brain caused by the larval form of the tapeworm *Taenia solium* and is a major cause of seizures and acquired epilepsy worldwide. Pigs serve as intermediate reservoir for larval vesicles (metacestode or cysticerci) and eggs (containing oncosphere – embryonic form of tapeworm) of *T. solium*. Humans are infected by consumption of raw or undercooked pork or by ingesting food and water contaminated with human or animal feces containing *T. solium* eggs. Eggs hatch into larva in the intestines, penetrate the intestinal wall, and migrate to the brain where they transform into cycticerci (Stringer, 2006). It can take several years to develop clinical symptoms, including seizures, after infection. Altered blood-brain barrier and inflammatory reaction around the cysts or associated with calcified granulomas appear in patients with NCC-associated seizures, but the factors crucial in causing seizures are unclear. Several rodent models of NCC have been developed using mice infected intracranially with *T. crassiceps* (Matos-Silva et al., 2012) or *Mesocestoides corti* (Mishra et al., 2013); however, seizures were not studied in these models. One study reported epileptiform activity in a rat model of NCC using granulomas associated with *T. crassiceps* infection (Stringer et al., 2003). In addition, seizures were observed in a recently reported rat model of NCC using activated *T. solium* oncospheres (Verastegui et

al., 2015).

Methods of generation

As reported in the study by Stringer et al., 2003, female BALB/c mice are first inoculated intraperitoneally with *T. crassiceps*. Live parasites do not cause much inflammation but the dying parasites initiate chronic granulomatous reaction in the peritoneal cavity. The development of granuloma can be histopathologically graded from stage 1-4 with increasing levels of inflammation and tissue damage. Granulomas indicative of each stage are isolated from the peritoneal cavity after 3 months of infection and the extract of granulomas is injected into the hippocampus or amygdala or other brain region of Sprague-Dawley rats (125-175 g) to model NCC. In another model (Verastegui et al., 2015), Holtzman rats aged 10-26 days are infected intracranially with activated *T. solium* oncospheres suspended in sterile physiologic salt solution.

Characteristics and defining features

Intrahippocampal electrodes are used to record epileptiform activity in the rats treated with granuloma extract. All rats injected with the extract from stage 1-2, but not stage 3-4, granulomas developed electrographic seizures of average 44 s within 3 min of injection. However, subsequent epileptiform activity, spreading of seizures out of hippocampus and behavioral seizures were not observed. Neuronal or glial cell loss was not detected in the brain. Such findings question the usefulness of this model to study the mechanism of epileptogenesis.

Epilepsy developed in 9% of rats (2/23) infected with activated *T. solium*

oncospheres at 5 months after infection. The seizures were characterized as generalized tonic-clonic and the frequency was at least once a week before necropsy. The presence of inflammatory cells and perivascular infiltrate were observed around cysts in cortical and subcortical limbic regions. This recent model overcomes some limitations of the previous models, but the numbers of rats developing epilepsy are very low. Future studies should conduct EEG recordings so as to characterize the seizures that occur as a consequence of the development of epilepsy in this model.

TMEV-induced murine model of limbic epilepsy

General description

Theiler's murine encephalomyelitis virus (TMEV) is a single-stranded positive-sense ribonucleic acid (RNA) virus belonging to *Picornaviridae* family and *Cardiovirus* genus. Several strains of TMEV have been characterized based on their neurovirulence. They are primarily grouped into two categories: 1) TO (Theiler's original) and 2) GDVII. The TO group contains less neurovirulent strains such as TO, DA (Daniels), BeAn8386 (BeAn), and WW; whereas the GDVII group contains highly neurovirulent strains including GDVII and FA. Mice infected with the TO group of TMEV strains generally survive the infection and exhibit a variety of pathological changes depending on the strain of both virus and mice, and therefore, they are useful to model several different diseases. C57BL/6J mice infected with the DA strain of TMEV develop acute seizures during the first two weeks of infection and develop limbic epilepsy after about two months of infection (Libbey et al., 2008; Stewart et al., 2010a).

Methods of generation

Five to seven weeks old C57BL/6J (B6) mice are briefly anesthetized with 3% isoflurane and infected with 20 µl of DA-TMEV solution intracortically in the right hemisphere by inserting the needle at a 90° angle to the skull. The injection region is located slightly medial to the equidistant point on the imaginary line connecting the eye and the ear. A sterilized syringe containing a plastic jacket on the needle exposing 2.5 mm of needle is used for infection to restrict the injection site to the somatosensory cortex without damaging the hippocampus. The schematic in Figure 1.1 summarizes the timeline of TMEV infection and the development of acute and chronic seizures.

Characteristics and defining features

Age

Generally, 5-7 weeks old mice are used for TMEV infection. However, 3 months old mice have also been observed to respond similarly to TMEV infection-induced seizures (Libbey et al., 2011a).

Sex

TMEV-induced seizure patterns are similar among male and female mice (Libbey et al., 2008).

Species

Development of seizures is C57BL/6J strain-specific. SJL/J (male and female), BALB/c (male), and FVB/N (male) mice do not show seizures following intracortical

infection with DA-TMEV (Broer et al., 2016; Libbey et al., 2008).

Acute seizures

Mice develop acute behavioral seizures from 3-10 dpi. Handling the mice or mildly agitating the cages induces seizures during the acute infection period. Seizures follow a pattern of focal onset with secondarily generalized tonic-clonic seizures and the seizure severity can be characterized by a modified Racine scale from stage 1 to 6 where stage 1 – mouth and facial movement, stage 2 – head nodding, stage 3 – forelimb clonus, stage 4 – forelimb clonus, rearing, stage 5 – forelimb clonus, rearing, and falling, and stage 6 – intense running, jumping, repeated falling, and severe clonus (Racine, 1972). Generally, mild seizures (stage 1-3) appear in about 25-50% of the infected mice by 3 dpi. As the infection progresses, additional mice develop seizures and the seizure intensity and duration steadily increases (stage 4-6) by 5 dpi. Numbers of seizures gradually decrease after 5 dpi without reduction in the intensity and most of the mice cease to have seizures by 8 dpi (Bhuyan et al., 2015). Mice do not generally develop status epilepticus during the acute infection period.

Seizures are afebrile in nature and their properties, including frequency, intensity, duration, and latency to first appearance, vary among mice. The percentage of infected mice developing seizures is positively correlated with the titer of DA-TMEV used for infection. A dose-response study demonstrated that seizure incidence increased from 30% with $3x10^3$ PFU, to 40% with $3x10^4$ PFU, to 65% with $3x10^5$ PFU, and to 80% with $3x10^6$ PFU (Libbey et al., 2011b). Mice experience 10-15% weight loss during acute seizures and regain the weight slowly afterwards. Mice appear sick during the acute

infection period with varying symptoms of hunched posture, lethargy, decreased locomotion, and ruffled fur; however, mortality is very rare. Mice clear the virus from the brain by 2 weeks postinfection and survive the infection.

EEG seizures

A long-term continuous video encephalography (vEEG) study in mice surgically implanted with a recording electrode on the cortical surface 10-14 days before infection have been used to detect and monitor seizures (Figure 1.2) (Stewart et al., 2010a). Electrographic seizures are characterized as rhythmic spikes or sharp-wave discharges with amplitudes at least 2 times higher than baseline and lasting longer than 6 s and are associated with convulsive seizures (Figure 1.2). In this study, 75% (12/16) of mice were found to have seizures by vEEG monitoring compared to an incidence of only 52% (54/103) by twice-daily observations during the first 2 weeks of infection with $2x10^4$ PFU per mouse (Libbey et al., 2008; Stewart et al., 2010a). This first vEEG study reported average seizure incidence of 14.5 ± 10.5 (mean ± SD) seizures per mouse and an average seizure duration that increased from 24 ± 13 to 50 ± 17 s (mean ± SD) from 3 to 5 dpi.

Chronic seizures and epilepsy

Chronic spontaneous seizures and the development of epilepsy have been studied by vEEG up to 8 months post-TMEV infection (Stewart et al., 2010a). In this study, 14 mice which had acute behavioral seizures detected by visual observation in the first two weeks of infection were implanted with cortical surface electrodes at 8 weeks

postinfection. The continuous vEEG recordings conducted at 2-months postinfection for one week, and at 4 and 7 months postinfection for one month each detected electrographic seizures accompanied by stage 4-5 behavioral seizures in 9/14 (64%), 4/7 (57%), and 2/5 (40%) mice, respectively. All mice had epileptiform activity defined as an abnormal electrographic activity characterized by large amplitude, multispike morphology and either associated with sudden cessation of activity or no distinct behavioral correlate. Chronic seizure frequency was 2.1 seizures per mouse per week at 2 months and <1 seizure per mouse per week during the 5^{th}- and 7^{th}-month recording periods. A more recent vEEG study also demonstrated that all infected mice exhibit epileptiform EEG activity well after the infection has cleared and early seizures have resolved (Broer et al., 2016). In addition, this group also found that DA-TMEV infection results in spontaneous recurrent seizures in about 38% of the mice examined (Broer et al., 2016) and, as previously described, the frequency of these seizures was very low.

Neuropathology

Localization of TMEV in the brain

Many viruses associated with seizures exhibit tropism for neurons in limbic brain structures (Misra et al., 2008). The DA-TMEV strain has also been shown to infect primarily neurons in the limbic and temporal regions of B6 mice. TMEV antigens can be detected bilaterally in the hippocampus, septal nuclei, periventricular thalamic nuclei, and parietal, piriform, and entorhinal cortices of B6 mice during 3-7 dpi (Stewart et al., 2010b). Pyramidal neurons of the CA2 and CA1 region of the hippocampus are highly susceptible to TMEV infection, whereas CA3 and dentate gyrus of the hippocampus are

usually devoid of TMEV antigens. TMEV is largely undetectable in the brain by 14 dpi. Antigens of DA-TMEV have also been found in the brainstem at 2 dpi (Buenz et al., 2009). The cell surface receptor(s) that TMEV uses for insertion into the cells has not been determined, but sialic acid (carbohydrate co-receptor) has been implicated in cellular attachment of DA-TMEV (Lipton et al., 2006).

Inflammation following infection

Infection in the host is known to induce a variety of defense mechanisms that are intended to fight the infectious agents. However, the immune defense is akin to a double-edged sword. Optimal functions of the immune system are desirable; whereas excessive and prolonged activation of immune mediators can cause autoimmune inflammatory conditions and tissue damage. Several studies investigating the role of immune cells and molecules have been conducted in the TMEV model of epilepsy. These studies were aimed to address the following key important questions regarding this model: 1) do the infection-induced inflammatory conditions in the brain primarily drive the seizure activity and/or is the inflammation actually a consequence of seizure activity; 2) what is the relative contribution of the cells of the innate and adaptive immune system in seizure induction; and 3) do the neurological changes and seizure development accompanying TMEV infection recapitulate the clinical findings from patients suffering from infectious encephalitis-induced epilepsy? The outcome of these studies are summarized and discussed here.

Role of innate immune system

The innate immune system is the first line of defense against tissue damage caused by mechanical, chemical, or biological insult. A temporally and spatially regulated well-coordinated response comprised of a variety of proteins including cytokines, chemokines, complement proteins, growth factors, adhesion molecules, and intracellular signaling components rapidly develops upon stimuli such as infection and even seizures. The cell types implicated in driving the acute immune response in the CNS are microglia, astrocytes, endothelial cells of the blood vessels, and the immune cells of the peripheral compartment (macrophages, neutrophils, natural killer cells, and dendritic cells) that can infiltrate into the central compartment due to compromised blood-brain barrier and sometimes neurons.

TGFβ (transforming growth factor-β). Initial studies measured the level of TGFβ in the brain after infection because activation of the TGFβ signaling pathway contributes to seizure generation and epileptogenesis during and following CNS injury (Cacheaux et al., 2009). A significant increase in the level of TGFβ was found in the hippocampus from 5-7 days post-TMEV infection in seized mice (Libbey et al., 2008). TGFβ was highly expressed in the pyknotic neurons in the pyramidal layer of hippocampus and less extensively in the cortical neurons. Activation of TGFβ signaling in astrocytes in blood-brain barrier injury models of epilepsy contributes to astrocyte dysfunction and the impairment in the regulation of neuronal functions underlying the development of epilepsy (Vezzani et al., 2011). Interestingly, losartan, which is known to inhibit peripheral TGFβ signaling, significantly reduced the numbers of rats developing chronic seizures and the average seizure frequency (Bar-Klein et al., 2014) in the models of

vascular injury. This study provides evidence that TGFβ signaling could be targeted as a potential antiepileptogenic strategy. The validity of this strategy should be evaluated in the TMEV infection-induced model of epilepsy.

Cytokines. IL-1, IL-6, and TNFα are among the most widely investigated cytokines in various animal models of epilepsy as well as in clinical studies (Vezzani et al., 2008). The constitutive protein levels of these cytokines in the brain are normally barely detectable but they rapidly increase following seizure-inducing stimuli.

In the TMEV model, analysis of messenger RNA (mRNA) expression of cytokines – IL-1, IL-6, and TNFα – in the whole brain lysate at 6 dpi showed an increase in the levels of IL-1β in the seized mice (16-fold) and in the nonseized mice (9-fold), whereas the levels of IL-1α was increased by 4.3-fold in the seized mice and by 4.7-fold in the nonseized mice (Kirkman et al., 2010). TNFα level was dramatically increased by 128.5-fold in mice having acute seizures and by 13.5-fold in TMEV infected mice without seizures. IL-6 levels were also significantly increased by 67-fold in the seized mice and 44.5-fold in the nonseized mice. There was no difference in the mRNA levels of IL-1 and TNFα at 2 dpi before the induction of the first seizure. These data suggest an association between the mRNA levels of cytokines, especially TNFα and IL-6, and the acute seizure activity. To confirm the contribution of these cytokines in the development of seizures, mice strains deficient either in these cytokines or their receptors or signaling protein were tested for their seizure response following TMEV infection (Kirkman et al., 2010). Both IL-1α and IL-1β bind to IL-1R and initiate signaling via the adaptor protein known as myeloid differentiation primary response gene 88 (MyD88). About 38% of IL-1R1$^{-/-}$ mice (n = 16) and 47% of MyD88$^{-/-}$ mice (n = 45) had behavioral seizures in the

first two weeks of infection compared to 52% of WT mice (n = 103). These effects were not statistically significant. In contrast, only 15% of IL-$6^{-/-}$ mice (n = 20) and 10% of TNFα receptor $1^{-/-}$ mice (TNFR$1^{-/-}$, n = 20) developed seizures compared to the control group. It is concluded from these experiments that IL-1 signaling via IL-1R and MyD88 may not be involved in seizure induction in TMEV model, whereas TNFα and IL-6 signaling contribute significantly in seizure generation during the acute infection period.

The fact that IL-1-mediated signaling is not strongly implicated in TMEV-induced seizures is surprising, as IL-1β has been established by studies from multiple groups as an important cytokine that underlies proconvulsant effects in various animal models of epilepsy (Vezzani et al., 2011). The animal studies exploring the functions of IL-6 in seizure generation present dichotomous results (Campbell et al., 1993; Penkowa et al., 2001). Similarly, studies in other animal models of epilepsy have shown either proconvulsive or anticonvulsive effects of TNFα. TNFα is a pleiotropic cytokine having important functions in inflammation and immunoregulation. TNFα exerts its effects via two receptors: TNFR1 and TNFR2. The effects of TNFα on neural circuit function depends on various factors, including relative expression levels of TNFRs (TNFR1 and 2) in the tissue and the cell types expressing them (McCoy and Tansey, 2008). Indeed, TNFR1-mediated signaling has been implicated in causing hyperexcitatory and ictogenic effects of TNFα, whereas TNFR2 mediated antiseizure effects of TNFα in rodents treated with kainic acid (Balosso et al., 2005; Weinberg et al., 2013). Further studies should thoroughly investigate the roles of these cytokines in acute and chronic seizure development in the TMEV model. The mRNA levels were measured in the whole brain but there are currently no published data on the expressions of IL-1, IL-6, and TNFα in

the hippocampus, which is the epicenter of TMEV-induced damage and a likely region of seizure initiation. The contributions of the TNFRs in seizure generation should also be evaluated in the future.

In conclusion, inflammation mediated by cytokines, especially TNFα and IL-6, appears to contribute significantly in the development of acute seizures in the TMEV model. Cytokines can modulate neurotransmission by affecting the levels of excitatory and inhibitory neurotransmitters and their receptors, enzymes involved in the metabolism of neurotransmitters, and cellular signaling proteins (Wilcox and Vezzani, 2014). Hyperexcitable conditions and seizures can cause neurotoxicity which could in turn fuel the inflammatory process and contribute to the process of epileptogenesis. However, inflammation is also crucial to clear the viral infection, and therefore, some functions of cytokines in the TMEV model are likely to be beneficial and this needs further investigation. There must be a tightly regulated threshold in the level of inflammation, and violation of that threshold due to impaired regulatory processes could "prime" the neuronal circuits for hyperexcitation and development of either acute or chronic spontaneous seizures.

The complement system. The complement system is another component of the innate immune system that recognizes and eliminates pathogens through direct cell lysis and mobilizing innate and adaptive immunity (Ricklin et al., 2010). It is comprised of several serum proteins synthesized in the CNS by neurons, glia, and blood endothelial cells (Alexander et al., 2008). The expression of complement component proteins increases after viral infection primarily in microglia and macrophages. The activation of C3, the most abundant complement protein, can induce the release of TNFα and IL-6

(Zhang et al., 2007). Therefore, the role of the complement system in seizure development was also recently evaluated in the TMEV model.

The mRNA level of C3 was increased over 100-fold at 6 dpi in the brain of TMEV-infected mice, both with or without behavioral seizures (Kirkman et al., 2010). Interestingly, only 17% of $C3^{-/-}$ C57BL/6J mice (n = 41) had behavioral seizures in the first 3 weeks of TMEV infection compared to 52% in WT C57BL/6J mice (n = 103), indicating that C3 is involved in seizure generation in this model (Kirkman et al., 2010). About 40% of C57BL/6J mice (n = 22) pretreated with cobra venom factor to deplete C3 in the periphery developed behavioral seizures during acute TMEV infection, which was comparable to WT C57BL/6J mice (Kirkman et al., 2010). These data along with increased mRNA level of C3 in the brain indicate that the increased expression of C3 in the CNS is implicated in seizure generation in the TMEV model. The contribution to seizure induction by C3 could be either directly, by manipulating the synaptic functions in the CNS, and/or indirectly by increasing the release of TNFα or IL-6.

Chemokines. Chemokines are specific types of cytokines that are important for chemotaxis and recruitment of various immune cells in the blood to the sites of infection or injury. The mRNA expression of several chemokine ligands and receptors involved in the recruitment of polymorphonuclear granulocytes (PMNs), macrophages/monocytes, and natural killer (NK) cells were found to be elevated in the brains of TMEV-infected mice with seizures at 6 dpi compared to PBS-injected control mice (Libbey et al., 2011a). This study did not clearly correlate the particular type of infiltrating cell with the development of acute behavioral seizures because there are overlapping functions of many chemokines in the attraction of various infiltrating cells; however, it underscores

that infiltrating immune cells from the peripheral compartment could be important in the regulation of seizures.

Other inflammatory proteins. The functions of other inflammatory mediators such as toll-like receptors, adhesion molecules, prostaglandins, interferons, and inflammatory signaling proteins, for example, nuclear factor kappa-light-chain-enhancer of activated B cells (NF-κB) and mammalian target of rapamycin (mTOR), which are implicated in the development of seizures and epilepsy in some experimental animal models and in some human epilepsies, are not clear in the TMEV model and warrant future investigation.

Immune cells of innate immunity. Cells of the innate immune system include PMNs (neutrophils, basophils, and eosinophils), macrophages, monocytes, NK cells, and dendritic cells in the peripheral compartment. In the CNS, glial cells (microglia and astrocytes) are particularly involved in innate immune response. These cells are "activated" under pathogenic conditions and are known to release cytokines in order to neutralize the threat or insult.

Gliosis, which is the activation of glial cells in response to CNS injury, has been observed in mice during TMEV-infection (Loewen et al., 2016). Immunohistochemical analysis has revealed a significant increase in *Ricinus communi*s agglutinin-I-positive cells (marker for activated microglia/macrophage) at 5, 7, 14, 21, and 35 days post-TMEV infection and in glial fibrillary acidic protein (GFAP)-positive cells (marker for activated astrocytes) at 7 and 14 days post-TMEV infection in the brains of mice with seizures compared to nonseized and PBS-injected mice (Kirkman et al., 2010). Gliosis was also confirmed by confocal microscopy which showed an increase in

immunoreactivity for ionized calcium-binding adapter molecule 1 (IBA-1, another marker for activated microglia) and GFAP in the hippocampus of TMEV-infected mice during and after behavioral seizures during the acute infection period (4 and 14 dpi) (Loewen et al., 2016). Glial proliferation also occurs in the hippocampus of TMEV-infected mice during seizures (4 dpi). Astrogliosis was also found in the hippocampus at 4-6 months post-TMEV infection (Stewart et al., 2010a), suggesting that although TMEV is cleared from the CNS within 2 weeks of infection, chronic inflammatory conditions are sustained in the brains of TMEV-infected mice that had acute seizures. Further studies should elucidate the network consequences of long-term astrogliosis in the TMEV-infected mice.

Activated microglia, astrocytes, and infiltrating immune cells in the TMEV-infected brain could be involved in seizure development through increased production and release of cytokines, especially TNFα and IL-6. Mice treated with minocycline during the first week of TMEV infection to inhibit activation and recruitment of monocytes/macrophages and activation of microglia were significantly less susceptible to developing acute seizures compared to vehicle treated mice (Libbey et al., 2011a), supporting the role of both CNS and peripheral immune cells in seizure development. The relative contribution of resident CNS cells versus infiltrating cells in the development of seizures was studied by inhibiting activation and/or infiltration of particular peripheral immune cell in the CNS. The numbers of mice developing acute seizures in the first 3 weeks of infection were not significantly different in mice pretreated with either anti-Gr-1 antibody (targeting neutrophils, 50% seized, n = 20), or anti-CXCR2 antibody (targeting PMNs, 58% seized, n = 19), or anti-NK1.1 antibody

(targeting NK cells, 40% seized, n = 15) compared to control mice (61% seized, n = 28) indicating that PMNs especially neutrophils and NK cells may not be instrumental in the development of seizures (Libbey et al., 2011a). These experiments along with gliosis studies show that infiltrating macrophages/monocytes, microglia, and astrocytes may be involved in TMEV-induced seizure development.

The contribution of infiltrating macrophages/monocytes and glial cells in inducing the release of TNFα and IL-6 has been addressed using chimeric mice. Wildtype and IL-$6^{-/-}$ C57BL/6J mice were lethally irradiated to destroy the bone marrow, and were transplanted with bone marrow cells from either WT or IL-$6^{-/-}$ donor mice to generate chimeric mice that were deficient in IL-6 specifically either in the CNS (WT→IL-$6^{-/-}$) or in the periphery (IL-$6^{-/-}$→WT) (Libbey et al., 2011a). Only 25% of WT→IL-$6^{-/-}$ mice (n = 16) and 17% of IL-$6^{-/-}$→WT mice (n = 18) developed behavioral seizures compared to 65% of age-matched WT control mice (n = 40), implicating IL-6 production by both resident CNS cells and infiltrating cells in the development of seizures. TMEV infection was conducted at 3 months of age for this experiment instead of the usual age of 4-7 weeks, suggesting that the older mice are also similarly susceptible to TMEV-induced seizures. Similarly, the experiments using lethally irradiated WT C57BL/6J mice transplanted with GFP^{+} bone marrow cells, in which the majority of infiltrating macrophages, but not microglia, were GFP-labelled, showed a significant increase in the infiltration of macrophages in the brain following TMEV infection (Cusick et al., 2013). Flow cytometric analysis of the brain samples from TMEV-infected GFP^{+} chimeric mice revealed significantly higher numbers of GFP^{+} macrophages labelled with IL-6, whereas GFP^{-} microglial cells were labelled with TNFα, indicating that significantly more TNFα

and IL-6 are produced by resident microglia and infiltrating macrophages, respectively (Cusick et al., 2013).

Role of adaptive immune system

The roles of B cells and CD4+ T cells have not been elucidated in the TMEV model. CD8+ cytotoxic T cells were detected around the perivascular cuffs in the hippocampus of TMEV-infected mice with and without acute seizures during 5-7 dpi (Libbey et al., 2008). The extent of perivascular cuffing and the infiltration of T cells were similar between seized and nonseized mice, indicating that T cells may not be implicated in seizure induction per se, but they could be involved in the clearance of viral-infected cells. The contribution of cytotoxic T cells in viral clearance and in the development of acute seizures was investigated using OT-I transgenic mice in which the majority of CD8+ T cells are highly specific for detecting ovalbumin. The seizure susceptibility of OT-I and WT C57BL/6J mice was similar during acute TMEV infection which suggests that the TMEV-specific CD8+ T cells do not modulate seizure activity (Kirkman et al., 2010). Similar to WT mice, acute seizures resolved in OT-I mice after 10 dpi. However, both RNA and protein of virus were detected in the brains of TMEV-infected OT-I mice with and without seizures during 12-17 dpi, whereas WT mice clear the virus from the brain by 14 dpi (Kirkman et al., 2010). This suggests that the persistence of virus in the brain is not correlated with observable seizure activity. The innate inflammatory immune response directed against viral infection, and subsequently intensified due to seizures, is one of the most probable driving factors causing TMEV-induced behavioral seizures. The experiments involving OT-I mice also indicate that

CD8+ T cells, along with C3 as mentioned above, are important for viral clearance from the brain.

Oxidative stress

Increased levels of cytokines, chemokines and other inflammatory mediators in response to TMEV infection can directly damage mitochondria, resulting in oxidative stress. In addition, oxidative stress can facilitate seizure generation by damaging the neurons and intensifying the inflammatory processes. Cross-talk between inflammation and oxidative stress could be involved in the development of seizures following TMEV infection. TMEV-infected mice have a significant reduction of reduced glutathione (GSH) and a concomitant increase in oxidized glutathione (GSSG) in the hippocampus during acute seizures that persists after cessation of seizures (Bhuyan et al., 2015). The GSH and GSSG levels were similar between infected and control mice before the induction of seizures. The ratio of 3-nitrotyrosine/tyrosine (3NT/Tyr) which is a marker for reactive oxygen and nitrogen species was also increased at 3, 4 and 14 dpi (Bhuyan et al., 2015). There was no change in these markers of oxidative stress in the cerebellum. These data suggest that oxidative stress occurs in the TMEV model concurrently with inflammation and acute seizures and may prove to be an important therapeutic target for treatment of acute seizures and perhaps even the process of epileptogenesis.

Neural injury

TMEV exhibits tropism for limbic structures of the brain and, as mentioned earlier, TMEV antigens are found in hippocampus, cortical structures, and thalamus.

Neuronal death occurs bilaterally in the neurons of the CA1/CA2 pyramidal layer of hippocampus, entorhinal and parietal cortices, and periventricular thalamic nuclei during acute infection (Stewart et al., 2010b), thus, overlapping in the areas with the presence of virus. However, the cell death may not be exclusively due to virus itself. In fact, one study found that majority of degenerating hippocampal neurons were not infected with TMEV and the authors concluded that CA1 pyramidal neurons die as "bystanders" (Buenz et al., 2009). Inflammation, oxidative stress, and seizures may all contribute to the observed neuronal damage. Hippocampal neurodegeneration and sclerosis result in significant bilateral hippocampal atrophy and coincident increase in the size of the lateral ventricles as early as 1 month postinfection (Stewart et al., 2010a). Other neuropathological changes that have been described in the hippocampus during acute infection include perivascular cuffs (accumulation of leukocytes around vessels that is commonly observed in viral encephalitis) and pyknosis (chromatin condensation in necrotic cells) (Libbey et al., 2008). Demyelination in the spinal cord, which occurs in SJL mice infected with DA-TMEV, does not occur in TMEV-infected C57BL/6J mice (Stewart et al., 2010b).

Neurophysiological changes

Acute seizures that occur with viral encephalitis are associated with an increased risk of developing chronic spontaneous seizures. The hyperexcitability in TMEV-infected mice was assessed by seizure threshold tests and corneal kindling at 2 months postinfection (Stewart et al., 2010b). The seizure thresholds for limbic and forebrain seizures, but not hindlimb seizures, and the numbers of corneal stimulations required to

achieve the fully kindled state were significantly reduced in TMEV-infected mice which indicate that TMEV-infected mice with acute seizures have a hyperexcitable neural circuit in the forebrain and limbic structures which is associated with an increased susceptibility to develop chronic seizures.

A significant increase in c-fos staining, a marker for increased neuronal activity, was observed in CA1-3 and dentate gyrus regions of hippocampus of TMEV-infected mice within 2 h of acute seizures (Smeal et al., 2012). These findings suggested that the hippocampus of TMEV-infected mice was involved in seizure generation and/or spread. Subsequent patch-clamp recordings of CA3 pyramidal cells were consistent with the findings of c-fos expression by revealing a significant increase in the amplitude and frequency of spontaneous excitatory postsynaptic currents (sEPSCs) during the acute infection (3-7 dpi) as well as 2 months postinfection (Smeal et al., 2012). The amplitude and frequency of miniature EPSCs (mEPSCs) in the CA3 cells were also significantly increased during both time points, suggesting that the excitatory synaptic changes occur early during the infection and can be sustained for a long time. CA3 cells receive excitatory input from the mossy fibers from the dentate gyrus, recurrent collateral connections of CA3 cells, and also via the perforant path from the entorhinal cortex. The increases in the larger amplitudes of mEPSCs (>20 pA), which are known to have mossy fiber origin (Henze et al., 1997), were similar between acute and chronic time points. The proportion of mEPSCs of 11-20 pA, associated with CA3 recurrent collaterals, was significantly increased during acute infection and decreased during 2 months postinfection. The different pattern of changes in mEPSC amplitudes suggests that the dynamic alterations in the hippocampal tri-partite circuit occur during epileptogenesis

and may reflect different seizure generating or sustaining circuits at the later time point. A recent patch-clamp study in CA3 pyramidal cells also shows a reduction in the amplitudes of spontaneous as well as miniature inhibitory postsynaptic currents (sIPSCs and mIPSCs) during the acute infection period (3-7 dpi) but not at 2 months postinfection (Smeal et al., 2015). From a mechanistic standpoint, TNFα seems to provide a key contribution in acute seizure development in the TMEV model. TNFα signaling has been shown to increase the membrane insertion of glutamate receptors and to decrease membrane expression of $GABA_A$ receptor subunits (Stellwagen and Malenka, 2006). Thus, it is possible that TNFα-mediated synaptic scaling might contribute to hyperexcitation in the CA3 circuit during acute TMEV infection. However, it is crucial to test this hypothesis at various time points after infection.

Comorbidities

TMEV-infected mice display impairment in motor functions and coordination. TMEV-infected mice have a significant righting reflex deficiency during the acute infection period (Libbey et al., 2008). Following the acute infection period, TMEV-infected mice show anxiety-like behavior as observed by their impaired performances in open field and light-dark box tests (Umpierre et al., 2014). While TMEV-infected mice do not have apparent signs of depressive-like behavior in a saccharin preference test (Umpierre et al., 2014), they were cognitively impaired in a novel object place recognition task and in the Morris water maze test. Impairment in spatial memory in TMEV-infected mice was also reported by another research group (Buenz et al., 2006) and is consistent with the neural loss that is observed in the hippocampus.

Use in therapy and biomarker development

Efforts are currently ongoing to incorporate the TMEV model into the repertoire of animal models used for the National Institute of Neurological Disorders and Stroke (NINDS)-sponsored Epilepsy Therapy Screening Program. Recently, the efficacy and disease-modifying potential of carbamazepine (CBZ) and valproic acid (VPA) was assessed in the TMEV model (Barker-Haliski et al., 2015). VPA (200 mg/kg) and CBZ (20 mg/kg) given twice daily during the first week of TMEV infection did not decrease the proportion of mice developing acute seizures, although VPA reduced the seizure burden. CBZ, in fact, increased the numbers of mice developing seizures and the concomitant seizure burden, and decreased the latency to first seizure. Treatment with either drug did not improve anxiety-like behavior associated with TMEV-infected mice. However, this study did not assess the ability of early treatment with these drugs to prevent the subsequent development of chronic spontaneous seizures. In addition, as mentioned earlier, the mechanisms driving provoked and spontaneous seizures in this model are likely to be different, and CBZ and VPA may have different effects on the seizures that occur after epilepsy develops. Inflammation plays an instrumental role in seizure development in the TMEV model. Indeed, minocycline and wogonin, which decrease inflammation by suppressing activation of microglia/macrophages and infiltration of macrophages in the CNS, were both found to reduce TMEV-induced acute seizures (Cusick et al., 2013). Thus, this model provides the opportunity to study the etiologically relevant epileptogenesis mechanisms to identify novel classes of therapies to prevent seizures as well as the epileptogenesis process.

In contrast, the low frequency of chronic seizures during the epileptic phase in the

TMEV model highlights a challenge for using chronic seizures as an outcome measure for drug development. Alternatively, predictive biomarkers such as reduced seizure thresholds, behavioral comorbidities such as anxiety-like behavior and cognitive performance, or changes in the levels of inflammatory proteins, may prove useful to identify potential disease-modifying therapies in this model.

Advantages

The TMEV model is not technically challenging to establish and has been successfully replicated (Broer et al., 2016). TMEV is a natural pathogen of mice, and it does not infect humans and is not known to cause any adverse human health issues. Therefore, the TMEV model does not pose specific challenges to the researchers. Finally, because the strain of mouse used (C57BL/6) is the common background on which many transgenic mouse models are generated, it is possible to use powerful genetic manipulations to test hypotheses relevant to epileptogenesis in this model.

Limitations and model optimization considerations

While clearly this first model of infection-induced TLE is an important model of a common cause of human TLE, the frequency and incidence of spontaneous seizures after the virus clears are fairly low. Thus, the detailed studies of epileptogenesis and drug treatment in the later time period would require a very large cohort of mice monitored by 24/7 vEEG for prolonged periods of time. However, the numbers of mice developing seizures during the acute infection period are correlated with TMEV titer and the initial chronic vEEG experiments were conducted in mice that had been infected using $2x10^4$

PFU of TMEV. Future experiments should investigate whether the development of subsequent TLE following infection with a higher titer of TMEV increases the incidence of seizures. In addition, focal seizures without a behavioral correlate may have been missed in the original report. Therefore, subsequent studies using hippocampal depth electrodes may provide additional outcome measures (e.g., interictal spiking, hippocampal paroxysmal discharges, etc.) that can be quantified and associated with the development of TLE.

Insight into human disorders

TMEV-infected mice exhibit seizures during the acute infection period, survive the infection, clear the virus, develop spontaneous seizures, and show evidence of inflammation, neuropathological abnormalities, and behavioral and cognitive comorbidities (Table 1.1). Thus, the TMEV model mimics many aspects of seizures that occur in patients during and following infection and provides a unique opportunity to study mechanisms of infection-induced seizures, subsequent epileptogenesis, and behavioral comorbidities.

The nature of neuropathological changes in the brain and the involvement of numbers of inflammatory markers in seizure development following TMEV infection substantiates that the TMEV model could be a relevant model for human mesial TLE. First, the limbic region is a critical area of the brain in patients with TLE, as epileptiform and ictal activity, as well as pathological damage, have been observed (Sharma et al., 2007). Second, many studies in human epilepsy patients have reported increases in the mRNA and protein levels of cytokines in the serum, cerebrospinal fluid, and sometimes

in surgically resected brain tissues (Vezzani et al., 2011). The complement system has also been suspected to contribute to seizures and epileptogenesis in patients with mesial TLE (Aronica et al., 2007). Third, there is evidence of oxidative stress in patients with TLE (Rowley and Patel, 2013). Finally, activation of microglia, astrocytes, macrophages, and PMNs has been reported in human epilepsy cases (Vezzani et al., 2011). Despite these useful clinical reports, it is important to mention that the human studies are constrained by the limited availability of sufficient brain samples and appropriate control samples for biochemical and physiological analysis and therefore, they often involve measuring the levels of inflammatory molecules in the serum. Thus, these data may not be sufficient to establish a cause-and-effect relationship between the increased levels of inflammatory molecules and the seizure activity. Nevertheless, it is evident that inflammatory markers are present at high levels in epileptic patients, thus warranting in-depth investigation where TMEV model could be useful to understand how excessive inflammation affects neuronal functions to cause seizures.

The prevalence of neurological and psychiatric disorders such as anxiety, depression, cognitive impairment, and migraine is significantly higher in patients with epilepsy than in the general population (Brooks-Kayal et al., 2013). Antiseizure medications can suppress seizures but do not generally treat the cognitive and behavioral comorbidities associated with epilepsy. A detailed study of the mechanisms of comorbidities in experimental models is necessary to develop new therapies which not only decrease seizures but also improve the quality of the patient's life. Since the TMEV model reflects several clinically relevant behavioral comorbidities, it provides an excellent platform for future drug discovery efforts targeting seizures and comorbidities

of epilepsy.

Conclusion

Animal models of epilepsy have been enormously useful in generating fundamental knowledge about the changes at the genetic, molecular, cellular, and circuit levels in the brain during seizures and epileptogenesis. This knowledge has been crucial in successfully discovering and developing many antiseizure drugs. Despite having numerous animal models for epilepsy and over 20 approved antiseizure drugs, around one third of epilepsy patients are still pharmacoresistant (Loscher and Schmidt, 2011) and many of these patients have epilepsy that is the result of CNS infection. A limitation of previous antiseizure drug discovery efforts may be that similar and conventional animal models were used, without necessarily considering the underlying disease-modifying mechanisms underlying the development of epilepsy in patients. The heterogeneous nature of epileptogenesis in patients suggests that there is a clear need for better animal models that more closely recapitulate clinical events. Therefore, valuable progress has been made in the past 10 years in developing the etiologically relevant animal model of infection-induced epilepsy that is described here. It is expected that the TMEV model, as well as other infection-induced models of epilepsy, will fill a void by providing a better understanding of the mechanism(s) of epilepsy and by providing a discovery platform that will drive the next generation of drug and novel therapy discovery efforts.

References

Alexander, J.J., Anderson, A.J., Barnum, S.R., Stevens, B., Tenner, A.J., 2008. The complement cascade: Yin-Yang in neuroinflammation, neuroprotection, and

neurodegeneration. J. Neurochem. 107, 1169-1187.

Aronica, E., Boer, K., van Vliet, E.A., Redeker, S., Baayen, J.C., Spliet, W.G., van Rijen, P.C., Troost, D., da Silva, F.H., Wadman, W.J., Gorter, J.A., 2007. Complement activation in experimental and human temporal lobe epilepsy. Neurobiol. Dis. 26, 497-511.

Balosso, S., Ravizza, T., Perego, C., Peschon, J., Campbell, I.L., De Simoni, M.G., Vezzani, A., 2005. Tumor necrosis factor-alpha inhibits seizures in mice via p75 receptors. Ann. Neurol. 57, 804-812.

Bar-Klein, G., Cacheaux, L.P., Kamintsky, L., Prager, O., Weissberg, I., Schoknecht, K., Cheng, P., Kim, S.Y., Wood, L., Heinemann, U., Kaufer, D., Friedman, A., 2014. Losartan prevents acquired epilepsy via TGF-beta signaling suppression. Ann. Neurol. 75, 864-875.

Barker-Haliski, M.L., Dahle, E.J., Heck, T.D., Pruess, T.H., Vanegas, F., Wilcox, K.S., White, H.S., 2015. Evaluating an etiologically relevant platform for therapy development for temporal lobe epilepsy: effects of carbamazepine and valproic acid on acute seizures and chronic behavioral comorbidities in the Theiler's murine encephalomyelitis virus mouse model. J. Pharmacol. Exp. Ther. 353, 318-329.

Beers, D.R., Henkel, J.S., Schaefer, D.C., Rose, J.W., Stroop, W.G., 1993. Neuropathology of herpes simplex virus encephalitis in a rat seizure model. J. Neuropathol. Exp. Neurol. 52, 241-252.

Bhuyan, P., Patel, D.C., Wilcox, K.S., Patel, M., 2015. Oxidative stress in murine Theiler's virus-induced temporal lobe epilepsy. Exp. Neurol. 271, 329-334.

Birbeck, G.L., Molyneux, M.E., Kaplan, P.W., Seydel, K.B., Chimalizeni, Y.F., Kawaza, K., Taylor, T.E., 2010. Blantyre Malaria Project Epilepsy Study (BMPES) of neurological outcomes in retinopathy-positive paediatric cerebral malaria survivors: a prospective cohort study. Lancet Neurol. 9, 1173-1181.

Broer, S., Kaufer, C., Haist, V., Li, L., Gerhauser, I., Anjum, M., Bankstahl, M., Baumgartner, W., Loscher, W., 2016. Brain inflammation, neurodegeneration and seizure development following picornavirus infection markedly differ among virus and mouse strains and substrains. Exp. Neurol. 279, 57-74.

Brooks-Kayal, A.R., Bath, K.G., Berg, A.T., Galanopoulou, A.S., Holmes, G.L., Jensen, F.E., Kanner, A.M., O'Brien, T.J., Whittemore, V.H., Winawer, M.R., Patel, M., Scharfman, H.E., 2013. Issues related to symptomatic and disease-modifying treatments affecting cognitive and neuropsychiatric comorbidities of epilepsy. Epilepsia 54 Suppl. 4, 44-60.

Buenz, E.J., Rodriguez, M., Howe, C.L., 2006. Disrupted spatial memory is a consequence of picornavirus infection. Neurobiol. Dis. 24, 266-273.

Buenz, E.J., Sauer, B.M., Lafrance-Corey, R.G., Deb, C., Denic, A., German, C.L., Howe, C.L., 2009. Apoptosis of hippocampal pyramidal neurons is virus independent in a mouse model of acute neurovirulent picornavirus infection. Am. J. Pathol. 175, 668-684.

Cacheaux, L.P., Ivens, S., David, Y., Lakhter, A.J., Bar-Klein, G., Shapira, M., Heinemann, U., Friedman, A., Kaufer, D., 2009. Transcriptome profiling reveals TGF-beta signaling involvement in epileptogenesis. J. Neurosci. 29, 8927-8935.

Campbell, I.L., Abraham, C.R., Masliah, E., Kemper, P., Inglis, J.D., Oldstone, M.B., Mucke, L., 1993. Neurologic disease induced in transgenic mice by cerebral overexpression of interleukin 6. Proc. Natl. Acad. Sci. U. S. A. 90, 10061-10065.

Chen, S.F., Huang, C.C., Wu, H.M., Chen, S.H., Liang, Y.C., Hsu, K.S., 2004. Seizure, neuron loss, and mossy fiber sprouting in herpes simplex virus type 1-infected organotypic hippocampal cultures. Epilepsia 45, 322-332.

Cusick, M.F., Libbey, J.E., Patel, D.C., Doty, D.J., Fujinami, R.S., 2013. Infiltrating macrophages are key to the development of seizures following virus infection. J. Virol. 87, 1849-1860.

Dyhrfjeld-Johnsen, J., Berdichevsky, Y., Swiercz, W., Sabolek, H., Staley, K.J., 2010. Interictal spikes precede ictal discharges in an organotypic hippocampal slice culture model of epileptogenesis. J. Clin. Neurophysiol. 27, 418-424.

Epstein, L.G., Shinnar, S., Hesdorffer, D.C., Nordli, D.R., Hamidullah, A., Benn, E.K., Pellock, J.M., Frank, L.M., Lewis, D.V., Moshe, S.L., Shinnar, R.C., Sun, S., 2012. Human herpesvirus 6 and 7 in febrile status epilepticus: the FEBSTAT study. Epilepsia 53, 1481-1488.

Getts, D.R., Matsumoto, I., Muller, M., Getts, M.T., Radford, J., Shrestha, B., Campbell, I.L., King, N.J., 2007. Role of IFN-gamma in an experimental murine model of West Nile virus-induced seizures. J. Neurochem. 103, 1019-1030.

Henze, D.A., Card, J.P., Barrionuevo, G., Ben-Ari, Y., 1997. Large amplitude miniature excitatory postsynaptic currents in hippocampal CA3 pyramidal neurons are of mossy fiber origin. J. Neurophysiol. 77, 1075-1086.

Kirkman, N.J., Libbey, J.E., Wilcox, K.S., White, H.S., Fujinami, R.S., 2010. Innate but not adaptive immune responses contribute to behavioral seizures following viral infection. Epilepsia 51, 454-464.

Labar, D.R., Harden, C., 1998. Infection and inflammatory diseases., in: Engel, J., Jr.,

Pedley, T.A. (Eds.), Epilepsy: A Comprehensive Textbook Lippincott, Williams & Wilkins, New York, pp. 2587-2596.

Libbey, J.E., Kennett, N.J., Wilcox, K.S., White, H.S., Fujinami, R.S., 2011a. Interleukin-6, produced by resident cells of the central nervous system and infiltrating cells, contributes to the development of seizures following viral infection. J. Virol. 85, 6913-6922.

Libbey, J.E., Kennett, N.J., Wilcox, K.S., White, H.S., Fujinami, R.S., 2011b. Lack of correlation of central nervous system inflammation and neuropathology with the development of seizures following acute virus infection. J. Virol. 85, 8149-8157.

Libbey, J.E., Kirkman, N.J., Smith, M.C., Tanaka, T., Wilcox, K.S., White, H.S., Fujinami, R.S., 2008. Seizures following picornavirus infection. Epilepsia 49, 1066-1074.

Lipton, H.L., Kumar, A.S., Hertzler, S., Reddi, H.V., 2006. Differential usage of carbohydrate co-receptors influences cellular tropism of Theiler's murine encephalomyelitis virus infection of the central nervous system. Glycoconj. J. 23, 39-49.

Loewen, J.L., Barker-Haliski, M.L., Dahle, E.J., White, H.S., Wilcox, K.S., 2016. Neuronal injury, gliosis, and glial proliferation in two models of temporal lobe epilepsy. J. Neuropathol. Exp. Neurol. 75, 366-378.

Loscher, W., Schmidt, D., 2011. Modern antiepileptic drug development has failed to deliver: ways out of the current dilemma. Epilepsia 52, 657-678.

Matos-Silva, H., Reciputti, B.P., Paula, E.C., Oliveira, A.L., Moura, V.B., Vinaud, M.C., Oliveira, M.A., Lino-Junior Rde, S., 2012. Experimental encephalitis caused by Taenia crassiceps cysticerci in mice. Arq. Neuropsiquiatr. 70, 287-292.

McCoy, M.K., Tansey, M.G., 2008. TNF signaling inhibition in the CNS: implications for normal brain function and neurodegenerative disease. J. Neuroinflammation 5, 45.

Mishra, P.K., Morris, E.G., Garcia, J.A., Cardona, A.E., Teale, J.M., 2013. Increased accumulation of regulatory granulocytic myeloid cells in mannose receptor C type 1-deficient mice correlates with protection in a mouse model of neurocysticercosis. Infect. Immun. 81, 1052-1063.

Misra, U.K., Tan, C.T., Kalita, J., 2008. Viral encephalitis and epilepsy. Epilepsia 49 Suppl 6, 13-18.

Ndimubanzi, P.C., Carabin, H., Budke, C.M., Nguyen, H., Qian, Y.J., Rainwater, E., Dickey, M., Reynolds, S., Stoner, J.A., 2010. A systematic review of the

frequency of neurocyticercosis with a focus on people with epilepsy. PLoS Negl. Trop. Dis. 4, e870.

Oostenbrink, R., Moons, K.G., Derksen-Lubsen, G., Grobbee, D.E., Moll, H.A., 2002. Early prediction of neurological sequelae or death after bacterial meningitis. Acta Paediatr. 91, 391-398.

Penkowa, M., Molinero, A., Carrasco, J., Hidalgo, J., 2001. Interleukin-6 deficiency reduces the brain inflammatory response and increases oxidative stress and neurodegeneration after kainic acid-induced seizures. Neuroscience 102, 805-818.

Racine, R.J., 1972. Modification of seizure activity by electrical stimulation. II. Motor seizure. Electroencephalogr. Clin. Neurophysiol. 32, 281-294.

Ricklin, D., Hajishengallis, G., Yang, K., Lambris, J.D., 2010. Complement: a key system for immune surveillance and homeostasis. Nat. Immunol. 11, 785-797.

Rowley, S., Patel, M., 2013. Mitochondrial involvement and oxidative stress in temporal lobe epilepsy. Free Radic. Biol. Med. 62, 121-131.

Sharma, A.K., Reams, R.Y., Jordan, W.H., Miller, M.A., Thacker, H.L., Snyder, P.W., 2007. Mesial temporal lobe epilepsy: pathogenesis, induced rodent models and lesions. Toxicol. Pathol. 35, 984-999.

Smeal, R.M., Fujinami, R., White, H.S., Wilcox, K.S., 2015. Decrease in CA3 inhibitory network activity during Theiler's virus encephalitis. Neurosci. Lett. 609, 210-215.

Smeal, R.M., Stewart, K.A., Iacob, E., Fujinami, R.S., White, H.S., Wilcox, K.S., 2012. The activity within the CA3 excitatory network during Theiler's virus encephalitis is distinct from that observed during chronic epilepsy. J. Neurovirol. 18, 30-44.

Solbrig, M.V., Adrian, R., Chang, D.Y., Perng, G.C., 2006. Viral risk factor for seizures: pathobiology of dynorphin in herpes simplex viral (HSV-1) seizures in an animal model. Neurobiol. Dis. 23, 612-620.

Stellwagen, D., Malenka, R.C., 2006. Synaptic scaling mediated by glial TNF-alpha. Nature 440, 1054-1059.

Stewart, K.A., Wilcox, K.S., Fujinami, R.S., White, H.S., 2010a. Development of postinfection epilepsy after Theiler's virus infection of C57BL/6 mice. J. Neuropathol. Exp. Neurol. 69, 1210-1219.

Stewart, K.A., Wilcox, K.S., Fujinami, R.S., White, H.S., 2010b. Theiler's virus infection chronically alters seizure susceptibility. Epilepsia 51, 1418-1428.

Stringer, J.L., 2006. Models available for infection-induced seizures, in: Pitkänen, A.,

Schwartzkroin, P.A., Moshé, S.L. (Eds.), Models of Seizures and Epilepsy, First ed. Elsevier, pp. 521-526.

Stringer, J.L., Marks, L.M., White, A.C., Jr., Robinson, P., 2003. Epileptogenic activity of granulomas associated with murine cysticercosis. Exp. Neurol. 183, 532-536.

Stroop, W.G., Schaefer, D.C., 1989. Neurovirulence of two clonally related herpes simplex virus type 1 strains in a rabbit seizure model. J. Neuropathol. Exp. Neurol. 48, 171-183.

Theodore, W.H., 2014. Epilepsy and viral infections. Epilepsy Curr. 14, 35-42.

Umpierre, A.D., Remigio, G.J., Dahle, E.J., Bradford, K., Alex, A.B., Smith, M.D., West, P.J., White, H.S., Wilcox, K.S., 2014. Impaired cognitive ability and anxiety-like behavior following acute seizures in the Theiler's virus model of temporal lobe epilepsy. Neurobiol. Dis. 64, 98-106.

Verastegui, M.R., Mejia, A., Clark, T., Gavidia, C.M., Mamani, J., Ccopa, F., Angulo, N., Chile, N., Carmen, R., Medina, R., Garcia, H.H., Rodriguez, S., Ortega, Y., Gilman, R.H., 2015. Novel rat model for neurocysticercosis using Taenia solium. Am. J. Pathol. 185, 2259-2268.

Vezzani, A., Balosso, S., Ravizza, T., 2008. The role of cytokines in the pathophysiology of epilepsy. Brain. Behav. Immun. 22, 797-803.

Vezzani, A., French, J., Bartfai, T., Baram, T.Z., 2011. The role of inflammation in epilepsy. Nat. Rev. Neurol. 7, 31-40.

Vezzani, A., Fujinami, R.S., White, H.S., Preux, P.M., Blumcke, I., Sander, J.W., Loscher, W., 2016. Infections, inflammation and epilepsy. Acta Neuropathol. 131, 211-234.

Weinberg, M.S., Blake, B.L., McCown, T.J., 2013. Opposing actions of hippocampus TNFalpha receptors on limbic seizure susceptibility. Exp. Neurol. 247, 429-437.

Wilcox, K.S., Vezzani, A., 2014. Does brain inflammation mediate pathological outcomes in epilepsy? Adv. Exp. Med. Biol. 813, 169-183.

Wu, H.M., Huang, C.C., Chen, S.H., Liang, Y.C., Tsai, J.J., Hsieh, C.L., Hsu, K.S., 2003. Herpes simplex virus type 1 inoculation enhances hippocampal excitability and seizure susceptibility in mice. Eur. J. Neurosci. 18, 3294-3304.

Wu, H.M., Liang, Y.C., Chen, S.H., Huang, C.C., Tsai, J.J., Hsieh, C.L., Hsu, K.S., 2004. Valacyclovir treatment ameliorates the persistently increased pentylenetetrazol-induced seizure susceptibility in mice with herpes simplex virus type 1 infection. Exp. Neurol. 189, 66-77.

Zhang, X., Kimura, Y., Fang, C., Zhou, L., Sfyroera, G., Lambris, J.D., Wetsel, R.A., Miwa, T., Song, W.C., 2007. Regulation of Toll-like receptor-mediated inflammatory response by complement in vivo. Blood 110, 228-236.

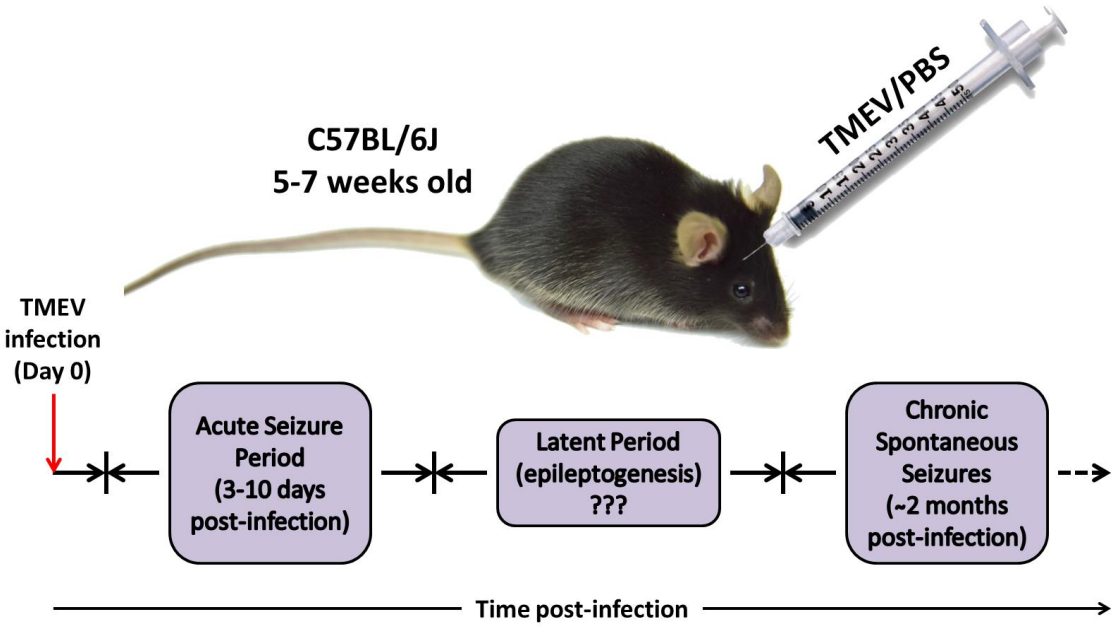

Figure 1.1 Schematic of the TMEV-infection mouse model of temporal lobe epilepsy. C57BL/6J mice are infected with Theiler's murine encephalitis virus or sham (PBS, phosphate-buffered saline) and monitored for acute and chronic seizures as described in the chapter. TMEV-infected mice present with acute behavioral seizures between 3 to 10 days postinfection and survive the infection. Mice then undergo the process of epileptogenesis during the latent period. Mice develop late spontaneous seizures after about 2 months postinfection.

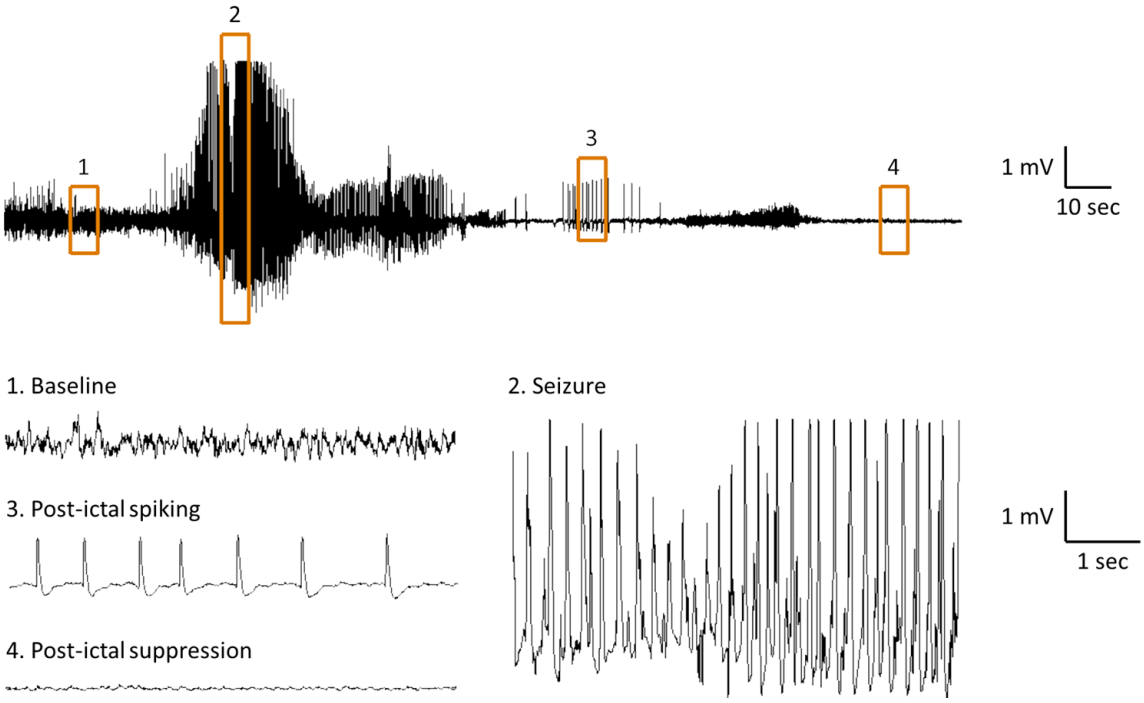

Figure 1.2 Electroencephalographic (EEG) recording from TMEV-infected mice. An example of EEG recording from an electrode implanted on the cortical surface of TMEV-infected mouse is shown during an acute seizure at 4 days postinfection. The expanded traces corresponding to the boxes are shown below, illustrating EEG activity during 1) before seizure (baseline), 2) seizure, 3) postictal spiking, and 4) behavioral arrest following seizure (postictal suppression).

Table 1.1 Salient features of the TMEV model of limbic epilepsy.

❖ C57BL/6J mice infected intracortically with TMEV exhibit acute seizures during 3-10 days postinfection.
❖ Mice survive the infection, clear the virus from the brain after about 2 weeks of infection, and later develop chronic seizures. Therefore, this is a 'hit and run' type of infection which results into development of limbic epilepsy.
❖ Frequency of chronic unprovoked seizures during the epilepsy phase is low.
❖ TMEV-infected mice have brain damage in the limbic structures. Loss of CA1 pyramidal neurons and tissue sclerosis in the hippocampus appear within a week of infection.
❖ Excessive inflammatory response driven mainly by the cells of innate immunity (microglia, macrophages and astrocytes) contributes to the development of seizures.
❖ Cytokines, primarily TNFα and IL-6, and complement protein C3 are strongly associated with the development of seizures.
❖ TMEV-infected mice with acute seizures have a hyperexcitable neurocircuit in the forebrain and limbic structures and exhibit increased susceptibility to develop chronic seizures.
❖ CA3 hippocampal neurons are hyperexcitable, however, the pattern of changes in excitatory and inhibitory functions differ between acute and chronic seizures, which suggests that the dynamic alterations in the hippocampal tri-partite circuit occur during epileptogenesis.
❖ TMEV-infected mice with acute seizures show later behavioral and cognitive comorbidities (anxiety and impairment in episodic and spatial memories).

CHAPTER 2

OXIDATIVE STRESS IN MURINE THEILER'S VIRUS-INDUCED TEMPORAL LOBE EPILEPSY[2]

Abstract

Temporal lobe epilepsy (TLE) is the most common form of acquired epilepsy that can be caused by several inciting events including viral infections. However, one-third of TLE patients are pharmacoresistant to current antiepileptic drugs and therefore, there is an urgent need to develop antiepileptogenic therapies that prevent the development of the disease. Oxidative stress and redox alterations have recently been recognized as important etiological factors contributing to seizure-induced neuronal damage. The goal of this study was to determine if oxidative stress occurs in the TMEV (Theiler's murine

---

[2]Reprinted from Experimental Neurology, 271, Pallavi Bhuyan[†], Dipan C. Patel[†,]*, Karen S. Wilcox, and Manisha Patel, Oxidative stress in murine Theiler's virus-induced temporal lobe epilepsy, 329-34, 2015, with permission from Elsevier.

[†]Co-first authors

*Conducted TMEV infection and acute seizures monitoring in mice, harvested brain tissue samples for the analysis of oxidative stress markers, and contributed to the writing of the manuscript.

encephalomyelitis virus) model of temporal lobe epilepsy (TLE). C57BL/6J mice were injected with TMEV or with saline intracortically and observed for acute seizures. At various time points after TMEV injection, hippocampi were analyzed for levels of reduced glutathione (GSH), oxidized glutathione (GSSG) and 3-nitrotyrosine (3NT). Mice infected with TMEV displayed behavioral seizures between 3 and 7 days postinfection (dpi). The intensity of seizures increased over time with most of the seizures being a stage 4 or 5 on the Racine scale at 6 dpi. Mice exhibiting at least one seizure during the observation period were utilized for the biochemical analyses. The levels of GSH were significantly depleted in TMEV-infected mice at 3, 4 and 14 dpi. with a concomitant increase in GSSG levels as well as an impairment of the redox status. Additionally, there was a substantial increase in 3NT levels in TMEV-infected mice at these time points. These redox changes correlated with the occurrence of acute seizures in this model. Interestingly, we did not see changes in any of the indices in the cerebellum of TMEV-infected mice at 3 dpi indicating that these alterations are localized to the hippocampus and perhaps other limbic regions. This is the first study to demonstrate the occurrence of oxidative stress in the TMEV model of infection-induced TLE. The redox alterations were observed at time points coinciding with the appearance of acute behavioral seizures suggesting that these changes might be a consequence of seizure activity. Our results support the hypothesis that redox changes correlate with seizure activity in acquired epilepsies, regardless of the inciting insults, and suggest oxidative stress as a potential therapeutic target for their treatment.

Introduction

Temporal lobe epilepsy or TLE, the most common form of acquired epilepsy is initiated by a variety of insults including traumatic brain injury, stroke, status epilepticus and infections, which can cause early seizures, and following a latent period, lead to the development of spontaneous seizures or epilepsy. The cascade of biochemical, molecular and structural alterations following a precipitating injury and culminating in the development of epilepsy, that is, epileptogenesis, is thought to involve processes such as neuronal loss, gliosis, axonal sprouting, neurogenesis and inflammation (Dudek and Staley, 2011; Sharma et al., 2007). A recent study indicates that patients that exhibit seizures during viral encephalitis are 22 times more likely to develop epilepsy than the control population (Misra et al., 2008). Thus, patients with encephalitis are at high risk for developing epilepsy. A novel mouse model of infection-induced TLE which recapitulates clinical observations has been recently developed which offers a unique opportunity to study the molecular mechanism(s) underlying epileptogenesis and to identify novel therapeutic strategies (Libbey et al., 2008). Theiler's murine encephalomyelitis virus (TMEV)-infected C57BL/6J mice show acute behavioral seizures between 3 and 7 days postinfection (dpi), exhibit neurodegeneration, and glial activation in the hippocampus. A significant proportion of mice surviving the infection develop epilepsy after a latent period (Kirkman et al., 2010; Stewart et al., 2010a, b). In addition, the brains of TMEV-infected mice show increased expression of mRNA for proinflammatory cytokines, including tumor necrosis factor-α (TNFα) and interleukin-6 (IL-6), during the acute seizure period (Kirkman et al., 2010). Given that TNFα receptor 1 and IL-6 knockout mice have a significantly reduced incidence of seizures during the

acute TMEV infection period, inflammation seems to play an important role in the induction of seizures in this animal model (Kirkman et al., 2010).

Oxidative stress is an important mechanism known to occur following brain injuries, sufficient to cause epilepsy (Liang et al., 2000). Endogenous antioxidants can overcome normal production of reactive oxygen and nitrogen species (ROS and RNS). However, their excessive production can overwhelm the natural antioxidant defenses and shift the redox state to a more oxidized environment which can lead to oxidative damage of various cellular targets. In fact, both mitochondrial and extracellular ROS play a role in mediating seizure-induced neuronal death (Liang et al., 2000; Patel et al., 2005). Additionally, oxidative stress has been shown to occur throughout epilepsy development in chemoconvulsant models of TLE (Liang and Patel, 2006; Patel, 2004; Waldbaum and Patel, 2010). Whether oxidative stress is a common mechanism underlying diverse epileptogenic injuries is unclear. We hypothesized that oxidative stress occurs in the Theiler's virus infection model of TLE for the following reasons. (1) Viral infections often cause increased formation of ROS and RNS either due to direct effects of the virus on the cells or as a consequence of host inflammatory responses to the infections (Schwarz, 1996; Valyi-Nagy et al., 2000). In response to viral infections, increased levels of cytokines, chemokines and other inflammatory mediators can directly damage mitochondria, resulting in oxidative stress. Herpes simplex virus (HSV) and Japanese encephalitis virus (JEV) are among the most common viruses which cause encephalitis and are both associated with acute seizures in patients (Theodore, 2014). Acute and chronic HSV-1 infection in mice results in inflammation and oxidative damage to the neurons and nonneuronal cells in the brain (Valyi-Nagy and Dermody, 2005). JEV

infection has also been shown to stimulate the formation of oxidative stress in rat cultured cortical glial cells and in an acute JEV rat model (Liao et al., 2002; Srivastava et al., 2009). (2) Oxidative stress and mitochondrial dysfunction have the potential to lower seizure threshold by a variety of mechanisms including impaired ATP production (Jamme et al., 1995) and altered expression of transporters and enzymes crucial in the homeostasis of synaptic levels of neurotransmitter and intracellular calcium levels, thus tilting the balance of synaptic neurotransmission towards hyperexcitation (Waldbaum and Patel, 2010). Oxidative stress can further damage neurons by directly inducing apoptosis or necrosis and such aberrant neuronal loss can facilitate seizure generation (Kannan and Jain, 2000). Therefore, both inflammation and oxidative stress following viral infection may contribute to the development of acute seizures in the TMEV model.

While inflammation has been well documented in the TMEV model of infection-induced epilepsy, it is currently unknown if oxidative stress is observed during the acute seizure stage in TMEV infected mice. Therefore, the goal of the present study was to investigate the time course of oxidative stress in the TMEV-infection mouse model of TLE. We report here that TMEV-infected animals have a significant depletion of reduced glutathione (GSH), an increase in oxidized glutathione (GSSG) levels, as well as an increase in 3-nitrotyrosine/tyrosine (3NT/Tyr) ratio. This data suggests that oxidative stress occurs in the TMEV model of CNS infection-induced epilepsy coincident with inflammation and acute seizure activity.

Methods

Animals

Male C57BL/6J mice aged between 4 and 5 weeks old were purchased from Jackson Laboratory (Bar Harbor, ME, USA). After arrival, mice were allowed to acclimatize for 3 days prior to the experiment. Mice were provided food and water *ad libitum* and kept in a facility providing 12 h of light and lark cycle starting at 6:00 AM. All the procedures performed were in accordance with the guidelines provided and approved by the Institutional Animal Care and Use Committee of the University of Utah.

Treatment of mice and seizure monitoring

Mice were anesthetized briefly using a mixture of isoflurane and compressed air. Mice were then injected with 20 µl of either phosphate-buffered saline (PBS, n = 30) or $3x10^5$ PFU (plaque forming units) of Daniels strain of TMEV (n = 50) intracortically to a depth of 2 mm in the temporal region of the right hemisphere (posterior and medial of the right eye). Mice were agitated by briefly shaking their cages and monitored for behavioral seizures for 1 h, twice a day and a minimum of 2 h apart from 8:00 AM to 5:00 PM, until 10 dpi as previously described (Libbey et al., 2008). The intensity of the seizure activity was graded using the Racine scale as follows: stage 1, mouth and facial movements; stage 2, head nodding; stage 3, forelimb clonus; stage 4, rearing; and stage 5, rearing and falling (Racine, 1972). Mice were sacrificed at 8 h postinfection, and 1, 2, 3, 4, and 14 dpi. For 3, 4, and 14 dpi, only TMEV-infected mice that had acute behavioral seizures were used, while nonseized mice from the TMEV group were excluded from the studies. The ipsilateral and contralateral portions of the hippocampus were

microdissected and collected separately. Cerebellum was also collected. All the tissue samples were flash-frozen using 2-methylbutane chilled on dry ice and stored at -80 ºC. The samples were shipped overnight on dry ice to the laboratory of Dr. Manisha Patel at the University of Colorado, Aurora, CO for the analysis.

HPLC determination of GSH and GSSG

Reduced and oxidized forms of GSH were measured by HPLC with electrochemical detection (HPLC-EC) following minor modifications to previously described methods (Lakritz et al., 1997; Liang and Patel, 2006). GSH and GSSG were detected using a CoulArray system (Model 5600, ESA) on two coulometric array cell modules, each containing eight electrochemical sensors attached in series. Electrochemical detector potentials were 150/300/450/570/690/800/850 mV. Frozen hippocampi obtained from Dr. Karen Wilcox's laboratory were sonicated with 0.1 N perchloric acid ($HClO_4$) immediately before thawing in a 1:10 weight by volume ratio. The homogenates were centrifuged at 13,000 x g for 10 min at 4 ºC. Aliquots of the supernatant (20 µL) were injected into the HPLC and separated on a 5 µM, 250 x 4.6-mm C-18 ODS-80Tm column (Tosoh Bioscience, Japan). The mobile phase was comprised of 100 mM sodium phosphate, 1% methanol, pH 2.7 and a flow rate of 0.6 ml/min was maintained. Control values were normalized to one hundred percent and data is represented as percent of control (% control).

HPLC determination of 3-nitrotyrosine

3-Nitroyrosine (3NT) and tyrosine levels were measured using a HPLC method similar to GSH and GSSG measurements and as previously described (Ryan et al., 2014). Frozen hippocampi samples were processed in the same way as described above and 20 µl of the supernatant was injected into an ESA 5600 CoulArray HPLC (Chelmsford, MA). Separation was achieved using the same column and mobile phase as mentioned above.

Statistical analyses

GraphPad Prism 6 was used for all statistical analyses performed. Group differences were determined by analysis of variance (ANOVA) with Sidak's multiple comparison tests.

Results

Acute behavioral seizures in TMEV-infected mice

Behavioral seizures occur between 3 and 7 dpi in the TMEV model (Stewart et al., 2010a). Accordingly, seizures were not observed in animals sacrificed prior to day 3. As it was not possible to predict which animals would have gone on to develop seizures, the number of animals was increased (n = 8 per group) for the TMEV samples that were obtained at 8 h postinfection and at 1 and 2 dpi. The remaining animals (n = 26) were then assessed for seizure activity and 81% of those animals were observed to have had at least one seizure prior to sacrifice. However, on any given observation day, approximately only 50% of the animals had a seizure (Figure 2.1a). As previously

described, seizure severity increased over the course of the observation period, with the majority of seizures observed being either a stage 4 or 5 seizure by 6 dpi (Figure 2.1b and 2.1c). Only those animals that exhibited at least one seizure during the observation periods were used for harvesting tissue for the remaining time points (3, 4, and 14 dpi; n = 5 per group).

Impaired glutathione redox status in TMEV model

To determine if oxidative stress occurs in TMEV infected mice, we measured the tissue redox status in the ipsi- and contralateral hippocampus of PBS- and TMEV-injected mice. GSH is the most abundant nonprotein thiol as well as an extremely important nonenzymatic antioxidant in the body. The ratio of GSH to its oxidized form GSSG, a disulfide redox partner, is an excellent indicator of the overall tissue redox status and can be measured by HPLC analysis (Liang and Patel, 2006; Schafer and Buettner, 2001). A higher GSH/GSSG ratio indicates a reduced environment whereas a decrease in this ratio denotes a relatively oxidized tissue environment. Decreased GSH/GSSG correlates with structural damage to cellular membranes, DNA damage, posttranslational modifications to proteins and inactivation of essential enzymes, which can all affect neuronal excitability (Andersen, 2004; Waldbaum and Patel, 2010). Whole hippocampal (ipsilateral) GSH (Figure 2.2a) decreased significantly in TMEV-infected mice at 72 h (mean ± SEM = 74.712 ± 3.6%), 96 h (73.494 ± 4.236%), and 14 days (83.91 ± 5.010%) postinfection with a concomitant increase in GSSG (Figure 2.2b) levels (203.422 ± 45.697%, 238.291 ± 14.27%, 231.849 ± 41.642% for 72 h, 96 h and 14 days, respectively), compared to PBS injected control mice. The ratio of GSH/GSSG (Figure

2.2c) was also significantly decreased at these time points. The contralateral hippocampi displayed similar levels as PBS injected mice. This correlates with the onset of acute behavioral seizures indicating that tissue redox status is decreased as a consequence of either seizure activity and/or inflammation in the TMEV model, which is consistent with previous findings in the lithium-pilocarpine and kainate chemoconvulsant models of TLE (Jarrett et al., 2008; Ryan et al., 2014; Waldbaum et al., 2010).

Increased 3-nitrotyrosine levels in TMEV-infected mice

3-Nitrotyrosine (3NT) is a marker for protein nitration, a posttranslational modification that can lead to protein dysfunction or turnover. A major source of 3NT is peroxynitrite ($ONOO^-$), produced from the reaction between nitric oxide (NO) and superoxide ($O_2\bullet^-$), two highly reactive free radical species. $ONOO^-$ attacks tyrosine residues of proteins specifically, to form 3NT (Sawa et al., 2000). The levels of 3NT and free tyrosine (Tyr) can be measured utilizing HPLC and a higher ratio of 3NT/Tyr is an indicator of oxidative and/or nitrosative stress in tissues. The ratio of 3NT/Tyr in the ipsilateral hippocampus was significantly elevated at 72 h, 96 h, and 14 days (means ± SEM of 3NT/Tyr x 1000 = 4.707 ± 0.566, 6.297 ± 0.801 and 4.44 ± 0.428, respectively) postinfection compared to their respective controls (Figure 2.3). Thus, this data demonstrate that acute seizure activity in mice infected with TMEV leads to an increase in protein nitration suggestive of increased production of reactive oxygen and nitrogen species.

No change in oxidative stress indices in the cerebellum of TMEV-infected mice

In order to determine if the alterations in oxidative and nitrosative stress are localized to any regions other than the hippocampus, we measured GSH, GSSG, and 3NT levels in the cerebellum of mice injected with TMEV and PBS at 3 dpi. There were no significant differences between PBS- and TMEV-infected mice in any of the oxidative stress indices measured (Figure 2.4) indicating that the redox changes are specific to the hippocampus and perhaps other limbic areas in this model.

Discussion

This study demonstrates for the first time, that acute seizures resulting from TMEV infection in mice leads to the occurrence of oxidative and nitrosative stress which along with inflammation, might be contributing to the development of epilepsy in this model. We have shown that (1) the glutathione redox status is significantly impaired and (2) 3-nitrotyrosine levels are significantly increased following acute seizures in the TMEV model of infection-induced epilepsy. These results are consistent with previous findings in the lithium-pilocarpine and kainate chemoconvulsant models of TLE and verify that ROS and RNS are elevated as a consequence of acute seizure activity regardless of the initiating injury and point to the fact that oxidation- and nitration-induced posttranslation modifications might play an important role in epileptogenesis and associated pathologies.

The TMEV mouse model of epilepsy was generated by the injection of the Daniel's strain of TMEV into the right cortex of C57BL/6J mice whereby the mice

develop short-term encephalitic seizures within 3 to 7 dpi. Previously published research has demonstrated similar results as well as confirmed the development of chronic, spontaneous seizures starting at around 2 months postinfection by video-EEG recordings (Stewart et al., 2010a). The development of epilepsy was also associated with hippocampal sclerosis and astrogliosis in these animals, hallmarks of mesial TLE (Stewart et al., 2010a). Viral infection-induced models of epilepsy, such as the West Nile (WNV), measles, and herpes simplex viruses (HSV), have been difficult to address experimentally due to a variety of reasons including fatality from acute viral encephalitis, or lack of spontaneous seizures or the persistence of the virus throughout the animal's life. The TMEV-infected mice not only survive the infection and develop spontaneous seizures, but also clear the virus by 14 dpi (Kirkman et al., 2010). Therefore, TMEV-infected C57BL/6J mice present us with a potential model to study the mechanisms underlying the development of acute seizures, epileptogenesis, and consequent epilepsy following a viral infection of the CNS (Stewart et al., 2010a, b). In addition, this model may be useful in identifying novel disease-modifying therapies for the prevention of epilepsy.

One distinguishing feature of the TMEV model is the occurrence of inflammatory changes in the brains of the infected mice which is believed to contribute to the development of acute seizures. Specifically, activation of the innate but not the adaptive immune system in response to the infection was implicated which included substantial increases in TNFα and IL-6 mRNA levels, along with microglial infiltration and astrogliosis (Kirkman et al., 2010). Viral infections of the CNS have also been associated with the production of ROS and oxidative stress. Oxidative damage is an important

component of acute encephalitis caused by HSV-1, HIV, and measles virus. Increased ROS and RNS production can be a direct effect of the virus and a result of the inflammatory response of the host (Valyi-Nagy and Dermody, 2005). Oxidative stress and tissue redox status in turn can stimulate the production of proinflammatory cytokines (Iyer et al., 2009). Here, we show that ROS and RNS are increased acutely, as measured by the tissue GSH redox status and 3NT/Tyr ratios, resulting from seizure activity that arises due to induction of innate immune responses, highlighting the relationship between oxidative stress and inflammation in this model.

GSH is an important antioxidant responsible for scavenging harmful reactive species and maintaining a reduced environment in tissues. GSH depletion occurs in several disease states including TLE and the ratio of GSH/GSSG serves as a very important indicator of the tissue redox status and oxidative stress. GSH depletion has been implicated in aging as well as other acute and chronic neuronal disorders (Liu et al., 2004; Sims et al., 2004). Here, we show that the GSH levels are significantly depleted at 3, 4, and 14 dpi concomitant with increases in GSSG levels rendering the overall tissue redox status more oxidized. This is consistent with our previous findings of ROS production and altered redox state in two different chemoconvulsant models of TLE, the kainate and lithium-pilocarpine models, where status-epilepticus is the initiating cause of redox changes (Liang and Patel, 2006; Ryan et al., 2014; Waldbaum et al., 2010). The decrease in the GSH redox status persisted at 14 dpi which represents the latent phase in this model during which the mice do not have any behavioral seizures. Seizures in TMEV- infected mice reemerge spontaneously 8 weeks postinfection (Stewart et al., 2010b) which indicates that the persistent redox changes occurring in the TMEV mice

could have a potential role in epilepsy development. However, mechanistic studies are needed to definitively conclude whether these changes in oxidative stress are causal to seizure progression. Nevertheless, our results confirm that decreased GSH redox status is a common phenomenon occurring in animal models of TLE despite the type of precipitating injury, indicating that this could be an important mechanism contributing to spontaneous seizures in TLE.

A variety of mechanisms could lead to the decreased GSH/GSSG ratio in this model. First, it has been previously shown that chemoconvulsant-induced status epilepticus leads to an increase in steady-state mitochondrial $O_2\bullet^-$ levels resulting in the production of hydrogen peroxide (H_2O_2) which can diffuse out of the mitochondria into the cellular space and deplete cellular GSH pools (Liang et al., 2000). Second, posttranslational inactivation of the iron-sulfur (Fe-S)-containing TCA cycle enzyme, aconitase, mediated by $O_2\bullet^-$, which can also pose an additional oxidative burden by producing equimolar amounts of H_2O_2 per mole of $O_2\bullet^-$. It is noteworthy here that the production of $O_2\bullet^-$ precedes neuronal death in the kainate model and the latter can be prevented by treatment with a broad-spectrum antioxidant, as well as by overexpressing mitochondrial superoxide dismutase or SOD2 in mice (Liang et al., 2000). Stewart et al., have previously published that TMEV-infected mice have increased neuronal death in the hippocampus at 4–6 dpi (Stewart et al., 2010a). Thus, altered GSH redox state which is observed starting 3 dpi could be a major factor contributing to the brain pathology of TMEV-infected mice and the development of epileptic seizures. Therefore, future studies investigating the ability of antioxidants to prevent cell death in this model is warranted.

Another important finding of this paper is the increase in the levels of 3NT, a

product resulting from nitration of tyrosine residues in proteins by mainly peroxynitrite ($ONOO^-$). $ONOO^-$ is the product of the reaction between $O_2\bullet^-$ and NO, both of which can be generated as a consequence of seizure activity as shown previously in the kainate model (Liang et al., 2000; Ryan et al., 2014). Interestingly, inflammatory cytokines can also lead to the formation of extracellular $O_2\bullet^-$ and NO by activation of the NADPH oxidases (Nox) and inducible nitric oxide synthase (iNOS), respectively (Dikalov, 2011). Furthermore, our previous work has also illustrated activation of Nox2 in the kainate model (Patel et al., 2005). Therefore, in the TMEV-infected mice, 3NT formation could be a consequence of NO production from acute seizures or it could be a direct consequence of the release of proinflammatory molecules. The increase in 3NT levels presents with a unique hypothesis where ROS/RNS-induced posttranslational modifications (PTMs) underlie the damaging subcellular events that promote epileptogenesis. PTMs associated with altered redox status are associated with cysteine (Cys) residues with low pKa or thiol groups in proteins (Giustarini et al., 2004; Jones, 2008). Such modifications can either exert a protection from further oxidation or if the Cys residue is functionally important, PTMs can disrupt the protein's biological function. As an example, Ryan et al., have recently demonstrated that carbonylation of complex I of the electron transport chain (ETC) is increased in the acute and chronic phases of epileptogenesis in the kainate model, which correlated with decreases in complex I activity. Mass spectrometric analysis of this PTM identified the site as Arg76 within the 75 kDa subunit of the complex (Ryan et al., 2012). Moreover, 3NT was shown to accumulate in the hippocampal neurons and not astrocytes in the kainate model implicating RNS as the species contributing to cell death in TLE (Ryan et al., 2014). All

this evidence brings forth the notion that PTMs resulting from seizure-induced ROS or RNS production can mediate neuronal death and the development of spontaneous seizures in the TMEV model. Further investigation into the role of ROS/RNS in the TMEV model can be warranted by determining the effect of an antioxidant on cell death and epileptic seizures in this model.

To summarize, we have demonstrated that acute seizures, arising from inflammation in the TMEV model of infection-induced epilepsy, lead to the production of ROS and RNS. In our studies we have reported a decrease in the GSH redox status as well as an increase in 3NT levels indicative of oxidative and nitrosative damage respectively. These results agree with previous findings illustrating the occurrence of oxidative and nitrosative stress in SE models of TLE, suggesting that these biochemical changes are common phenomena in animal models of TLE, irrespective of the initiating injury. Furthermore, our results point to the role of ROS- and RNS-mediated PTMs as well as highlight the interaction between redox and inflammatory processes in the TMEV model, which could be the mechanisms underlying the pathology observed in this model. Finally, this study underscores the relationship between redox mechanisms and seizure activity in the TMEV model and lays the groundwork for further investigation and development of therapeutic strategies targeting redox processes for the treatment of acquired epilepsies.

Acknowledgements: This work was funded by the Skaggs Scholar Award (KSW and MP), R01 NS065434 (KSW) and R01 NS086423 (MP).

References

Andersen, J.K., 2004. Oxidative stress in neurodegeneration: cause or consequence? Nat. Med. 10, S18-S25 (Suppl.).

Dikalov, S., 2011. Cross talk between mitochondria and NADPH oxidases. Free Radic. Biol. Med. 51, 1289-1301.

Dudek, F.E., Staley, K.J., 2011. The time course of acquired epilepsy: implications for therapeutic intervention to suppress epileptogenesis. Neurosci. Lett. 497, 240-246.

Giustarini, D., Rossi, R., Milzani, A., Colombo, R., Dalle-Donne, I., 2004. S-glutathionylation: from redox regulation of protein functions to human diseases. J. Cell. Mol. Med. 8, 201-212.

Iyer, S.S., Accardi, C.J., Ziegler, T.R., Blanco, R.A., Ritzenthaler, J.D., Rojas, M., Roman, J., Jones, D.P., 2009. Cysteine redox potential determines pro-inflammatory IL-1beta levels. PLoS One 4, e5017.

Jamme, I., Petit, E., Divoux, D., Gerbi, A., Maixent, J.M., Nouvelot, A., 1995. Modulation of mouse cerebral Na+,K(+)-ATPase activity by oxygen free radicals. Neuroreport 7, 333-337.

Jarrett, S.G., Liang, L.P., Hellier, J.L., Staley, K.J., Patel, M., 2008. Mitochondrial DNA damage and impaired base excision repair during epileptogenesis. Neurobiol. Dis. 30, 130-138.

Jones, D.P., 2008. Radical-free biology of oxidative stress. Am. J. Physiol. Cell Physiol. 295, C849-C868.

Kannan, K., Jain, S.K., 2000. Oxidative stress and apoptosis. Pathophysiology 7, 153-163.

Kirkman, N.J., Libbey, J.E., Wilcox, K.S., White, H.S., Fujinami, R.S., 2010. Innate but not adaptive immune responses contribute to behavioral seizures following viral infection. Epilepsia 51, 454-464.

Lakritz, J., Plopper, C.G., Buckpitt, A.R., 1997. Validated high-performance liquid chromatography-electrochemical method for determination of glutathione and glutathione disulfide in small tissue samples. Anal. Biochem. 247, 63-68.

Liang, L.P., Ho, Y.S., Patel, M., 2000. Mitochondrial superoxide production in kainate-induced hippocampal damage. Neuroscience 101, 563-570.

Liang, L.P., Patel, M., 2006. Seizure-induced changes in mitochondrial redox status. Free Radic. Biol. Med. 40, 316-322.

Liao, S.L., Raung, S.L., Chen, C.J., 2002. Japanese encephalitis virus stimulates superoxide dismutase activity in rat glial cultures. Neurosci. Lett. 324, 133-136.

Libbey, J.E., Kirkman, N.J., Smith, M.C., Tanaka, T., Wilcox, K.S., White, H.S., Fujinami, R.S., 2008. Seizures following picornavirus infection. Epilepsia 49, 1066-1074.

Liu, H., Wang, H., Shenvi, S., Hagen, T.M., Liu, R.M., 2004. Glutathione metabolism during aging and in Alzheimer disease. Ann. N. Y. Acad. Sci. 1019, 346-349.

Misra, U.K., Tan, C.T., Kalita, J., 2008. Viral encephalitis and epilepsy. Epilepsia 49 Suppl 6, 13-18.

Patel, M., 2004. Mitochondrial dysfunction and oxidative stress: cause and consequence of epileptic seizures. Free Radic. Biol. Med. 37, 1951-1962.

Patel, M., Li, Q.Y., Chang, L.Y., Crapo, J., Liang, L.P., 2005. Activation of NADPH oxidase and extracellular superoxide production in seizure-induced hippocampal damage. J. Neurochem. 92, 123-131.

Racine, R.J., 1972. Modification of seizure activity by electrical stimulation. II. Motor seizure. Electroencephalogr. Clin. Neurophysiol. 32, 281-294.

Ryan, K., Backos, D.S., Reigan, P., Patel, M., 2012. Posttranslational oxidative modification and inactivation of mitochondrial complex I in epileptogenesis. J. Neurosci. 32, 11250-11258.

Ryan, K., Liang, L.P., Rivard, C., Patel, M., 2014. Temporal and spatial increase of reactive nitrogen species in the kainate model of temporal lobe epilepsy. Neurobiol. Dis. 64, 8-15.

Sawa, T., Akaike, T., Maeda, H., 2000. Tyrosine nitration by peroxynitrite formed from nitric oxide and superoxide generated by xanthine oxidase. J. Biol. Chem. 275, 32467-32474.

Schafer, F.Q., Buettner, G.R., 2001. Redox environment of the cell as viewed through the redox state of the glutathione disulfide/glutathione couple. Free Radic. Biol. Med. 30, 1191-1212.

Schwarz, K.B., 1996. Oxidative stress during viral infection: a review. Free Radic. Biol. Med. 21, 641-649.

Sharma, A.K., Reams, R.Y., Jordan, W.H., Miller, M.A., Thacker, H.L., Snyder, P.W., 2007. Mesial temporal lobe epilepsy: pathogenesis, induced rodent models and lesions. Toxicol. Pathol. 35, 984-999.

Sims, N.R., Nilsson, M., Muyderman, H., 2004. Mitochondrial glutathione: a modulator of brain cell death. J. Bioenerg. Biomembr. 36, 329-333.

Srivastava, R., Kalita, J., Khan, M.Y., Misra, U.K., 2009. Free radical generation by neurons in rat model of Japanese encephalitis. Neurochem. Res. 34, 2141-2146.

Stewart, K.A., Wilcox, K.S., Fujinami, R.S., White, H.S., 2010a. Development of postinfection epilepsy after Theiler's virus infection of C57BL/6 mice. J. Neuropathol. Exp. Neurol. 69, 1210-1219.

Stewart, K.A., Wilcox, K.S., Fujinami, R.S., White, H.S., 2010b. Theiler's virus infection chronically alters seizure susceptibility. Epilepsia 51, 1418-1428.

Theodore, W.H., 2014. Epilepsy and viral infections. Epilepsy Curr. 14, 35-42.

Umpierre, A.D., Remigio, G.J., Dahle, E.J., Bradford, K., Alex, A.B., Smith, M.D., West, P.J., White, H.S., Wilcox, K.S., 2014. Impaired cognitive ability and anxiety-like behavior following acute seizures in the Theiler's virus model of temporal lobe epilepsy. Neurobiol. Dis. 64, 98-106.

Valyi-Nagy, T., Dermody, T.S., 2005. Role of oxidative damage in the pathogenesis of viral infections of the nervous system. Histol. Histopathol. 20, 957-967.

Valyi-Nagy, T., Olson, S.J., Valyi-Nagy, K., Montine, T.J., Dermody, T.S., 2000. Herpes simplex virus type 1 latency in the murine nervous system is associated with oxidative damage to neurons. Virology 278, 309-321.

Waldbaum, S., Liang, L.P., Patel, M., 2010. Persistent impairment of mitochondrial and tissue redox status during lithium-pilocarpine-induced epileptogenesis. J. Neurochem. 115, 1172-1182.

Waldbaum, S., Patel, M., 2010. Mitochondria, oxidative stress, and temporal lobe epilepsy. Epilepsy Res. 88, 23-45.

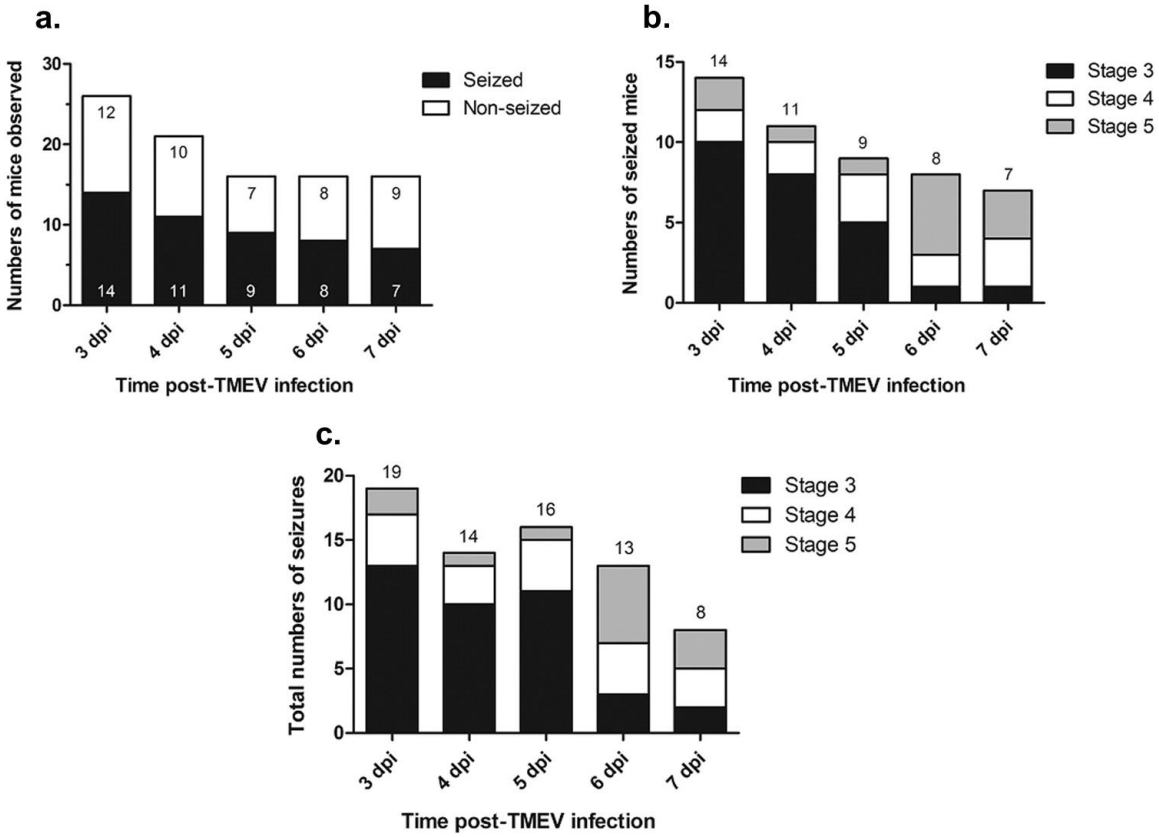

Figure 2.1 Acute behavioral seizures in TMEV-infected mice. Mice infected with TMEV show acute behavioral seizures between 3 and 7 days postinfection. (a) While 81% of the TMEV-infected animals exhibited at least one seizure during the observation period, only approximately 50% of the mice were observed to have behavioral seizures on any given day between 3 and 7 dpi. (b) Distribution of mice which experienced acute seizures following TMEV infection based on the seizure intensity graded according to the Racine scale. For a mouse which had more than one seizure on any given day, the highest scale of seizure intensity was considered for the plot. Decreasing numbers of animals over time reflect the fact that animals were being sacrificed at different time points throughout the study. (c) Consistent with previous studies (Stewart et al., 2010b; Umpierre et al., 2014), the total numbers of seizures based on the Racine scale on each day during seizure monitoring show that seizure intensity increases over the course of observation period. (dpi, days postinjection).

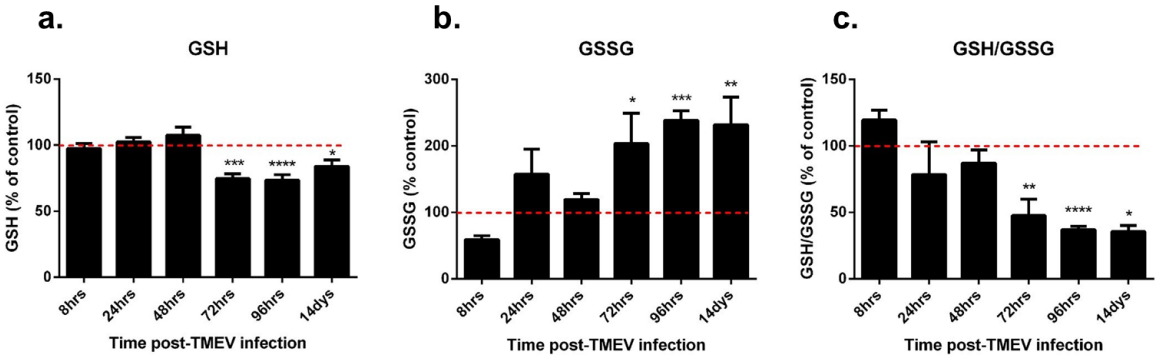

Figure 2.2 Impaired GSH redox status in TMEV-infected mice. Hippocampal GSH redox status is impaired in mice infected with TMEV. Levels of GSH (a), GSSG (b) and the ratio of GSH/GSSG (c) were measured in the mouse ipsilateral hippocampus using HPLC with electrochemical detection. Mice were injected with PBS or TMEV and sacrificed at indicated times (n≥5 mice per group). Values were normalized to percent of control values and presented as values ± SEM. The dotted line indicates 100%. Statistics: *=$p<0.05$, **=$p<0.01$, ***=$p<0.001$ and ****=$p<0.0001$ versus respective PBS controls; two-way ANOVA with Sidak's Multiple Comparison test.

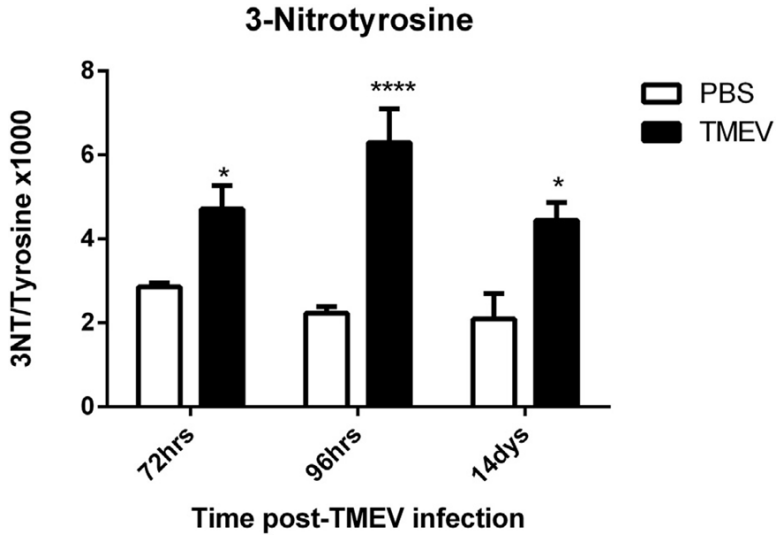

Figure 2.3 Increased levels of 3NT in TMEV-infected mice. Hippocampal 3NT levels were elevated in TMEV-infected mice. Mice were injected with PBS or TMEV and 3NT levels were measured at the indicated times with HPLC-EC (n = 4-5 mice per group). Data are represented as the ratio of 3-nitrotyrosine to tyrosine (3NT/Tyrosine x 1000) as values ± SEM. Statistics: *=$p<0.05$ and ****=$p<0.0001$ versus respective PBS controls; two-way ANOVA with Sidak's Multiple Comparison test.

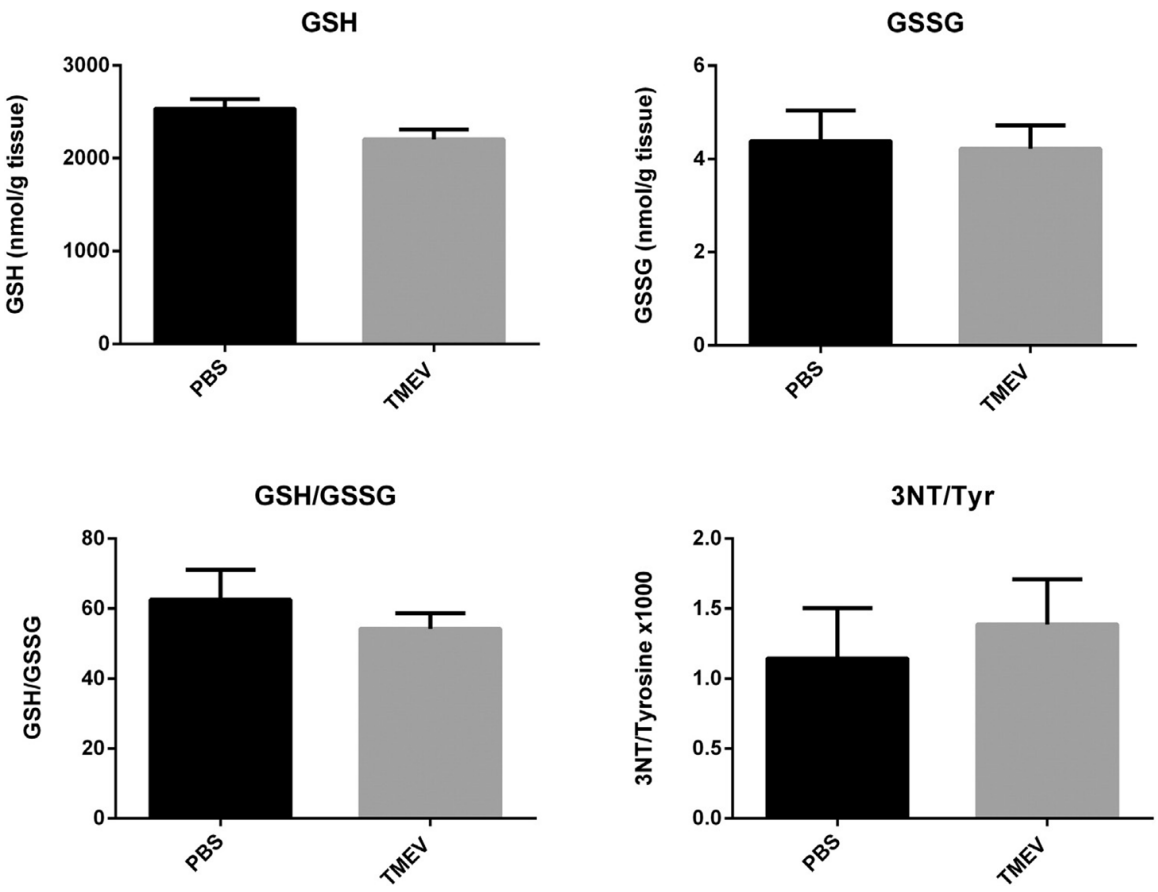

Figure 2.4 No oxidative stress in cerebellum of TMEV mice at 3 dpi. Mice were injected with PBS or TMEV and GSH, GSSG, 3NT and Tyr levels were measured at 3dpi with HPLC-EC (n = 5 mice per group). GSH and GSSG levels are presented as nmols/g tissue and as the ratio of GSH/GSSG. 3NT levels are presented as the ratio of 3NT to tyrosine (3NT/Tyr x 1000). All data is represented as values ± SEM. Statistical analysis used here was an unpaired t test

CHAPTER 3

HIPPOCAMPAL TNFα SIGNALING CONTRIBUTES TO HYPEREXCITABILITY IN AN INFECTION-INDUCED MOUSE MODEL OF LIMBIC EPILEPSY

Introduction

Encephalitis as a consequence of viral infections of the CNS is often associated with the occurrence of acute seizures and a dramatically increased probability of the subsequent development of acquired epilepsy (Vezzani et al., 2016). Indeed, a retrospective epidemiological study found an overall 22-fold increase in the risk for developing epilepsy following viral encephalitis if patients present with acute seizures (Misra et al., 2008). CNS infection can cause intense inflammatory responses and parenchymal damage in the brain contributing to acute seizures which, in turn, can exacerbate inflammatory conditions, ensuring further CNS damage and the development of recurring chronic seizures (Vezzani et al., 2011; Vezzani et al., 2016). Therefore, investigating the role of inflammation as a consequence of CNS infection could provide valuable insight for the development of next generation disease-modifying therapies for the prevention of epilepsy.

Theiler's murine encephalomyelitis virus (TMEV)-infected C57BL/6J mice have

acute seizures between 3 and 8 days postinfection (dpi), exhibit pathological and physiological changes such as astrogliosis, microgliosis, neuronal loss in CA1, and increased excitatory synaptic transmission in CA3 pyramidal neurons in the hippocampus. Importantly, the mice survive the infection, clear the virus from the brain, present with cognitive impairment and anxiety-like symptoms and develop chronic spontaneous seizures after a latent period (Broer et al., 2016; Kirkman et al., 2010; Libbey et al., 2008; Loewen et al., 2016; Smeal et al., 2012; Stewart et al., 2010a; Umpierre et al., 2014). Thus, TMEV-infected mice recapitulate many clinical observations from patients suffering from infection-induced temporal lobe epilepsy (TLE) and offer a unique opportunity to study the molecular mechanism(s) underlying the process of infection-induced epileptogenesis.

TMEV infection results in a dramatic increase in the expression of cytokines, chemokines, oxidative stress markers, and infiltration of macrophages in the first week of infection which may contribute to the initiation and/or propagation of seizures during the acute infection period in this model (Bhuyan et al., 2015; Cusick et al., 2013; Kirkman et al., 2010). The level of tumor necrosis factor-α (TNFα) mRNA in the whole brain of TMEV-infected mice exhibiting acute seizures was increased by 128-fold at 6 dpi compared to control mice (Kirkman et al., 2010). Further, only 10% of TNFα receptor 1 knock-out (TNFR1 KO) mice developed acute behavioral seizures compared to 52% of wild-type (WT) control mice, which implies a significant role of TNFR1-mediated effects of TNFα in seizure development in this model (Kirkman et al., 2010).

TNFα signaling through the TNFR1 pathway has been shown to contribute to the regulation of homeostatic synaptic scaling by modulating the postsynaptic expression of

α-amino-3-hydroxy-5-methyl-4-isoxazolepropionic acid receptors (AMPARs) under both physiological and pathogenic conditions (Beattie et al., 2010). TNFα increases the expression of GluR1-containing and GluR2-lacking AMPARs on the surface of cultured hippocampal neurons and in pyramidal cells in acute rat hippocampal slices (Beattie et al., 2002; Stellwagen et al., 2005; Stellwagen and Malenka, 2006). Whole cell patch-clamp recordings from CA1 pyramidal neurons in acute hippocampal slices pretreated with TNFα show significant increases in average amplitudes of miniature excitatory postsynaptic currents (mEPSCs) (Stellwagen et al., 2005). This suggests that TNFα may contribute to hyperexcitability by augmenting excitatory synaptic strength by increased trafficking of AMPARs subunits to postsynaptic membranes (Stellwagen et al., 2005; Stellwagen and Malenka, 2006). The effects of TNFα on regulating excitatory synaptic strength have also been described in rodent models of spinal injury (Ferguson et al., 2008), pain (Choi et al., 2010), and glaucoma (Cueva Vargas et al., 2015).

The present experiments were performed to evaluate the role of hippocampal TNFα signaling in seizure generation during the acute period following TMEV infection. We found a significant increase in expression of both hippocampal mRNA and protein levels of TNFα following TMEV infection that was coincident with focal seizure activity. In addition, a significant increase in the TNFR1:TNFR2 ratio in hippocampus suggests that signaling through the TNFR1 pathway predominates during the acute infection period. Consistent with increased TNFR1 signaling, increases in hippocampal cell surface AMPA receptor expression was also observed during the acute period. While treatment with XPro1595, a mutant form of human soluble TNFα (sTNFα) that acts as a dominant-negative selective inhibitor of sTNFα, had no effect on seizures during the acute TMEV-

infection period, several lines of transgenic animals deficient in either TNFα or its receptors were found to have robust changes in seizure incidence and severity following TMEV infection. Taken together the present results suggest that increases in TNFα signaling, likely through the TNFR1 pathway, contributes to hyperexcitability and the increased probability of seizures in the hippocampus following TMEV infection. Therefore, this pathway may provide a novel target for antiseizure and disease modifying treatments following CNS infection.

Methods

Animals

C57BL/6J mice (WT (#006460), $TNFR2^{-/-}$ (#002620), $TNFR1^{-/-}TNFR2^{-/-}$ (#003243), and $TNF\alpha^{-/-}$ (#005540)) aged between 4-6 weeks were purchased from Jackson Laboratory. $TNFR2^{-/-}$, $TNFR1^{-/-}TNFR2^{-/-}$, and $TNF\alpha^{-/-}$ mice were bred at our vivarium. All the KO mice were on C57BL/6J background and the deletion of the target protein was confirmed by PCR. All the experiments were carried out in male mice unless otherwise specified. After arrival, mice were allowed to acclimatize for at least 3 days prior to the experiment. Mice were provided food and water *ad libitum* and kept in a facility providing 12 h of light and lark cycle starting at 6:00 AM. All the procedures performed were in accordance with the guidelines provided and approved by the Institutional Animal Care and Use Committee of the University of Utah.

Method of TMEV infection and seizure monitoring

Mice are briefly anesthetized with 3% isoflurane and injected with 20 µl of either phosphate-buffered saline (PBS) or DA-TMEV solution intracortically in the right hemisphere by inserting the needle at a 90° angle to the skull. The injection region is located slightly medial to the equidistant point on the imaginary line connecting the eye and the ear. A sterilized syringe containing a plastic jacket on the needle exposing 2.5 mm of needle is used for infection to restrict the injection site to the somatosensory cortex without damaging the hippocampus. TMEV titer injected per mouse ranged from $2x10^4$ to $3x10^5$ PFU (plaque forming units) depending on the experiment.

Mice were briefly agitated by shaking their cages and monitored for behavioral seizures twice daily in the morning and afternoon separated by a minimum of 2 h until 10 dpi. Seizure intensity was graded using modified Racine scale as follows: stage 1, mouth and facial movements; stage 2, head nodding; stage 3, forelimb clonus; stage 4, forelimb clonus, rearing; and stage 5, forelimb clonus, rearing, and falling; stage 6, intense running, jumping, repeated falling, and severe clonus. Seizure frequency was reported as an average number of seizures during the entire acute seizure period, whereas seizure severity/intensity was represented as an average cumulative seizure burden at each dpi during acute seizure period. Cumulative seizure burden at each dpi for a mouse was calculated by summing all of its seizure scores up to that dpi.

Tissue collection for mRNA and protein analysis

TMEV-infected mice that had acute behavioral seizures were used for all the biochemical studies. TMEV- and PBS-treated mice were sacrificed at 1, 4, 5, and 14 dpi

depending on the experiment. The ipsilateral and contralateral hippocampi were rapidly isolated and collected separately. All the tissue samples were flash frozen using 2-methylbutane chilled on dry ice and stored at -80 ºC until further processing.

Multiplex cytokine array

The protein levels of an array of cytokines were measured in mouse ipsilateral hippocampal lysates using a multiplex kit (V-PLEX™, K15048D) from Mesoscale Discovery according to manufacturer's instructions. Briefly, ipsilateral hippocampi were homogenized in MSD Tris lysis buffer in a 1:10 weight by volume ratio, centrifuged and the supernatant collected. Protein concentration was determined using the Bradford assay and 250 µg of protein was loaded per well to measure cytokines. The levels of analytes were determined by measuring the intensity of emitted light at 620 nm using a Sector Imager 2400.

Gel electrophoresis and western blot

Protein expressions of TNFRs were quantified by western blot analysis. The ipsilateral hippocampi were homogenized in 10 µl of lysis buffer (25 mM Tris-HCl, 150 mM NaCl, 1 mM EDTA, 1% Igepal CA-630, 5% glycerol, protease inhibitors (cocktail tablet, Roche), and 1 mM sodium orthovanadate) per mg of tissue and the supernatant was collected after centrifugation. Total protein concentration was measured by BCA protein assay (Pierce) and 10 µg of total protein was electrophoresed using polyacrylamide gel (4-12% Bis-Tris gel, NuPAGE™, Invitrogen) under denaturing conditions. The proteins were transferred to a PVDF membrane and detected by

chemiluminescence (NEL105001EA, PerkinElmer) using rabbit polyclonal antibodies against TNFR1 (#ab64006, 1:25000, Abcam), TNFR2 (#3727, 1:1000, Cell Signaling Technologies) and actin (#A2103, 1:250000, Sigma) followed by HRP-conjugated secondary antibody (#65-6120, 1:3000, Invitrogen). Densitometric analysis of protein levels was performed using ImageJ software (National Institute of Health, NIH).

Quantitative reverse transcription polymerase chain reaction (RT-qPCR)

Total RNA was isolated from the hippocampi samples by Trizol/chloroform extraction and purified to remove genomic DNA contamination by DNase treatment followed by a spin column-based method (RNeasy Mini Kit, Qiagen) according to manufacturer's instructions. Quality and quantity of RNA were validated by spectrophotometry and acrylamide gel electrophoresis which showed intense discrete ribosomal RNA bands devoid of genomic DNA. cDNA was synthesized from RNA using random primers (SuperScript® VILO Master Mix, Invitrogen) and amplified by qPCR (LightCycler®480, Roche) using 1 μg cDNA with Luminaris Color HiGreen qPCR Master Mix (Thermo Fisher Scientific) and 0.3 μM primers for TNFR1 (Forward (F), 5'-AGAGAAAGTGAGTGCGTCCC-3'; Reverse (R), 5'-AGCCTTCTCCTCTTTGAC-AGG-3'), TNFR2 (F, 5'-AGCTGCAGTTCTTCCTGTACC-3'; R, 5'-GATGCTACA-GATGCGGTGGG-3'), TNFα (F, 5'-CTGAACTTCGGGGTGATCGG-3', R, 5'-GGC-TTGTCACTCGAATTTTGAGA-3', β-actin (F, 5'-AGATCAAGATCATTGCTCC-TCC-3', R, 5'-ACGCAGCTCAGTAACAGTCC-3') and GAPDH (F, 5'-AGCTAC-TCGCGGCTTTACG-3', R, 5'-GGCCAAATCCGTTCACACC-3'). LC480 software

used a second derivative formula to calculate threshold cycle (C_T). Primer efficiency for each analyte was determined using four dilutions of cDNA, and the primer efficiency was used to calculate ΔC_T and $\Delta\Delta C_T$ relative to the reference gene as well as PBS-treated control group. Primer specificity was confirmed by melt curves followed by agarose gel electrophoresis for the expected size product.

Treatment of TMEV-infected mice with XPro1595

TMEV-infected mice were treated with 10 or 100 mg/kg of XPro1595 subcutaneously either every third day or daily. Vehicle contained 150 mM NaCl, 10 mM L-histidine, and 0.01% w/v Tween-20 in deionized water (pH 6.51). For intracerebroventricular (i.c.v.) administration of XPro1595, the guide cannula was surgically implanted into the left lateral ventricle using stereotaxic coordinates of -1.1 mm lateral, -0.5 mm posterior, and -3.0 mm ventral from the bregma as described in detail previously (DeVos and Miller, 2013). Briefly, mice were anesthetized by 10 ml/kg i.p. injection of a mixture of ketamine and xylazine solution in sterile PBS (final concentration: ketamine – 10.4 mg/ml, Xylazine – 1.6 mg/ml) and the skull was exposed in a sterile surgical environment. Guide cannulas (C315GS-5/SP, 3 mm below pedestal, PlasticsOne) were inserted into the left lateral ventricle using a sharp beveled end of the cannula and glued to the skull. A dummy cannula (C315DCS-5/SPC, PlasticsOne) was placed in the guide cannula to prevent the exposure of the ventricle to the outside environment. Mice were allowed to recover from surgery for 12-15 days before initiating the experiment. Mice were immobilized during drug infusion by anesthetizing them using isoflurane (VetEquip® isoflurane vaporizer) and the dummy cannula was removed just

before the drug infusion in a laminar flow hood under aseptic conditions. An internal cannula (C315IS-5/SPC, PlasticsOne) connected to a 10 µl Hamilton® syringe via tubing was inserted into the guide cannula to infuse either XPro1585 or the vehicle solution. An infusion pump (PHD 2000 programmable, Harvard Apparatus) was used to infuse either 5 µl of 40 mg/ml XPro1595 at 1 µl/min (0 and 2 dpi) or 2.5 µl of 80 mg/ml XPro1595 at 0.5 µl/min (4 and 6 dpi). The internal cannula was kept in place for about 1 min after infusion and then slowly removed to avoid leakage. The dummy cannula was secured into the guide cannula immediately.

Cell surface biotinylation assay

Horizontal brain slices (350 µm) from control and TMEV-infected mice with seizures were prepared by vibratome at 5 dpi in ice-cold sucrose solution (concentrations in mM: 200 sucrose, 3 KCl, 26 $NaHCO_3$, 1.4 NaH_2PO_4, 10 glucose, and 3 $MgSO_4$ and 1 $CaCl_2$ added before use; 4°C) and collected in artificial cerebrospinal fluid (aCSF, concentrations in mM: 126 NaCl, 3 KCl, 26 $NaHCO_3$, 1.4 NaH_2PO_4, 10 glucose, and 2 $MgSO_4$ and 2 $CaCl_2$ added before use; pH, 7.33-7.35; osmolality, 297-303 mOsm/kg) at room temperature. Only brain slices ipsilateral to the injection were used for further processing. The slices were incubated in aCSF (31°C) for 45-50 min to recover from the surface damage inflicted during slicing. All the remaining steps were conducted at 4°C. The slices were washed with aCSF to remove dead surface cells and debris and incubated in 1 mg/ml solution of Sulfo-NHS-SS-biotin (Pierce) for 30 min to biotinylate cell surface proteins. The excess biotin solution was washed off using aCSF, quenched by incubating the slices in 100 mM glycine solution, and again washed with aCSF. The

hippocampal regions were dissected out quickly, collected in 250 µl lysis buffer (recipe same as described in western blot procedure), homogenized, centrifuged (14,000 x g, 15 min, 4°C) and the supernatant was collected. All the solutions used for processing brains and brain slices were continuously oxygenated with the mixture of 95% oxygen and 5% carbon dioxide.

Total protein (biotinylated surface proteins and nonbiotinylated intracellular proteins) concentrations in the supernatant were measured by a BCA protein assay (Pierce). To isolate biotinylated surface proteins (SP) from the total proteins (TP), 50 µg of TP was incubated with 25 µl of streptavidin beads (NeutrAvidin™, Thermo scientific) overnight at 4°C on a rotator. The appropriate ratio of beads to TP for each protein of interest was empirically measured by incubating a constant volume of beads with a range of TP in order to isolate the corresponding SP, as described in detail (Gabriel et al., 2014). We chose a ratio of beads to TP of 1:2, which was found to isolate SP in a linear range. The mixture of beads and TP was centrifuged and the beads were washed with lysis buffer. The SP were eluted by incubating the beads in 20 µl of 2X SDS-PAGE reducing sample buffer containing 50 mM DTT in the final mixture (4X SDS-PAGE sample buffer: 106 mM Tris-HCl, 141 mM Tris-base, 0.51 mM EDTA, 2% SDS, 10% glycerol) for 30 min with continuous gentle mixing at room temperature. The supernatant containing SP was collected after centrifugation (17,000 x g, 2 min). The expression of GluA1 and GluA2 subunits of AMPARs were measured in both SP and TP fractions by SDS-PAGE and western blot (anti-GluA1 mAb #MAB2263 and anti-GluA2 mAb #MAB397, Millipore) as described above. The entire volume of supernatant containing SP (isolated from 50 µg of TP) and 10 µg of TP were electrophoresed in the same gel.

Patch-clamp electrophysiology

Mice were sacrificed and their brains were removed between 3-7 dpi, and 350 μM horizontal brain slices were cut in ice-cold sucrose solution and incubated in aCSF solution for 1 h at room temperature. Miniature EPSCs were recorded from the dentate granule cells (DGCs) by whole-cell patch-clamp in aCSF solution containing 1 μM tetrodotoxin as described previously (Smeal et al., 2012). The internal recording solution contained (in mM): 129 potassium gluconate, 6 CsCl, 10 HEPES, 1 EGTA, 0.5 $CaCl_2$, 10 glucose, 2 ATP, 0.5 GTP, 5 QX314, 1 NaCl, and 5 tetraethylammonium chloride. The equilibrium potential for ionotropic glutamate receptors (iGluR $E_{Na+/K+}$) was 4.66 mV at room temperature and mEPSCs were recorded by clamping the cell at -70 mV. Properties of the miniature currents analyzed included amplitude, interevent interval, frequency, rise time and decay time (Smeal et al., 2012).

Statistics

Datasets involving continuous variables are represented by the average and the standard error of the mean (SEM), and the datasets with ordinal variables by frequency distribution. Experimental design involving two groups with one continuous dependent variable was analyzed by unpaired two-tailed t test, whereas design involving more than two groups with two categorical independent variables and one continuous dependent variable was analyzed by two-way ANOVA. Multiple comparisons were performed by Bonferroni posttest. Average cumulative seizure burden, which was calculated from a ranked dataset, was analyzed by Scheirer-Ray-Hare test which is an extension of the Kruskal-Wallis test for two randomized factorial designs (Scheirer et al., 1976). Two

groups with binomial outcome were analyzed by Fisher's exact test. "Survival" (% seizure free) curves and cumulative distributions were analyzed by log-rank test and Kolmogorov-Smirnov test, respectively. Densitometry of immunoblot images and the analysis of mEPSCs were conducted by Image J (NIH) and Mini Analysis Program (Version 6.0.7, Synaptosoft), respectively. Statistical calculations were conducted using GraphPad Prism® 5 and Microsoft Excel.

Results

Increased expression of TNFα and other cytokines in the hippocampus following TMEV infection

Previous studies have demonstrated that TNFα mRNA levels increase dramatically by 128-fold in whole brain homogenates of TMEV-infected mice with acute behavioral seizures at 6 dpi compared to noninfected control mice (Kirkman et al., 2010). TMEV infection results in significant cell loss in the CA1 region, increased c-fos immunoreactivity in the hippocampus following TMEV-induced acute seizures, and increased excitability in the CA3 region of the hippocampus, a brain region often associated with seizure initiation in TLE (Smeal et al., 2012). Therefore, it is important to determine the role of hippocampal TNFα in TMEV-induced seizures. We measured the expression levels of TNFα mRNA and protein in the hippocampus of TMEV-infected mice and PBS-injected control mice. TMEV-infected mice exhibit acute behavioral and electrographic seizures between 3-8 dpi. Therefore, we measured the levels of TNFα at 1, 5, and 14 dpi to compare the levels before, during, and after the acute seizure period. Only handling-induced behavioral seizures were evaluated in these and the following

studies, as the presence of depth electrodes could influence the cytokine response. The mRNA level of TNFα in TMEV-infected mice was not significantly different at 1 dpi compared to control mice (n = 4) (Figure 3.1a). However, it dramatically increased by 161-fold (n = 4, $p<0.001$) at 5 dpi during the peak of the acute seizure activity and it was still 88-fold higher at 14 dpi (n = 4, $p<0.001$) (Figure 3.1a). Similarly, immunoassay studies found no significant increase in the protein expression of TNFα in the hippocampus of TMEV-infected mice compared to control mice at 1 dpi, but TNFα was elevated 206-fold ($p<0.001$) and 35-fold ($p<0.05$) at 5 and 14 dpi, respectively (Figure 3.1b, Table 3.1) (Control: n = 5 (all time points); TMEV: n = 8 (1 dpi), 6 (5 dpi), and 5 (14 dpi)). The absolute average (± SEM) levels of TNFα were measured as follows: 4.89 ± 1.19 pg/ml (control) and 33.80 ± 3.09 pg/ml (TMEV) at 1 dpi; 0.54 ± 0.22 pg/ml (control) and 110.50 ± 7.96 pg/ml (TMEV) at 5 dpi; and 1.41 ± 0.65 pg/ml (control) and 48.92 ± 10.02 pg/ml (TMEV) at 14 dpi. Additionally, protein levels of many other cytokines were also increased in the hippocampus in TMEV-infected mice with seizures at 5 dpi (Table 3.1), notably interferon-γ (IFNγ) which was 21,734-fold elevated compared to control mice. In addition, the antiinflammatory cytokine, interleukin-10 (IL-10), was also increased by 47-fold, which suggests that negative immune feedback also occurs during acute TMEV infection to control excessive inflammation.

Increased protein expression ratio of TNFR1:TNFR2 in hippocampus during acute seizures

The TNFα receptors, TNFR1 and TNFR2, mediate contrasting effects of TNFα in various disease models (Fischer et al., 2015) and differential changes in the protein levels

of TNFR1 and TNFR2 have been shown in the hippocampus in a rat model of limbic epilepsy (Weinberg et al., 2013). Therefore, we measured the expression of TNFR1 and TNFR2 in hippocampus following TMEV infection by western blot. Figure 3.1c shows a representative western blot image for TNFR1, TNFR2, and actin (gel loading control) from TMEV-infected mice at 1, 4, and 14 dpi along with PBS-treated control mice. Optical density (OD) analysis revealed a slight but significant reduction in the expression of TNFR1 in TMEV-infected mice at 4 dpi (OD: 0.97 ± 0.012 vs. 0.83 ± 0.01, n = 5-6, $p<0.05$) and 14 dpi (OD: 0.95 ± 0.03 vs. 0.75 ± 0.064, n = 5-6, $p<0.01$) after normalizing the data with actin levels (Figure 3.1d). However, the expression of TNFR2 protein levels were dramatically reduced at 4 dpi (OD: 0.90 ± 0.029 vs. 0.51 ± 0.038, n = 5-6, $p<0.001$) and 14 dpi (OD: 0.99 ± 0.049 vs. 0.42 ± 0.087, n = 5-6, $p<0.001$) (Figure 3.1d). The ratio of TNFR1:TNFR2, indicating the relative expressions of both TNFRs in the hippocampus during the acute infection period, was significantly elevated (1.08 ± 0.033 vs. 1.67 ± 0139, $p<0.05$) at 4 dpi and was further increased at 14 dpi (0.97 ± 0.057 vs. 2.04 ± 0.255, $p<0.001$) (Figure 3.1d) which suggests that TNFα may mediate its downstream effects predominantly through TNFR1 in the hippocampus during the acute TMEV infection period.

We also measured the mRNA levels of both TNFRs using qPCR. In contrast to TNFα, we found opposite changes in the levels of both TNFR1 and TNFR2 for mRNA and protein expression. The expression of TNFR1 mRNA was significantly elevated by 2.59, 5.5, and 4.65-fold at 1, 5, and 14 dpi, respectively, (n = 4); whereas the protein levels were slightly reduced (Figure 3.1e). Similarly, mRNA expression of TNFR2 was increased by 12.94- and 16.8-fold at 5 and 14 dpi (n = 4); whereas the protein levels were

reduced by 0.57- and 0.42-fold at 4 and 14 dpi (Figure 3.1f). These changes result in a progressive decrease in the relative mRNA expression ratios of TNFR1:TNFR2 and an increase in the relative protein expression ratios of TNFR1:TNFR2 in the hippocampus during acute TMEV infection (Figure 3.1g). This suggests that TNFR expression undergoes posttranslational regulation.

Lack of seizure control following peripheral administration of XPro1595 on TMEV-induced acute seizures

There is a significant increase in whole brain and hippocampal TNFα mRNA, an increase in protein expression of TNFα, and an increase in the ratio of TNFR1:TNFR2 expression in the hippocampus as a consequence of TMEV infection. In addition, prior work has demonstrated that seizure incidence is dramatically reduced in TNFR1$^{-/-}$ mice (Kirkman et al., 2010). Therefore, we hypothesized that pharmacological inhibition of TNFR1 could decrease the incidence and/or severity of TMEV-induced acute seizures. TNFα is expressed as a homotrimeric transmembrane protein (tmTNFα) and the extracellular portion of tmTNFα can be cleaved by TNFα converting enzyme (TACE) to form a soluble TNFα (sTNFα). Both tmTNFα and sTNFα are active in their trimeric composition and mediate a variety of cellular activities via TNFRs (McCoy and Tansey, 2008). sTNFα predominantly mediates its effects via TNFR1, while TNFR2 is fully activated only by tmTNFα (Grell et al., 1995; Grell et al., 1998). While anti-TNFα antibodies are approved for the treatment of peripheral inflammatory conditions, they do not cross blood brain barrier (BBB) (Tracey et al., 2008). Therefore, we selected the investigational BBB-permeant compound, XPro1595, to test the hypothesis that TNFα

signaling through TNFR1 contributes to seizure generation. XPro1595 is a mutant form of human sTNFα and acts as a dominant-negative selective inhibitor of sTNFα (Steed et al., 2003). It dose-dependently exchanges with endogenous monomers of sTNFα to form an inactive heterotrimer which does not bind to TNFRs and lacks intrinsic bioactivity (Steed et al., 2003). Since sTNFα predominantly mediates its effects via TNFR1, XPro1595 indirectly inhibits TNFR1 functions. XPro1595 has been shown to provide beneficial effects in animal models of several peripheral as well as CNS inflammatory conditions including experimental autoimmune encephalomyelitis (EAE), Parkinson's disease, spinal cord injury, and focal cerebral ischemia by selectively inhibiting sTNFα-TNFR1 signaling and sparing beneficial functions of TNFR2 (Brambilla et al., 2011; Clausen et al., 2014; McCoy et al., 2006; Novrup et al., 2014; Zalevsky et al., 2007). Since the dosing regimen of 10 mg/kg of subcutaneous (s.c.) XPro1595 administered every third day was effective in models of other CNS diseases (Barnum et al., 2014; Brambilla et al., 2011; Clausen et al., 2014), we tested whether peripheral treatment of TMEV-infected mice with XPro1595 could prevent the development of handling-induced acute seizures. Handling sessions were captured by video monitoring and experimenters scoring seizures were blinded to the treatment groups as described in the methods. Administration of 10 mg/kg of XPro1595 (s.c.) at 1, 4, and 7 dpi did not decrease average number of seizures (Vehicle: 5.27 ± 0.37, XPro1595: 5.63 ± 0.45, n = 30, p=0.5313) or have any effect on average cumulative seizure burden at any time point during the acute seizure period when compared to vehicle-treated mice. To determine if the lack of efficacy on seizure incidence and severity was due to an inappropriate dosing regimen, we increased the dosing frequency of XPro1595 (10 mg/kg) to every day, starting from 2

h postinfection through 9 dpi. This dosing regime was also ineffective in decreasing either seizure frequency (Vehicle: 5.13 ± 0.71, XPro1595: 5.13 ± 0.77, n = 15, p=1.00) or severity. Finally, we increased the dose to 100 mg/kg and started treatment 2 days prior to infection through 7 dpi. Despite a 10-fold increase in the dose and initiating the treatment before infection, both XPro1595 and vehicle-treated groups had similar average numbers of seizures (Vehicle: 6.63 ± 1.24, XPro1595: 6.25 ± 0.77, n = 8, p=0.801) and average cumulative seizure burdens during the acute seizure period. Thus, systemic administration of high doses of XPro1595 was not effective in controlling seizures induced by TMEV infection.

Lack of seizure control following CNS administration of XPro1595 on TMEV-induced acute seizures

Despite numerous studies demonstrating central activity of XPro1595 in animal models of neurological disorders, a recent study found that systemic injection of XPro1595 was insufficient to provide therapeutic efficacy in a mouse model of spinal cord injury (SCI), whereas central administration of XPro1595 provided neuroprotection and ameliorated motor dysfunction in this model (Novrup et al., 2014). The concentration of XPro1595 in the CSF (1-6 ng/ml) has been found to be 1000-fold reduced compared to that in the plasma (1-8 μg/ml) from rats after 2-3 days of treatment with XPro1595 (10 mg/kg, s.c.) (Barnum et al., 2014). Furthermore, as in the model of SCI, where acute inflammatory response occurs rapidly in the CNS, the protein levels of TNFα and other inflammatory cytokines increase rapidly in the hippocampus after TMEV infection. Thus, we hypothesized that XPro1595 did not achieve a sufficient concentration in the brain to

prevent signaling through the TNFR1 system following subcutaneous treatment in TMEV-infected mice Therefore, we tested the effectiveness of CNS administration of XPro1595 by free-hand bolus injection of 5 µl of XPro1595, equivalent to about 10 mg/kg of mouse, at 2 dpi into the left lateral ventricle. Surprisingly, the average number of seizures was significantly reduced by treatment with XPro1595 (Vehicle: 5.6 ± 0.40, XPro1595: 3.1 ± 0.77, n = 10, p=0.0097), as well as average cumulative seizure burden at each day during 6-8 dpi (Figure 3.2a). However, the results could not be replicated when we repeated the free-hand i.c.v bolus experiment (average number of seizures, Vehicle: 5.2 ± 0.63, XPro1595: 5.3 ± 0.79, n = 10, p=0.9222) (Figure 3.2b). Single bolus administration of XPro1595 might not have been sufficient to suppress endogenous TNFα during the entire acute seizure activity period. Therefore, mice were implanted with guide cannulas into the left lateral ventricle for multiple drug infusion in the CNS. Infusions of XPro1595 (10 mg/kg starting at 5-6 h after infection) or vehicle were repeated every other day for a total 4 infusions. As was observed following systemic injections, central administration of XPro1595 had no effect on either average number of seizures (Vehicle: 4.18 ± 1.32, XPro1595: 2.75 ± 1.02, n = 11-12, p=0.3952) or average cumulative seizure burden at any day during 3-8 dpi (Figure 3.2c, 3.2d) compared to TMEV-treated mice receiving vehicle infusions. The placement of the guide cannula into the ventricle was confirmed in all the mice enrolled for this study by infusing 0.1% Evan's blue dye at 9 dpi (Figure 3.2e). Therefore, regardless of administration route, dosing regimen, or dose, XPro1595 was ineffective in preventing seizures following TMEV infections.

Differential susceptibility of TNFRs KO mice to develop TMEV-induced acute seizures

Previous work has demonstrated that only 10% of TNFR1$^{-/-}$ mice (n = 2/20) infected with 2x10^4 PFU of TMEV developed acute behavioral seizures, suggesting that TNFR1-mediated effects could be involved in seizure generation in this model (Kirkman et al., 2010). As XPro1595 did not block acute seizures, we used transgenic animals to further test the hypothesis that TNFα signaling contributes to hyperexcitability following infection. Seizure incidence and severity in TNFα$^{-/-}$, TNFR2$^{-/-}$, and TNFR1$^{-/-}$TNFR2$^{-/-}$ mice during the acute infection period was therefore evaluated (Figure 3.3). All the mice were infected with 2x10^4 PFU of TMEV to compare the data with the published findings in TNFR1$^{-/-}$ mice. Although the numbers of infected mice that developed acute behavioral seizures were similar for WT and TNFα$^{-/-}$ (67% seized mice, n = 18), seizure frequency and severity, as measured by average number of seizures and average cumulative seizure burden, were significantly reduced in TNFα$^{-/-}$ mice (Figure 3.3a). Interestingly, TNFR2$^{-/-}$ mice experienced severe seizures compared to WT as evidenced by an increase in the average (± SEM) number of seizures (WT: 2.8 ± 0.42, TNF2$^{-/-}$: 4.6 ± 0.43, p=0.0042, n = 27 (WT), n = 30 (TNFR2$^{-/-}$)) and an average cumulative seizure burden at 7 and 8 dpi (Figure 3.3b). The latency to develop the first seizure was also significantly reduced in TNFR2$^{-/-}$, as 11 of 30 TNFR2$^{-/-}$ mice experienced seizures at 3 dpi compared to just 1 of 27 WT mice. In addition, the overall percentage of seizure free-mice for TNFR2$^{-/-}$ and WT mice over the entire acute seizure period was significantly different (p=0.0046) (Figure 3.3c). Since previous work demonstrated that TNFR1$^{-/-}$ mice were less susceptible to developing acute seizures (Kirkman et al., 2010) and TNFR2$^{-/-}$

developed severe TMEV-induced seizures, we reasoned that TNFR1$^{-/-}$TNFR2$^{-/-}$ mice might have seizure patterns similar to WT mice. However, TNFR1$^{-/-}$TNFR2$^{-/-}$ exhibited a significantly reduced average number of seizures (WT: 3.1 ± 0.50, TNFR1$^{-/-}$TNF2$^{-/-}$: 1.0 ± 0.34, p=0.001, n = 28 (WT), n = 30 (TNFR1$^{-/-}$TNFR2$^{-/-}$)) as well as average cumulative seizure burden at 6, 7, and 8 dpi (Figure 3.3d) compared to WT mice. The percentages of total numbers of infected mice that developed acute behavioral seizures in TNFR1$^{-/-}$, TNFR1$^{-/-}$TNFR2$^{-/-}$, TNFα$^{-/-}$, WT, and TNFR2$^{-/-}$ were 10% (n = 2/20) (Kirkman et al., 2010), 33% (n = 10/30), 67% (n = 12/18), 73% (n = 40/55), and 93% (n = 28/30), respectively (Figure 3.3e). Both male and female mice had similar seizure responses in all the strains tested, and thus, the data from both genders are pooled. In contrast to the lack of seizure control observed with XPro1595 treatment, results in the transgenic mouse strains suggest that TNFα signaling through the TNFR1 pathway could indeed be a prominent mechanism through which hyperexcitability and seizure activity occur following TMEV infection. In addition, TNFα signaling through the TNFR2 pathway, as is the case in other neurological disorders, may be involved in dampening excitability, since mice lacking TNFR2 have a higher incidence and greater severity of seizures.

Increase in the surface levels of AMPAR subunits during acute seizures in WT B6 mice

AMPARs are the primary glutamate receptors that mediate fast excitatory neurotransmission in the brain (Traynelis et al., 2010). TNFα has been shown to increase AMPAR trafficking into postsynaptic neuronal membranes via neuronal TNFR1 (Beattie et al., 2002; Stellwagen et al., 2005). In addition, we have previously demonstrated that

the amplitudes of mEPSCs are increased during the acute infection period in CA3 pyramidal neurons, suggesting an increase in AMPA receptor surface expression (Smeal et al., 2012). Given the hypothesized role of TNFα in AMPAR trafficking and the observed increase in mEPSC amplitudes following TMEV infection, we evaluated hippocampal AMPA receptor expression using a cell surface biotinylation assay in mice treated with TMEV. Biotinylated surface proteins were separated from nonbiotinylated intracellular proteins using avidin beads in tissue prepared from acute hippocampal slices obtained from TMEV- and PBS-treated mice at 5 dpi as described here (Gabriel et al., 2014). The GluA1 and GluA2 subunits of AMPARs were probed in the surface protein (SP) as well as in the total protein (TP) fractions by western blot (Figure 3.4a). The ratios of surface/total levels of GluA1 that indicate the relative levels of GluA1 present on the cell surface were significantly elevated in the TMEV-infected mice with seizures compared to control (OD: 0.31 ± 0.011 vs. 0.45 ± 0.018, $p<0.0001$, n = 6). We also probed for phosphate-activated glutaminase (PAG), a mitochondrial protein, to control for the biotinylation of intracellular proteins. The levels of PAG in the SP fraction were less than 5% compared to those in the TP fraction (OD: 0.015 ± 0.0026 in PBS, 0.03 ± 0.0015 in TMEV) indicating that the biotinylation was largely restricted to cell surface proteins. The surface/total ratio for the levels of GluA2 was also significantly increased in TMEV-infected mice compared to control (OD: 0.53 ± 0.018 vs. 0.7 ± 0.025, $p=0.0007$, n = 6) (Figure 3.4b). The cell surface levels of GluA1 and GluA2 subunits were increased by 48% ($p<0.0001$) and 33% ($p=0.0002$), respectively, in TMEV-infected mice compared to PBS-injected mice (Figure 3.4c). The total protein levels of GluA1 and GluA2 in the TMEV-infected mice were significantly reduced by 46% and 55%,

respectively, compared to control mice (Figure 3.4d). Since TMEV-infected mice have a pronounced neuronal loss in the CA1 region, it is not surprising that the total protein levels of GluA1 and GluA2 are decreased in TMEV-infected mice.

Since TNFR2$^{-/-}$ mice had severe acute seizures compared to WT mice, we also conducted cell surface biotinylation assay in TNFR2$^{-/-}$ mice to test if TNFR2$^{-/-}$ mice had higher cell surface levels of GluA1 and GluA2 at 5 dpi. Similar to TMEV-infected WT C57BL/6J mice, the ratios of surface/total levels of GluA1 and GluA2 were significantly elevated in the TMEV-infected TNFR2$^{-/-}$ mice with seizures compared to PBS-injected TNFR2$^{-/-}$ mice (For GluA1, OD: 0.28 ± 0.012 vs. 0.40 ± 0.021, p=0.0011, n = 6; and for GluA2, OD: 0.45 ± 0.016 vs. 0.61 ± 0.036, p=0.0049, n = 6) (Figure 3.5a, 3.5b). The cell surface levels of GluA1 and GluA2 subunits were increased by 44% (p=0.0011) and 34% (p=0.0049), respectively, in the TMEV group compared to control mice (Figure 3.5c). The total protein levels of GluA1 and GluA2 in the TMEV-infected TNFR2$^{-/-}$ mice were significantly reduced by 42% and 48%, respectively, compared to control mice (Figure 3.5d), likely due to the widespread neurodegeneration observed in CA1 of the hippocampus.

mEPSCs recorded in DGCs are not affected by TMEV infection

TMEV exhibits a strong tropism for limbic brain regions and viral particles can be detected in CA1 and CA2 regions of hippocampus in the first week of infection (Buenz et al., 2009; Kirkman et al., 2010; Stewart et al., 2010b). Abundant c-Fos immunoreactivity, an indirect marker for neuronal activation, was found in the CA3 region and the dentate gyrus (DG) of hippocampus within 2 h after TMEV-induced acute seizures (Smeal et al.,

2012). Since the CA1 region is severely damaged by TMEV within 4-5 days of infection, initial studies investigating hyperexcitability in the hippocampus were focused on the CA3 region. Patch-clamp studies in acute brain slices found an increase in the amplitude and frequency of spontaneous and miniature EPSCs in CA3 pyramidal neurons during the period of 3-7 days post-TMEV infection (Smeal et al., 2012). The DG is another key region of the hippocampus that is frequently involved in seizure generation in limbic epilepsy models (Sloviter et al., 2012). Further, TNFα and TNFRs regulate homeostatic synaptic plasticity by enhancing excitatory synaptic strength in the DGCs in response to denervation-induced injury (Becker et al., 2015; Becker et al., 2013). Given our finding that there is an increased ratio of cell surface to total AMPA receptors in the biotinylation studies, we performed whole cell patch clamp recordings in DGCs to determine if there was an increase, as observed in CA3, in excitatory synaptic transmission during the acute infection period when seizures are observed. Miniature EPSCs in DGCs in hippocampal brain slices were obtained the during acute seizure period. Representative traces of mEPSCs from control and TMEV-infected mice are shown in Figure 3.6a. A total of 11 DGCs from 8 mice in the control group and 15 DGCs from 10 TMEV-infected mice with acute seizures were included in the analysis. The cumulative fraction analysis of mEPSC amplitude as well as interevent interval found no significant differences between treatment groups ($p>0.05$, KS test) (Figure 3.6b, 3.6c). The average (± SEM) mEPSC amplitudes were 14.3 ± 0.66 pA and 14.9 ± 0.59 pA in the control and TMEV mice, respectively ($p=0.5$), and the average (± SEM) frequencies were 2.30 ± 0.36 Hz and 2.35 ± 0.23 Hz for the control and TMEV mice, respectively ($p=0.9$). These data suggest that, unlike CA3 pyramidal neurons, DGCs do not have an increase in excitatory synaptic

transmission during the acute infection period.

Discussion

The present series of experiments evaluated the role of TNFα signaling in the hippocampus, a brain region involved in seizure generation, following TMEV infection. TNFα and its effects mediated via the activation of TNFR1, and/or reduced signaling through TNFR2, could be one of the major inflammatory pathways contributing to acute seizures. We demonstrate here, for the first time, that there is a substantial increase in the protein level of TNFα that is coincident with an increase in the protein expression ratios of TNFR1:TNFR2 in the hippocampus. The role of TNFα in contributing to seizure generation following TMEV infection was also supported by our findings in a number of transgenic mice. We found that there is a decrease in the seizure incidence, frequency, and severity of acute seizures in $TNFR1^{-/-}$ and $TNFR1^{-/-}TNFR2^{-/-}$ mice, whereas there is an increase in frequency and severity of acute seizures in $TNFR2^{-/-}$ mice. In addition, consistent with the hypothesized role of TNFα in hippocampal AMPA receptor trafficking, we demonstrated that there is a significant increase in the cell surface to total AMPA receptor ratio in TMEV transfected mice. This increase in cell surface expression likely underlies the increased amplitudes of mEPSCs that we have previously observed in recordings obtained in CA3 pyramidal cells in brain slices obtained from TMEV-infected mice (Smeal et al., 2012). While peripheral as well as central administration of XPro1595, an inhibitor of sTNFα, failed to inhibit TMEV-induced acute seizures, the data acquired here from WT and transgenic animals suggests that signaling through the TNFα system may play an important role in seizure generation during the acute infection

period and may serve as an important therapeutic target in conditions in which inflammation contributes to seizure generation.

TNFα signaling contributes to the regulation of homeostatic synaptic plasticity by modulating the postsynaptic surface levels of AMPARs under physiological conditions (Beattie et al., 2010). TNFα has been shown to induce synaptic scaling via neuronal TNFR1 by increasing the cell surface expression of GluA1-containing and GluA2-lacking AMPARs in cultured hippocampal neurons (Beattie et al., 2002; Stellwagen et al., 2005; Stellwagen and Malenka, 2006), in the rat hippocampal slice preparation (Stellwagen et al., 2005; Stellwagen and Malenka, 2006), in an animal model of SCI (Ferguson et al., 2008), and also in the dorsal spinal cord neurons in an intraplantar carrageenan model of inflammatory pain (Choi et al., 2010). Elevated levels of AMPARs in postsynaptic membranes can increase the strength of excitatory synaptic transmission. Furthermore, GluA2-lacking AMPARs are Ca^{2+}-permeable and increased intracellular concentration of Ca^{2+} can result into excitotoxicity (Liu and Zukin, 2007). We report that the levels of GluA1 and GluA2 subunits of AMPARs on the cell surface are elevated in the hippocampus of mice with acute seizures compared to noninfected mice. Differences in the trafficking of GluA2 subunits between SCI, pain models, and the present study may reflect the differences in underlying pathological, anatomical, and experimental conditions. Indeed, TNFα has been shown to exert varying effects on the regulation of excitatory synaptic strength contingent upon factors such as brain region. TNFα drives the internalization of GluA1 and GluA2 subunits of AMPARs in the medium spiny neurons in striatum, which is in contrast to its effects in hippocampal neurons (Lewitus et al., 2014). The data acquired here suggests that the increased cell surface expression of

AMPAR subunits most likely occurs in CA3 pyramidal neurons because 1) AMPA receptors are expressed in principal cells of the hippocampus (Osten et al., 2006), 2) CA1 pyramidal neurons start to degenerate by 3 dpi and exhibit extensive loss by 4 dpi (Loewen et al., 2016), 3) significant increases in amplitude and frequency of mEPSCs recorded from CA3 pyramidal neurons in TMEV-infected mice with seizures between 3-7 dpi (Smeal et al., 2012), and 4) no change in mEPSCs in DGCs in TMEV-infected mice with seizures between 3-7 dpi. AMPARs are also present in glial cells although with much less density than in neurons (Traynelis et al., 2010), and hippocampal interneurons express mainly GluA1 and GluA4, but lack GluA2 (Osten et al., 2006); therefore, we do not rule out the possibility of some postsynaptic AMPAR dynamics in these cells. A novel approach for real-time *in vivo* monitoring of AMPAR subunits has recently been described (Zhang et al., 2015), which could be utilized to address the question of spatial and cellular subunit targeting in the hippocampus where AMPAR trafficking occurs during TMEV-induced seizures.

TNFR1$^{-/-}$ and TNFR1$^{-/-}$TNFR2$^{-/-}$ mice were found to be highly resistant to developing TMEV-induced acute seizures, and those with seizures had much less severe seizures compared to WT mice. In addition, although the percentage of TMEV-infected TNFα$^{-/-}$ mice developing acute seizures was similar to WT mice, frequency and severity were significantly reduced in TNFα$^{-/-}$ mice. Taken together with the AMPAR trafficking findings, we conclude that TNFα is likely implicated in synaptic scaling via TNFR1 resulting in hippocampal hyperexcitability and seizures. However, additional studies that utilize pharmacological approaches to modulate the level of TNFα and the functions of TNFRs in the brain will be necessary to determine the mechanism through which

increased levels of TNFα impact excitatory strength and seizure generation.

Inhibition of sTNFα-TNFR1-mediated effects and sparing tmTNFα-TNFR2-mediated effects of TNFα has been a well-rationalized strategy to treat many peripheral and CNS inflammatory conditions which also minimizes adverse effects associated with absolute inhibition of TNFα (Fischer et al., 2015). In previous studies, the concentration of XPro1595 in CSF and plasma were found to be 1-6 ng/ml and 1-8 μg/ml, respectively, following subcutaneous treatment of rats with 10 mg/kg XPro1595 (Barnum et al., 2014). A 10-fold higher level of XPro1595, such as used in the present experiments, should therefore exchange 99% of endogenous sTNFα (Steed et al., 2003). In the present studies, the average concentration of TNFα in the hippocampus was 110.5 pg/ml at 5 days post-TMEV infection in mice with acute seizures. Thus, if the CSF concentration of XPro1595 in rats after 10 mg/kg s.c. dosing could be extrapolated to TMEV-infected mice, 10 mg/kg s.c. dosing should have been sufficient to remove the endogenously active form of sTNF. The present finding that XPro1595 treatment was unable to influence TMEV-induced seizures could be due to an insufficient concentration of XPro1595 in the hippocampus. This could also have been the limitation in a recent study where only CNS, but not peripheral, administration of XPro1595 had beneficial effects in the mouse model of SCI (Novrup et al., 2014). However, multiple i.c.v. infusion of XPro1595 also failed to reduce TMEV-induced seizures in the present study. Further data on the pharmacokinetics of XPro1595 in TMEV-infected mice could facilitate a better design of dosing regimen for treatment with this compound. However, even if XPro1595 sufficiently removed endogenous sTNFα, TNFR1 may still be activated by tmTNFα. Although sTNFα is a major ligand for TNFR1, tmTNFα has been shown to induce

inflammation and cytotoxicity through TNFR1 (Horiuchi et al., 2010). For example, a recent study using XPro1595 to prevent peripheral inflammation in a model of gout determined that the inflammatory response observed in that model was independent of sTNFα and was likely due to tmTNFα (Amaral et al., 2016). Thus, XPro1595 was unable to prevent the inflammation observed in that model. In addition, lymphotoxin (LTα3), formerly known as TNFβ, is structurally similar to sTNFα and binds to both TNFRs (Tracey et al., 2008). LTα3-TNFR1 signaling can cause inflammation similar to sTNFα-TNFR1 effects which could partly explain the lack of effects of XPro1595 on TMEV-induced seizures. Several TNFR1-specific inhibitors are under development (Fischer et al., 2015), which should be leveraged in the future to test the hypothesis of a pathogenic role of TNFR1-mediated signaling in TMEV-induced seizures. Finally, it has been found in previous studies that IL-6 signaling can also contribute to seizure generation during the TMEV acute infection period (Kirkman et al., 2010; Libbey et al., 2011). Animals deficient in IL-6, or treated with wogonin to reduce infiltrating macrophages, which are the major source of IL-6 (Cusick et al., 2013), also have a decrease in acute seizure activity in this model (Kirkman et al., 2010). Therefore a polytherapy approach involving both TNF and IL-6 modulators may prove the most efficacious in preventing seizure activity following TMEV infection.

In addition to increasing AMPAR trafficking to the synaptic membrane, TNFα has been proposed to increase excitation by modulating the functions of astrocytes. Pathogenic levels of TNFα in hippocampus may induce the release of glutamate from astrocytes into the synapse where glutamate can bind to presynaptic NMDA receptors to further increase the synaptic release of glutamate (Habbas et al., 2015; Santello et al.,

2011). TNFα has also been shown to decrease expression of the astrocyte glutamate transporter (GLT1) (Carmen et al., 2009). Recently, TNFα has been demonstrated to downregulate connexin-43 and GLT1 on spinal astrocytes, causing increased glutamatergic neurotransmission and neuropathic pain in mice (Morioka et al., 2015). Astrogliosis occurs throughout the hippocampus within 3 days of TMEV infection and persists up to 4-6 months postinfection (Loewen et al., 2016; Stewart et al., 2010a). It is a matter of future interest to determine if increased levels of TNFα affect the expression of glutamate transporters and gap junction proteins on astrocytes to tip the balance of synaptic function in favor of hyperexcitatory conditions.

Our results that TNFα contributes to neuronal hyperexcitability in the hippocampus through TNFR1-mediated signaling, whereas TNFR2-mediated signaling imparts antiictogenic effects, are not specific to the TMEV model. Similar diametric roles of TNFRs in modulating seizure activity have been reported in kainic acid and kindling models of limbic seizures (Weinberg et al., 2013). Our results also corroborate clinical findings in which the levels of TNFR1 and TNFR1-signaling proteins are increased in the resected hippocampal tissues from patients with refractory TLE (Yamamoto et al., 2006). Although animal studies that investigate the role of the TNFα system in various models of limbic seizures suggest that TNFR1-mediated signaling contributes to ictogenic effects, the consequences of pathogenic levels of TNFα on seizures are highly context-dependent. For example, overexpression of murine TNFα in astrocytes decreased kainate-induced seizures (Balosso et al., 2005), whereas overexpression of murine TNFα in neurons either caused seizures (Probert et al., 1995) or had no effects on kainate-induced seizure activity (Weinberg et al., 2013). Multiple factors in the CNS including the source

and the type of TNFα, the cell types expressing TNFRs, levels of TNFα and relative density of TNFRs in the tissue can influence the seizure outcome (Probert, 2015). These factors must be investigated in detail by designing animal studies that reflect clinical findings from the patients with TLE.

In conclusion, we have demonstrated that pathogenic level of TNFα and an increase in the expression ratio of TNFR1:TNFR2 in the hippocampus are associated with acute behavioral as well as focal hippocampal electrographic seizures in TMEV-infected mice. TNFα might cause hyperexcitation in TMEV-infected mice by strengthening excitatory synapses via a TNFR1-mediated mechanism, whereas TNFR2 may provide antiictogenic effects during acute infection. Inflammation occurs in other models of epilepsy and many patients with epilepsy present with CNS inflammatory conditions. Antiinflammatory therapies could be useful as stand-alone therapy or in combination with antiseizure medications. Anti-TNFα antibodies are widely prescribed for peripheral inflammatory conditions, however, they also cause serious adverse effects by inhibiting desirable functions of TNFα (Traynelis et al., 2010). Therefore, TNFR1-specific inhibitors and/or TNFR2-specific agonists might be a better strategy for reducing seizures.

References

Amaral, F.A., Bastos, L.F., Oliveira, T.H., Dias, A.C., Oliveira, V.L., Tavares, L.D., Costa, V.V., Galvao, I., Soriani, F.M., Szymkowski, D.E., Ryffel, B., Souza, D.G., Teixeira, M.M., 2016. Transmembrane TNF-alpha is sufficient for articular inflammation and hypernociception in a mouse model of gout. Eur. J. Immunol. 46, 204-211.

Balosso, S., Ravizza, T., Perego, C., Peschon, J., Campbell, I.L., De Simoni, M.G., Vezzani, A., 2005. Tumor necrosis factor-alpha inhibits seizures in mice via p75

receptors. Ann. Neurol. 57, 804-812.

Barnum, C.J., Chen, X., Chung, J., Chang, J., Williams, M., Grigoryan, N., Tesi, R.J., Tansey, M.G., 2014. Peripheral administration of the selective inhibitor of soluble tumor necrosis factor (TNF) XPro(R)1595 attenuates nigral cell loss and glial activation in 6-OHDA hemiparkinsonian rats. J. Parkinsons Dis. 4, 349-360.

Beattie, E.C., Stellwagen, D., Morishita, W., Bresnahan, J.C., Ha, B.K., Von Zastrow, M., Beattie, M.S., Malenka, R.C., 2002. Control of synaptic strength by glial TNFalpha. Science 295, 2282-2285.

Beattie, M.S., Ferguson, A.R., Bresnahan, J.C., 2010. AMPA-receptor trafficking and injury-induced cell death. Eur. J. Neurosci. 32, 290-297.

Becker, D., Deller, T., Vlachos, A., 2015. Tumor necrosis factor (TNF)-receptor 1 and 2 mediate homeostatic synaptic plasticity of denervated mouse dentate granule cells. Sci. Rep. 5, 12726.

Becker, D., Zahn, N., Deller, T., Vlachos, A., 2013. Tumor necrosis factor alpha maintains denervation-induced homeostatic synaptic plasticity of mouse dentate granule cells. Front. Cell. Neurosci. 7, 257.

Bhuyan, P., Patel, D.C., Wilcox, K.S., Patel, M., 2015. Oxidative stress in murine Theiler's virus-induced temporal lobe epilepsy. Exp. Neurol. 271, 329-334.

Brambilla, R., Ashbaugh, J.J., Magliozzi, R., Dellarole, A., Karmally, S., Szymkowski, D.E., Bethea, J.R., 2011. Inhibition of soluble tumour necrosis factor is therapeutic in experimental autoimmune encephalomyelitis and promotes axon preservation and remyelination. Brain 134, 2736-2754.

Broer, S., Kaufer, C., Haist, V., Li, L., Gerhauser, I., Anjum, M., Bankstahl, M., Baumgartner, W., Loscher, W., 2016. Brain inflammation, neurodegeneration and seizure development following picornavirus infection markedly differ among virus and mouse strains and substrains. Exp. Neurol. 279, 57-74.

Buenz, E.J., Sauer, B.M., Lafrance-Corey, R.G., Deb, C., Denic, A., German, C.L., Howe, C.L., 2009. Apoptosis of hippocampal pyramidal neurons is virus independent in a mouse model of acute neurovirulent picornavirus infection. Am. J. Pathol. 175, 668-684.

Carmen, J., Rothstein, J.D., Kerr, D.A., 2009. Tumor necrosis factor-alpha modulates glutamate transport in the CNS and is a critical determinant of outcome from viral encephalomyelitis. Brain Res. 1263, 143-154.

Choi, J.I., Svensson, C.I., Koehrn, F.J., Bhuskute, A., Sorkin, L.S., 2010. Peripheral inflammation induces tumor necrosis factor dependent AMPA receptor trafficking

and Akt phosphorylation in spinal cord in addition to pain behavior. Pain 149, 243-253.

Clausen, B.H., Degn, M., Martin, N.A., Couch, Y., Karimi, L., Ormhoj, M., Mortensen, M.L., Gredal, H.B., Gardiner, C., Sargent, II, Szymkowski, D.E., Petit, G.H., Deierborg, T., Finsen, B., Anthony, D.C., Lambertsen, K.L., 2014. Systemically administered anti-TNF therapy ameliorates functional outcomes after focal cerebral ischemia. J. Neuroinflammation 11, 203.

Cueva Vargas, J.L., Osswald, I.K., Unsain, N., Aurousseau, M.R., Barker, P.A., Bowie, D., Di Polo, A., 2015. Soluble Tumor Necrosis Factor Alpha Promotes Retinal Ganglion Cell Death in Glaucoma via Calcium-Permeable AMPA Receptor Activation. J. Neurosci. 35, 12088-12102.

Cusick, M.F., Libbey, J.E., Patel, D.C., Doty, D.J., Fujinami, R.S., 2013. Infiltrating macrophages are key to the development of seizures following virus infection. J. Virol. 87, 1849-1860.

DeVos, S.L., Miller, T.M., 2013. Direct intraventricular delivery of drugs to the rodent central nervous system. J Vis Exp, e50326.

Ferguson, A.R., Christensen, R.N., Gensel, J.C., Miller, B.A., Sun, F., Beattie, E.C., Bresnahan, J.C., Beattie, M.S., 2008. Cell death after spinal cord injury is exacerbated by rapid TNF alpha-induced trafficking of GluR2-lacking AMPARs to the plasma membrane. J. Neurosci. 28, 11391-11400.

Fischer, R., Kontermann, R., Maier, O., 2015. Targeting sTNF/TNFR1 Signaling as a New Therapeutic Strategy. Antibodies 4, 48.

Gabriel, L.R., Wu, S., Melikian, H.E., 2014. Brain slice biotinylation: an ex vivo approach to measure region-specific plasma membrane protein trafficking in adult neurons. J Vis Exp.

Grell, M., Douni, E., Wajant, H., Lohden, M., Clauss, M., Maxeiner, B., Georgopoulos, S., Lesslauer, W., Kollias, G., Pfizenmaier, K., Scheurich, P., 1995. The transmembrane form of tumor necrosis factor is the prime activating ligand of the 80 kDa tumor necrosis factor receptor. Cell 83, 793-802.

Grell, M., Wajant, H., Zimmermann, G., Scheurich, P., 1998. The type 1 receptor (CD120a) is the high-affinity receptor for soluble tumor necrosis factor. Proc. Natl. Acad. Sci. U. S. A. 95, 570-575.

Habbas, S., Santello, M., Becker, D., Stubbe, H., Zappia, G., Liaudet, N., Klaus, F.R., Kollias, G., Fontana, A., Pryce, C.R., Suter, T., Volterra, A., 2015. Neuroinflammatory TNFalpha Impairs Memory via Astrocyte Signaling. Cell 163, 1730-1741.

Horiuchi, T., Mitoma, H., Harashima, S., Tsukamoto, H., Shimoda, T., 2010. Transmembrane TNF-alpha: structure, function and interaction with anti-TNF agents. Rheumatology (Oxford) 49, 1215-1228.

Kirkman, N.J., Libbey, J.E., Wilcox, K.S., White, H.S., Fujinami, R.S., 2010. Innate but not adaptive immune responses contribute to behavioral seizures following viral infection. Epilepsia 51, 454-464.

Lewitus, G.M., Pribiag, H., Duseja, R., St-Hilaire, M., Stellwagen, D., 2014. An adaptive role of TNFalpha in the regulation of striatal synapses. J. Neurosci. 34, 6146-6155.

Libbey, J.E., Kennett, N.J., Wilcox, K.S., White, H.S., Fujinami, R.S., 2011. Interleukin-6, produced by resident cells of the central nervous system and infiltrating cells, contributes to the development of seizures following viral infection. J. Virol. 85, 6913-6922.

Libbey, J.E., Kirkman, N.J., Smith, M.C., Tanaka, T., Wilcox, K.S., White, H.S., Fujinami, R.S., 2008. Seizures following picornavirus infection. Epilepsia 49, 1066-1074.

Liu, S.J., Zukin, R.S., 2007. Ca2+-permeable AMPA receptors in synaptic plasticity and neuronal death. Trends Neurosci. 30, 126-134.

Loewen, J.L., Barker-Haliski, M.L., Dahle, E.J., White, H.S., Wilcox, K.S., 2016. Neuronal injury, gliosis, and glial proliferation in two models of temporal lobe epilepsy. J. Neuropathol. Exp. Neurol. 75, 366-378.

McCoy, M.K., Martinez, T.N., Ruhn, K.A., Szymkowski, D.E., Smith, C.G., Botterman, B.R., Tansey, K.E., Tansey, M.G., 2006. Blocking soluble tumor necrosis factor signaling with dominant-negative tumor necrosis factor inhibitor attenuates loss of dopaminergic neurons in models of Parkinson's disease. J. Neurosci. 26, 9365-9375.

McCoy, M.K., Tansey, M.G., 2008. TNF signaling inhibition in the CNS: implications for normal brain function and neurodegenerative disease. J. Neuroinflammation 5, 45.

Misra, U.K., Tan, C.T., Kalita, J., 2008. Viral encephalitis and epilepsy. Epilepsia 49 Suppl 6, 13-18.

Morioka, N., Zhang, F.F., Nakamura, Y., Kitamura, T., Hisaoka-Nakashima, K., Nakata, Y., 2015. Tumor necrosis factor-mediated downregulation of spinal astrocytic connexin43 leads to increased glutamatergic neurotransmission and neuropathic pain in mice. Brain. Behav. Immun. 49, 293-310.

Novrup, H.G., Bracchi-Ricard, V., Ellman, D.G., Ricard, J., Jain, A., Runko, E., Lyck, L., Yli-Karjanmaa, M., Szymkowski, D.E., Pearse, D.D., Lambertsen, K.L., Bethea, J.R., 2014. Central but not systemic administration of XPro1595 is therapeutic following moderate spinal cord injury in mice. J. Neuroinflammation 11, 159.

Osten, P., Wisden, W., Sprengel, R., 2006. Molecular mechanisms of synaptic function in the hippocampus: neurotransmitter exocytosis and glutamatergic, GABAergic, and cholinergic transmission, in: Andersen, P., Morris, R., Amaral, D., Bliss, T., O'Keefe, J. (Eds.), Hippocampus Book. Oxford University Press, USA, Cary, US.

Probert, L., 2015. TNF and its receptors in the CNS: The essential, the desirable and the deleterious effects. Neuroscience 302, 2-22.

Probert, L., Akassoglou, K., Pasparakis, M., Kontogeorgos, G., Kollias, G., 1995. Spontaneous inflammatory demyelinating disease in transgenic mice showing central nervous system-specific expression of tumor necrosis factor alpha. Proc. Natl. Acad. Sci. U. S. A. 92, 11294-11298.

Santello, M., Bezzi, P., Volterra, A., 2011. TNFalpha controls glutamatergic gliotransmission in the hippocampal dentate gyrus. Neuron 69, 988-1001.

Scheirer, C.J., Ray, W.S., Hare, N., 1976. The analysis of ranked data derived from completely randomized factorial designs. Biometrics 32, 429-434.

Sloviter, R.S., Bumanglag, A.V., Schwarcz, R., Frotscher, M., 2012. Abnormal dentate gyrus network circuitry in temporal lobe epilepsy, in: Noebels, J.L., Avoli, M., Rogawski, M.A., Olsen, R.W., Delgado-Escueta, A.V. (Eds.), Jasper's Basic Mechanisms of the Epilepsies, 4th ed, Bethesda (MD).

Smeal, R.M., Stewart, K.A., Iacob, E., Fujinami, R.S., White, H.S., Wilcox, K.S., 2012. The activity within the CA3 excitatory network during Theiler's virus encephalitis is distinct from that observed during chronic epilepsy. J. Neurovirol. 18, 30-44.

Steed, P.M., Tansey, M.G., Zalevsky, J., Zhukovsky, E.A., Desjarlais, J.R., Szymkowski, D.E., Abbott, C., Carmichael, D., Chan, C., Cherry, L., Cheung, P., Chirino, A.J., Chung, H.H., Doberstein, S.K., Eivazi, A., Filikov, A.V., Gao, S.X., Hubert, R.S., Hwang, M., Hyun, L., Kashi, S., Kim, A., Kim, E., Kung, J., Martinez, S.P., Muchhal, U.S., Nguyen, D.H., O'Brien, C., O'Keefe, D., Singer, K., Vafa, O., Vielmetter, J., Yoder, S.C., Dahiyat, B.I., 2003. Inactivation of TNF signaling by rationally designed dominant-negative TNF variants. Science 301, 1895-1898.

Stellwagen, D., Beattie, E.C., Seo, J.Y., Malenka, R.C., 2005. Differential regulation of AMPA receptor and GABA receptor trafficking by tumor necrosis factor-alpha. J. Neurosci. 25, 3219-3228.

Stellwagen, D., Malenka, R.C., 2006. Synaptic scaling mediated by glial TNF-alpha.

Nature 440, 1054-1059.

Stewart, K.A., Wilcox, K.S., Fujinami, R.S., White, H.S., 2010a. Development of postinfection epilepsy after Theiler's virus infection of C57BL/6 mice. J. Neuropathol. Exp. Neurol. 69, 1210-1219.

Stewart, K.A., Wilcox, K.S., Fujinami, R.S., White, H.S., 2010b. Theiler's virus infection chronically alters seizure susceptibility. Epilepsia 51, 1418-1428.

Tracey, D., Klareskog, L., Sasso, E.H., Salfeld, J.G., Tak, P.P., 2008. Tumor necrosis factor antagonist mechanisms of action: a comprehensive review. Pharmacol. Ther. 117, 244-279.

Traynelis, S.F., Wollmuth, L.P., McBain, C.J., Menniti, F.S., Vance, K.M., Ogden, K.K., Hansen, K.B., Yuan, H., Myers, S.J., Dingledine, R., 2010. Glutamate receptor ion channels: structure, regulation, and function. Pharmacol. Rev. 62, 405-496.

Umpierre, A.D., Remigio, G.J., Dahle, E.J., Bradford, K., Alex, A.B., Smith, M.D., West, P.J., White, H.S., Wilcox, K.S., 2014. Impaired cognitive ability and anxiety-like behavior following acute seizures in the Theiler's virus model of temporal lobe epilepsy. Neurobiol. Dis. 64, 98-106.

Vezzani, A., French, J., Bartfai, T., Baram, T.Z., 2011. The role of inflammation in epilepsy. Nat. Rev. Neurol. 7, 31-40.

Vezzani, A., Fujinami, R.S., White, H.S., Preux, P.M., Blumcke, I., Sander, J.W., Loscher, W., 2016. Infections, inflammation and epilepsy. Acta Neuropathol. 131, 211-234.

Weinberg, M.S., Blake, B.L., McCown, T.J., 2013. Opposing actions of hippocampus TNFalpha receptors on limbic seizure susceptibility. Exp. Neurol. 247, 429-437.

Yamamoto, A., Schindler, C.K., Murphy, B.M., Bellver-Estelles, C., So, N.K., Taki, W., Meller, R., Simon, R.P., Henshall, D.C., 2006. Evidence of tumor necrosis factor receptor 1 signaling in human temporal lobe epilepsy. Exp. Neurol. 202, 410-420.

Zalevsky, J., Secher, T., Ezhevsky, S.A., Janot, L., Steed, P.M., O'Brien, C., Eivazi, A., Kung, J., Nguyen, D.H., Doberstein, S.K., Erard, F., Ryffel, B., Szymkowski, D.E., 2007. Dominant-negative inhibitors of soluble TNF attenuate experimental arthritis without suppressing innate immunity to infection. J. Immunol. 179, 1872-1883.

Zhang, Y., Cudmore, R.H., Lin, D.T., Linden, D.J., Huganir, R.L., 2015. Visualization of NMDA receptor-dependent AMPA receptor synaptic plasticity in vivo. Nat. Neurosci. 18, 402-407.

Figure 3.1 Increase in the levels of TNFα and in a ratio of the protein expression of TNFR1:TNFR2 in the hippocampus of TMEV-infected mice during acute seizure activity period. (a) mRNA levels of TNFα, as measured by RT-qPCR, are significantly increased in TMEV-infected mice at 5 and 14 days postinfection (dpi) by 161- and 88-fold, respectively, compared to PBS-infected control mice (n = 4 for TMEV and control). (b) 206- and 35-fold increase in the protein expression levels of TNFα in TMEV-infected mice at 5 and 14 dpi compared to the PBS-injected control mice (Control: n = 5; TMEV: n = 8 (1 dpi), 6 (5 dpi), and 5 (14 dpi)). (c) Representative immunoblot shows the protein expression of TNFR1, TNFR2, and actin in the hippocampus from PBS- and TMEV-infected mice (n = 3). (d) Densitometric analysis of the immunoblots shows the expressions of TNFR1 and TNFR2 normalized to the expression levels of actin (Control: n = 5; TMEV: n = 5 (1 dpi), 6 (4 and 14 dpi); O.D., Optical density). The relative expression levels of TNFR1 and TNFR2 (TNFR1:TNFR2) are significantly increased by 1.54- and 2.1-fold at 4 and 14 dpi, respectively, in the TMEV-infected mice compared to control mice. (e-g) Comparison of mRNA and protein levels of TNFR1 and TNFR2 in the hippocampus of TMEV-infected mice before (1 dpi), during (5 dpi), and after (14 dpi) acute seizures. The ratio of TNFR1 to TNFR2 for mRNA is significantly reduced during the acute infection period (g, upper panel), whereas the ratio for the protein expression is significantly increased over the acute infection period (g, lower panel). The data are shown as mean ± SEM. Statistics: Two-way ANOVA followed by Bonferroni posttest; *$p<0.05$, **$p<0.01$, and ***$p<0.001$.

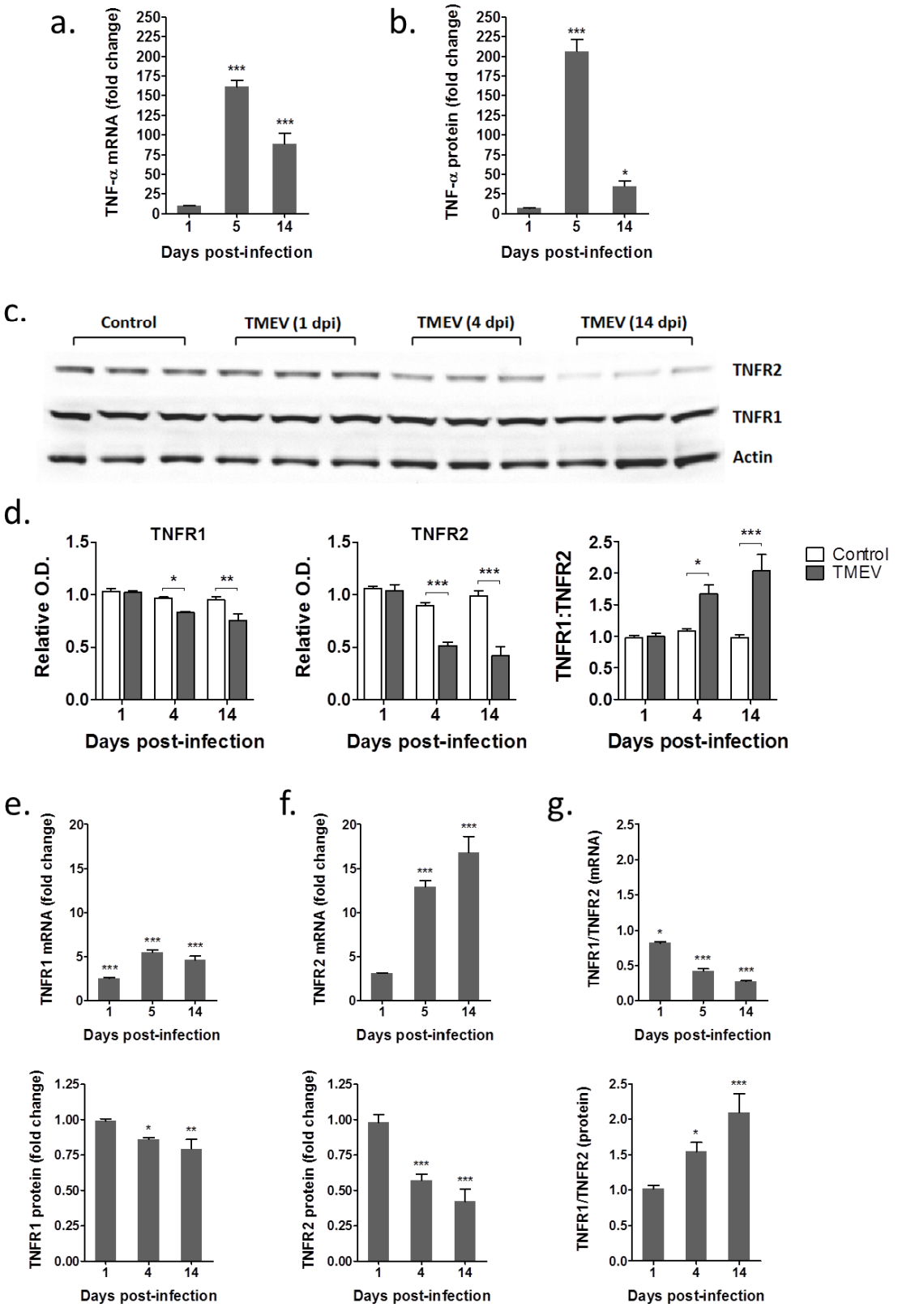
a.
TNF-α mRNA (fold change)
Days post-infection
b.
TNF-α protein (fold change)
Days post-infection
c.
Control
TMEV (1 dpi)
TMEV (4 dpi)
TMEV (14 dpi)
TNFR2
TNFR1
Actin
d.
TNFR1
TNFR2
Relative O.D.
TNFR1:TNFR2
Control
TMEV
Days post-infection
e.
TNFR1 mRNA (fold change)
TNFR1 protein (fold change)
f.
TNFR2 mRNA (fold change)
TNFR2 protein (fold change)
g.
TNFR1/TNFR2 (mRNA)
TNFR1/TNFR2 (protein)

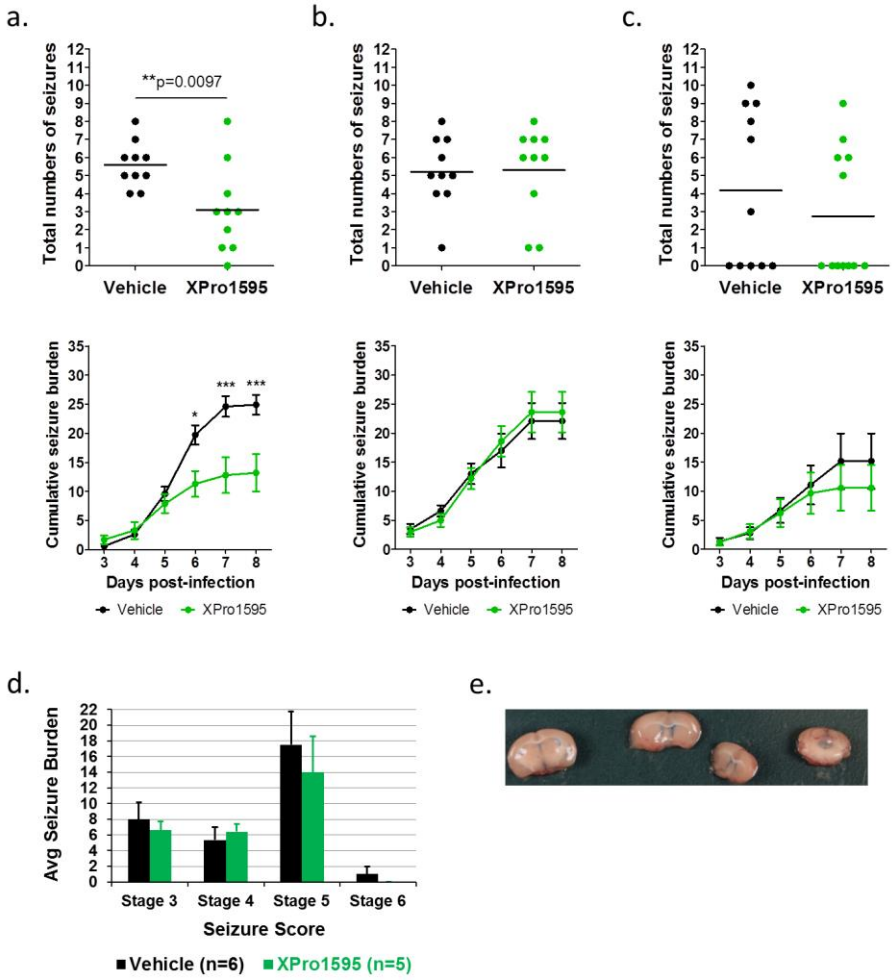

Figure 3.2 CNS administration of XPro1595 does not affect TMEV-induced acute seizure frequency and intensity. (a) Single i.c.v. bolus administration of XPro1595 (10 mg/kg) at 2 dpi in TMEV-infected mice (n = 10) significantly reduces an average number of generalized tonic-clonic seizures and an average cumulative seizure burden starting from 6 dpi compared to vehicle-treated TMEV-infected mice. (b) The repetition of single i.c.v. bolus administration study does not replicate the findings shown in (a). (c) Slow infusion of XPro1595 (10 mg/kg) at 0, 2, 4, and 6 dpi into the left lateral ventricle using a surgically implanted guide cannula does not reduce average seizure frequency and severity (n = 12, XPro1595; n = 11, vehicle). Each circle represents an individual mouse and the horizontal line shows average number of seizures per group. (d) Average seizure burden corresponding to each stage of modified Racine scale for generalized tonic-clonic seizures shows no difference between vehicle- and XPro1595-treated TMEV-infected mice. Only those mice which had acute seizures are included in this analysis. (e) The surgical placement of the guide cannula into the left lateral ventricle was confirmed by i.c.v. infusion of 0.1% Evans blue dye at 9 dpi in all TMEV-infected mice treated with either XPro1595 or vehicle. The panel shows an example of a diffusion of the dye into the ventricular system.

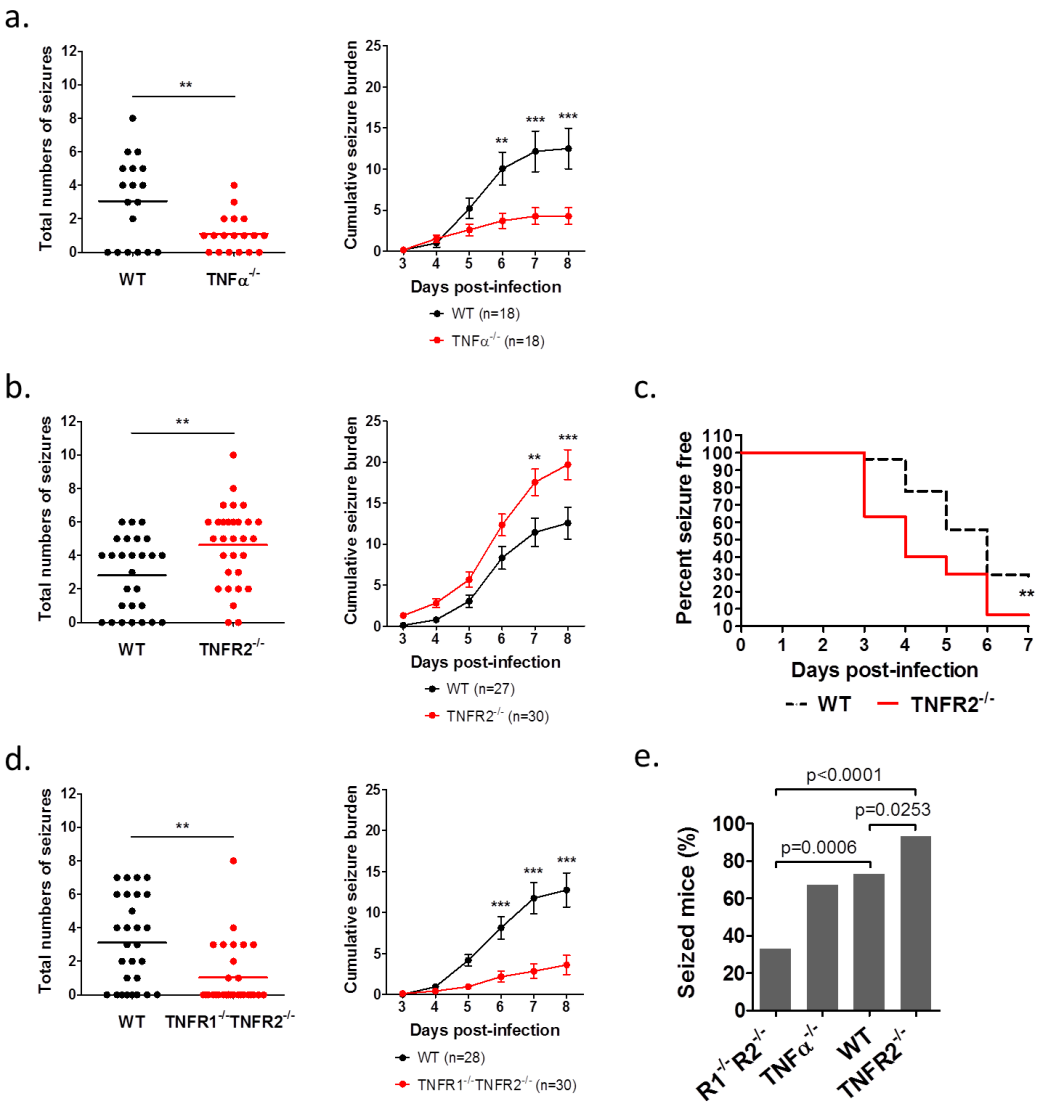

Figure 3.3 TMEV-induced acute behavioral seizure susceptibility in WT, TNFα$^{-/-}$, TNFR2$^{-/-}$, and TNFR1$^{-/-}$TNFR2$^{-/-}$ mice. (a) TNFα$^{-/-}$ mice have a significant reduction in the seizure frequency (upper panel), plotted as a total number of seizures per mouse, and in the seizure severity (lower panel) as measured by an average cumulative seizure burden during acute seizure period (3-8 dpi) compared to WT mice. Each circle represents individual mouse and the horizontal line shows an average number of seizures per group. (b) TNFR2$^{-/-}$ mice show an increase in the average seizure frequency as well as severity. (c) Reduced latency to develop a first TMEV-induced acute seizure in TNFR2$^{-/-}$ mice compared to WT mice. (d) Reduced average seizure frequency and severity in TNFR1$^{-/-}$TNFR2$^{-/-}$ mice. (e) Percentage of total infected mice that show acute behavioral seizures during 3-8 dpi. Statistics: unpaired t test (frequency), Scheirer-Ray-Hare test (severity), Fisher's exact test (% seized mice); and long-rank test (% seizure free); **p<0.01, ***p<0.001.

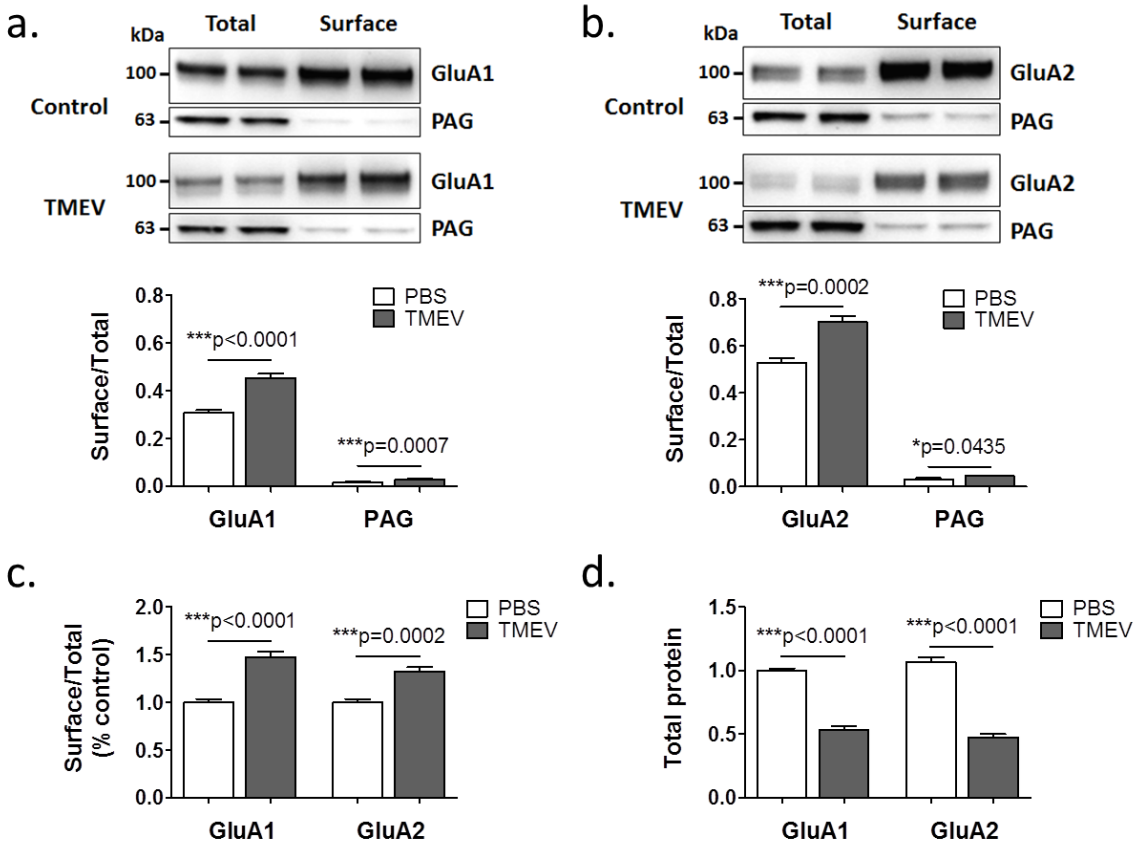

Figure 3.4 Increase in the cell surface levels of GluA1 and GluA2 subunits of AMPARs in TMEV-infected WT C57BL/6J mice during acute seizures. (a) Representative immunoblots from two mice show the levels of GluA1 in the total as well as the cell surface fractions of proteins isolated from ipsilateral hippocampus at 5 days postinjection of either PBS (control) or TMEV. Data in the first (total) and the third (surface) lanes from the left are from the same mouse, and the second (total) and the fourth (surface) lanes correspond to the other mouse. The surface proteins were isolated from the intracellular proteins by cell surface biotinylation procedure in acute hippocampal slices. The levels of GluA1 were quantified by densitometry and the data are shown as a ratio of surface to total protein which is significantly increased in TMEV-infected mice (n = 6). Phosphate-activated glutaminase (PAG) is a mitochondrial protein and serves as an intracellular control protein. (b) Similar to GluA1, the ratio of surface/total level for GluA2 is also increased in TMEV-infected mice (n = 6). (c) The ratios of surface/total protein expression for GluA1 and GluA2 are increased by 48% and 33%, respectively (data normalized to control). (d) About 50% decrease in the total expressions of GluA1 and GluA2 in TMEV-infected mice compared to the control group. Statistics: Unpaired two-tailed t test.

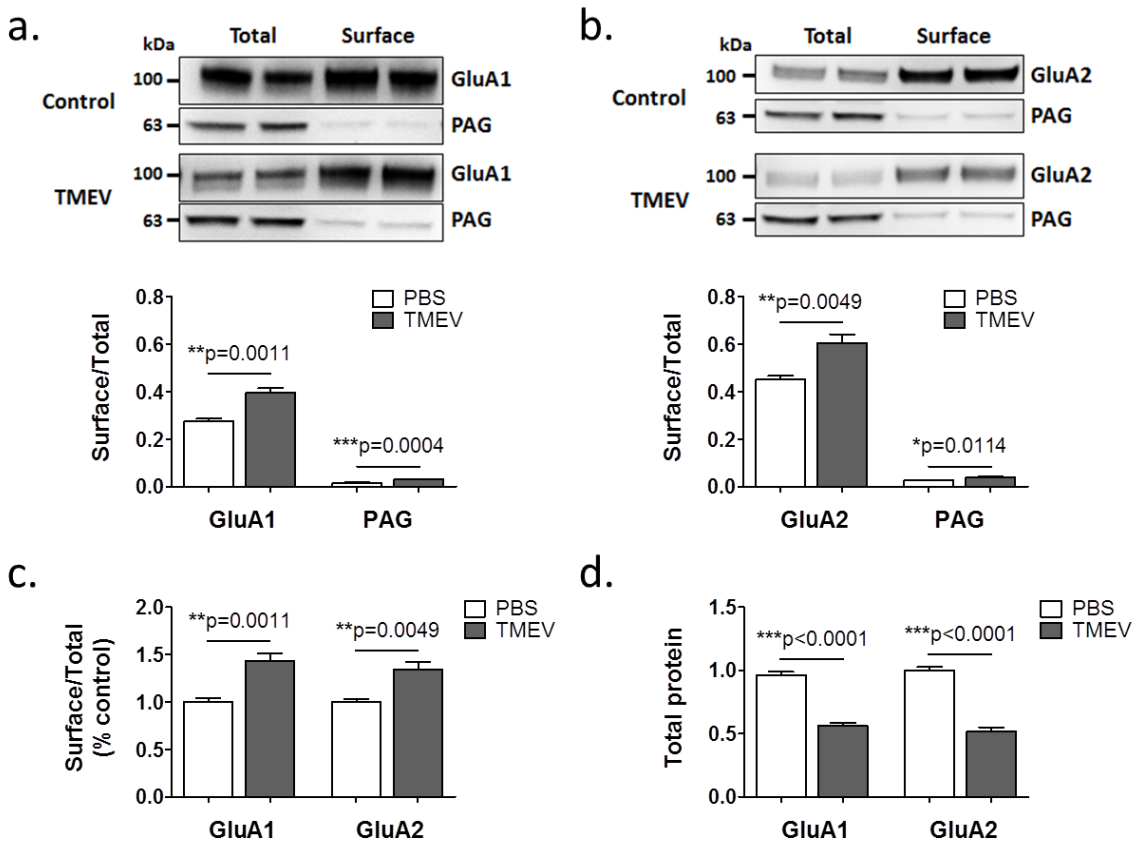

Figure 3.5 Increase in the cell surface levels of GluA1 and GluA2 subunits of AMPARs in TMEV-infected TNFR2$^{-/-}$ mice during acute seizures. (a) Representative immunoblots from two mice show the levels of GluA1 in the total as well as the cell surface fractions of proteins isolated from ipsilateral hippocampus at 5 days postinjection of either PBS (control) or TMEV. The surface proteins were isolated by cell surface biotinylation procedure in acute hippocampal slices. The levels of GluA1 were quantified by densitometry and the data are shown as a ratio of surface to total protein that is significantly increased in TMEV-infected mice (n = 6). Phosphate-activated glutaminase (PAG) is a mitochondrial protein and serves as an intracellular control protein. (b) Similar to GluA1, the ratio of surface/total level for GluA2 is also increased in TMEV-infected mice (n = 6). (c) The ratios of surface/total protein expression for GluA1 and GluA2 are increased by 44% and 34%, respectively (data normalized to control). (d) About 50% decrease in the total expressions of GluA1 and GluA2 in TMEV-infected mice compared to the control group. Statistics: Unpaired two-tailed t test.

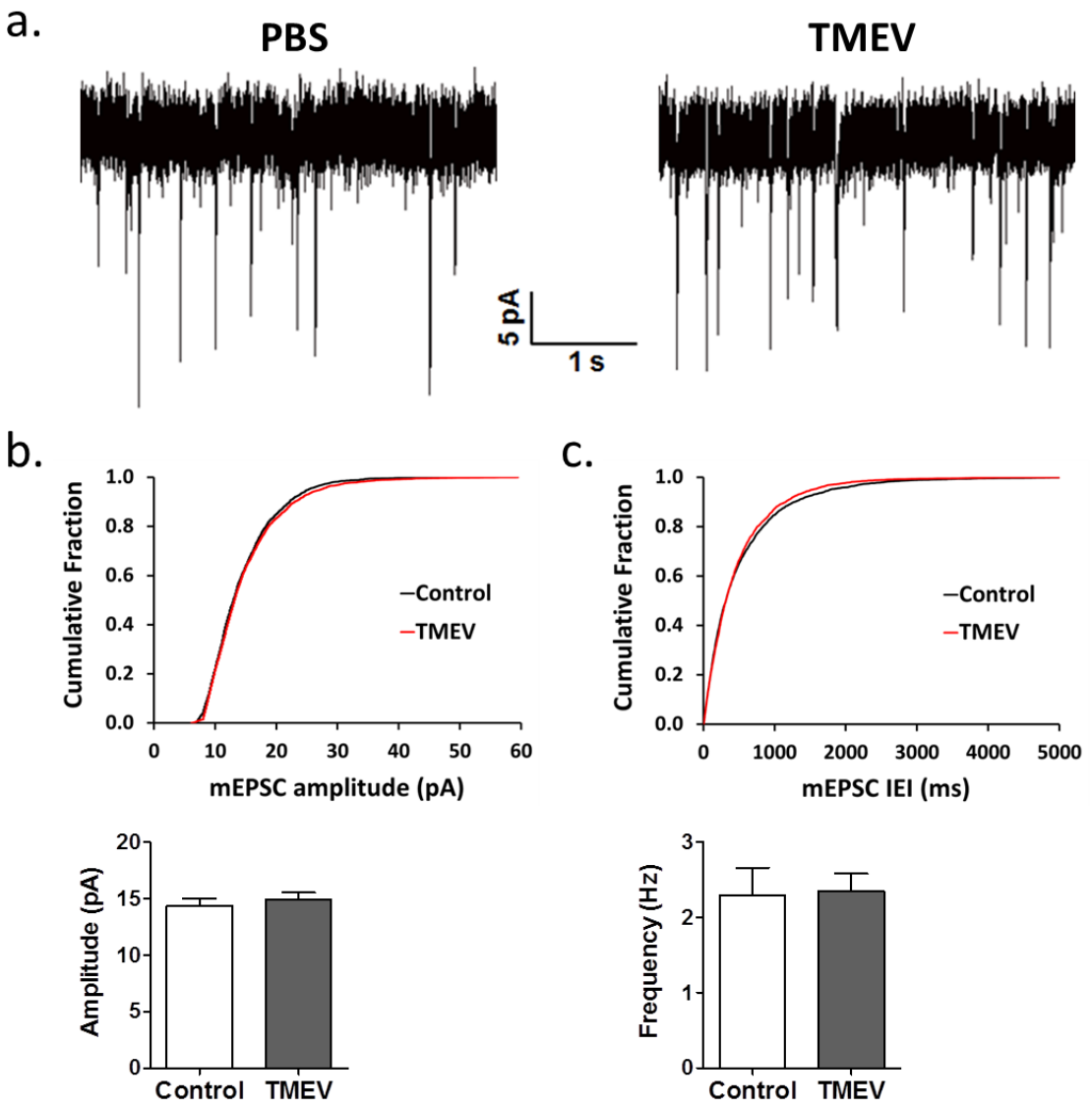

Figure 3.6 No difference in the properties of miniature excitatory postsynaptic currents (mEPSCs) of dentate granule cells (DGCs) between PBS-injected (control) and TMEV-infected mice during acute seizure activity period. (a) Representative traces of mEPSCs measured in the DGCs from the control group and TMEV-infected mice during 3-7 dpi. (b) Cumulative fraction distribution of the amplitude of mEPSCs shows no difference between the control and the TMEV groups. Average amplitudes of mEPSCs are plotted in the lower panel (Control: n = 8, TMEV: n = 10). (c) Cumulative fraction distribution of the interevent interval (IEI) of mEPSCs shows no difference between both the treatment groups. The lower panel shows the average frequency of mEPSCs. Statistics: Kolmogorov-Smirnov test (cumulative fraction), unpaired t test (average amplitude and frequency).

Table 3.1 Significant increase in the protein levels of various inflammatory mediators in the hippocampus of TMEV-infected mice during acute seizure activity period. Statistics: Two-way ANOVA, Bonferroni posttest, #p<0.05, *p<0.01, †p<0.001; SEM, standard error of the mean. (TNFα, tumor necrosis factor-α; IFNγ, interferon-γ; IL, interleukin; CXCL1, C-X-C motif chemokine ligand 1)

Cytokine	Fold change (relative to PBS-injected control mice)					
	Average	SEM	Average	SEM	Average	SEM
	1 dpi (n = 8)		5 dpi (n = 6)		14 dpi (n = 5)	
TNFα	6.9	0.6	206.2†	14.9	34.8#	7.1
IFNγ	4.5	0.8	21734.4†	3123.2	99.1	21.6
IL-1β	6.9	1.1	58.2†	5.4	46.6†	13.5
IL-10	2.3	0.3	47.2†	6.0	9.6	1.9
IL-12p70	2.5	0.3	3.0#	0.5	6.0†	1.0
IL-4	1.0	0.2	0.8	0.1	1.3	0.3
IL-2	2.4	0.3	14.4†	4.2	4.9	0.7
IL-5	2.0	0.1	10.8*	2.5	2.6	1.2
CXCL1	4.6	0.3	30.0†	4.3	2.4	0.3

CHAPTER 4

CANNABIDIOL TREATMENT PREVENTS SEIZURES FOLLOWING CNS INFECTION WITH THEILER'S MURINE ENCEPHALOMYELITIS VIRUS

Introduction

Theiler's Murine Encephalomyelitis Virus (TMEV) infection in the CNS of C57BL/6J mice causes a robust inflammatory response and oxidative stress in the hippocampus that is coincident with an acute seizure activity period. This acute seizure period is followed by a latent period and the majority of mice exhibiting acute seizures go on to develop epilepsy (Stewart et al., 2010). Protein levels of several cytokines and chemokines, including TNFα, IFNγ, IL-1β, IL-6, IL-2, IL-5, IL-12, and CXCL1, are significantly increased in the hippocampus of TMEV-infected mice during the acute behavioral seizure period (Table 3.1) (Cusick et al., 2013; Kirkman et al., 2010). In addition, mice deficient in TNFR1, TNFα, or IL-6 are much less susceptible to developing TMEV-induced acute seizures compared to WT mice (Figure 3.3a) (Kirkman et al., 2010). Oxidative and nitrative stress markers, such as elevated levels of 3-nitrotyrosine and impaired glutathione redox status, as evidenced by a decrease in the ratio of GSH:GSSG, have also been observed in the hippocampus of TMEV-infected mice with seizures as early as 3 dpi (Bhuyan et al., 2015). Thus, proinflammatory and

redox changes in the brain following TMEV infection may contribute to the development of acute seizures. Previous studies investigated the cellular sources of inflammatory mediators in the brain during acute TMEV infection period. In the CNS, glial cells, especially microglia, are the major source of cytokines and chemokines. In addition, neurons, endothelial cells, and infiltrating peripheral immune cells can also release inflammatory molecules under pathogenic conditions in the brain (Vezzani et al., 2011). Microgliosis, astrogliosis, and infiltration of macrophages have all been shown to occur in the hippocampus of TMEV-infected mice during acute seizures and thus likely contribute to the observed inflammatory response (Cusick et al., 2013; Loewen et al., 2016). Microglia and infiltrating macrophages are the major sources of TNFα and IL-6, respectively, in TMEV-infected mice with acute seizures (Cusick et al., 2013). Inhibiting infiltration of macrophages and microgliosis by minocycline or wogonin treatment has been shown to decrease the numbers of TMEV-infected mice that developed acute seizures (Cusick et al., 2013; Libbey et al., 2011). This further supports that inflammation likely plays a significant role in driving seizures in TMEV-infected mice, thus, antiinflammatory therapies, either as monotherapy and/or in combination with antiseizure drugs (ASDs), could be effective in reducing acute seizures and perhaps even prevent the development of epilepsy in TMEV-treated mice.

Cannabidiol (CBD), a nonpsychogenic phytoconstituent of the *Cannabis sativa* plant, has recently attracted clinical interest for the treatment of drug refractory epilepsy (Friedman and Devinsky, 2015). CBD imparts antiseizure effects in several animal models by altering neuronal excitability through a variety of mechanisms at doses devoid of adverse motor or psychoactive effects (Friedman and Devinsky, 2015; Rosenberg et

al., 2015). CBD may also modulate neuronal excitability by decreasing presynaptic release of glutamate by inhibiting G-protein-coupled receptor 55 (GRP55)-mediated release of intracellular Ca^{2+} (Sylantyev et al., 2013). CBD can also exert antioxidant and antiinflammatory effects (Burstein, 2015; Rosenberg et al., 2015). CBD decreases the release of TNFα in lipopolysaccharide-treated rats (Liou et al., 2008). CBD is also known to decrease the levels of other proinflammatory cytokines including IL-2, IFNγ, IL-6, IL-12p40, and IL-17 in mice (Hegde et al., 2011). Furthermore, CBD can enhance adenosine signaling by inhibiting adenosine uptake mechanisms (Carrier et al., 2006; Liou et al., 2008). Adenosine is known to function as an endogenous immunosuppressant (Hasko and Cronstein, 2004) and can also directly inhibit seizures and confer neuroprotective effects (Boison, 2012); therefore, CBD may also suppress inflammation and seizure activity through these mechanisms. In addition, CBD can ameliorate behavioral symptoms in an experimental autoimmune encephalomyelitis mouse model of multiple sclerosis potentially by suppressing T cell proliferation and microglial activity in the spinal cord (Kozela et al., 2011). CBD treatment also provides long-term improvement in motor deficits in TMEV-induced demyelinating disease, a model of multiple sclerosis in SJL/J mice, by decreasing infiltration of leukocytes, microglial activation, and proinflammatory cytokines IL-1β and TNFα (Mecha et al., 2013). Finally, isobolographic studies conducted by Dr. Misty D. Smith (University of Utah) found synergistic effects with 1:1 combination of CBD and levetiracetam in the 6 Hertz (6 Hz) psychomotor seizure test using CF1 mice (Smith et al., 2015). Based on these data, we hypothesized that CBD could be effective in suppressing acute behavioral seizures following TMEV infection.

The present studies were aimed at testing the efficacy of CBD in preventing acute

behavioral seizures in the TMEV model in C57BL/6J mice. While low doses of CBD had no effect on acute seizures that were induced by TMEV infection, the highest dose of CBD (180 mg/kg) significantly reduced the frequency and severity of acute seizures. The time to peak effect (TPE) of CBD in the 6 Hz psychomotor seizure test was observed at 2 h post-CBD treatment. This suggests that the lack of observed effects at the lower doses of CBD may have been due to the time at which animals were tested. Nevertheless, the results reported herein suggest that CBD may prove to be efficacious in this model of infection-induced seizures.

Methods

Animals

Male C57BL/6J mice (#006460) aged 5-6 weeks were purchased from Jackson Laboratory. After arrival, mice were allowed to acclimatize for at least 3 days prior to the experiment. Mice were provided food and water *ad libitum* and kept in a facility providing a 12 h light/dark cycle starting at 6:00 AM. All the procedures performed were in accordance with the guidelines provided and approved by the Institutional Animal Care and Use Committee of the University of Utah.

Method of TMEV infection and seizure monitoring

Mice are briefly anesthetized with 3% isoflurane and injected with 20 µl of either phosphate-buffered saline (PBS) or $2x10^5$ PFU (plaque forming units) DA-TMEV solution intracortically in the right hemisphere by inserting the needle at a 90° angle to the skull. The injection region is located slightly medial to the equidistant point on the

imaginary line connecting the eye and the ear. A sterilized syringe containing a plastic jacket on the needle exposing 2.5 mm of needle is used for infection to restrict the injection site to the somatosensory cortex.

Acute behavioral seizures were induced by briefly agitating the mice by shaking their cages and the seizures were video-monitored twice daily at 11:00 AM and at 4:00 PM between 2 to 8 days postinfection (dpi). Seizure intensity was graded using modified Racine scale as follows: stage 1, mouth and facial movements; stage 2, head nodding; stage 3, forelimb clonus; stage 4, forelimb clonus, rearing; stage 5, forelimb clonus, rearing, and falling; and stage 6, intense running, jumping, repeated falling, and severe clonus. Seizure scores were assigned after verifying seizure video recordings by an investigator blinded to the treatment groups. Seizure frequency was reported as the average number of seizures during the entire acute seizure period, whereas seizure severity/intensity was represented as the average cumulative seizure burden at each dpi during the acute seizure period. Cumulative seizure burden at each dpi for a mouse was calculated by summing all of the seizure score numbers up to that dpi.

CBD treatment

CBD was received from the National Institute on Drug Abuse (NIDA). Since CBD does not dissolve in aqueous solvents, it was formulated as an oil-in-water emulsion using a mixture of 100% ethanol, Kolliphor®, and 0.9% saline (1:1:18). CBD was first dissolved in 100% ethanol and equal amount of Kolliphor® (polyoxyl castor oil, BASF) was added. The mixture was vortexed and a small amount of 0.9% saline was added gradually while vortexing the mixture vigorously after every addition to make an

emulsion. The mixture of CBD in 100% ethanol and Kolliphor® appears transparent and after addition of a small amount of 0.9% saline, the emulsion appears milky. The emulsion was kept on ice and vortexed immediately before injecting each mouse i.p. at 10 ml/kg. Since the CBD emulsion destabilizes after about 1 h of preparation, it was made fresh and used within 20 min of preparation.

Statistics

The dataset involving continuous variables is represented by the mean and standard error of the mean (SEM), and the dataset with ordinal variables is presented as a frequency distribution. Experimental design involving two groups with one continuous dependent variable was analyzed by unpaired two-tailed t test, whereas design involving two categorical independent variables and one continuous dependent variable was analyzed by two-way ANOVA. Multiple comparisons were performed by Bonferroni posttest. Cumulative seizure burden, which was calculated from a ranked dataset, was analyzed by the Scheirer-Ray-Hare test, which is an extension of Kruskal-Wallis test for two randomized factorial designs (Scheirer et al., 1976). The statistical calculations were conducted using GraphPad Prism® 5 and Microsoft Excel.

Results

High dose CBD (180 mg/kg) effectively reduces TMEV-induced acute seizure frequency and intensity

The ED_{50} of CBD had been calculated previously in the 6 Hz seizure model of pharmacoresistant partial seizures (Smith et al., 2015). Male CF1 mice were treated with

different doses of CBD, ranging from 25-300 mg/kg i.p., and subjected to the 6 Hz psychomotor seizure test, and the numbers of mice protected from seizures, that is, an absence of jaw chomping, twitching of vibrissae, and forelimb clonus, were determined (Barton et al., 2001). From this dose-response study, the ED_{50} of CBD was calculated to be 180 mg/kg by probit analysis. Therefore, we used this dose to determine the antiseizure potential of CBD in the TMEV-induced infection model.

The first dosing regimen chosen for treatment with CBD was a "prophylactic" approach. CBD administration was begun two days prior to TMEV infection and continued for 8 days after infection. Therefore, as shown in Figure 4.1a, mice were treated with CBD (180 mg/kg; i.p. twice daily every 12 h) for a total 10 days. Acute seizures were video-monitored and assessed using a modified Racine seizure scale from stage 3 to 6 as described in the Methods and represented as a heat map (Figure 4.1b). All TMEV-infected mice in the vehicle treatment group developed acute seizures, whereas 3 mice in the CBD group did not have seizures. CBD-treated mice had a dramatic reduction in the average number of seizures that occurred over the acute seizure period (CBD: 1.5 ± 0.40, Vehicle: 8.3 ± 0.73, n = 10, $p<0.0001$. Data are presented as average seizures ± SEM.) (Figure 4.1c) and seizure severity between 4-8 dpi (Figure 4.1d) compared to vehicle-treated mice. Although 70% of CBD-treated mice had at least one behavioral seizure, CBD treatment delayed the development of seizures and significantly prolonged the seizure freedom period ($p<0.0001$, log-rank test) (Figure 4.1e).

After observing beneficial effects of CBD in the prophylactic regimen, we treated TMEV-infected mice with a more relevant therapeutic treatment regimen. Instead of beginning treatment before the infection, CBD treatment was started on day 3 after

infection. A significant portion of TMEV-infected mice begin to have acute seizures on 3 dpi, so the mice were treated with CBD between 3-7 dpi (Figure 4.2a). As in the first study, CBD was administered at 7:00 AM and 7:00 PM and seizures were evaluated at 4 and 9 h after the morning injection. The seizure scores for all the mice are presented in the heat map (Figure 4.2b). In both treatment groups, mice had similar numbers of seizures on 3 dpi (the first day of treatment). However, the seizure frequency and severity were dramatically reduced in the CBD group at 4 dpi and these effects were continued during the remaining period of CBD treatment. Average number of seizures was reduced by 67% in CBD-treated mice compared to vehicle-treated mice (CBD: 2.4 ± 0.60, Vehicle: 6.6 ± 0.75, n = 10, p=0.0004. Data are presented as average seizures ± SEM.) (Figure 4.2c). In addition, seizure severity was also significantly decreased in the CBD-treated mice between 5-8 dpi (Figure 4.2d). In contrast to the prophylactic treatment regimen, analysis of seizure freedom over time postinfection found no difference between the treatment groups in this treatment regimen (p=0.3751, log-rank test) since the majority of the mice in both the groups developed seizures within 3-4 dpi (Figure 4.2e).

Lower CBD doses have no effect on TMEV-induced acute seizures

Next we conducted a dose-response study to determine the ED_{50} of CBD in this model. Mice were divided into 6 groups (n = 10), with 5 of the groups being treated with different doses of CBD (22.5, 45, 90, and 180 mg/kg) or vehicle starting at 3 dpi through 7 dpi every 12 h. One group served as noninfected control and only injected with PBS intracortically. Surprisingly, all the doses of CBD, except 180 mg/kg, were ineffective in

reducing the average number of seizures (Vehicle: 10.2 ± 0.68, 22.5 mg/kg CBD: 8.3 ± 0.70, 45 mg/kg CBD: 9.6 ± 1.02, 90 mg/kg CBD: 10.1 ± 0.94, and 180 mg/kg CBD: 4.4 ± 0.85. Data are presented as average seizures ± SEM.) and average cumulative seizure burden compared to TMEV-infected vehicle-treated mice. However, as shown previously, the high dose of CBD (180 mg/kg) consistently reduced seizure frequency ($p<0.0001$ compared to vehicle, 45 and 90 mg/kg groups, $p<0.05$ compared to 22.5 mg/kg group) (Figure 4.3a) and the average cumulative seizure burden from 4-7 dpi was also significantly reduced compared to the vehicle treated group (Figure 4.3b).

Although CBD (180 mg/kg) was efficacious in reducing TMEV-induced seizures, mice treated with this dose of CBD lost weight starting from 4 dpi through 9 dpi compared to mice in the other treatment groups (Figure 4.3c). Weight loss was coincident with the CBD treatment period as mice started to recover after 8 dpi. CBD (180 mg/kg)-treated mice were also observed to have ruffled fur, which may suggest a hypothermic effect of treatment, and hypothermia can contribute to a reduction in seizures (Guilliams et al., 2013; Wang et al., 2011). Therefore, we measured body temperature of CBD (180 mg/kg)-treated mice up to 4 h post-CBD treatment from 3-7 dpi by a rectal temperature probe. As shown in Figure 4.3d, average body temperature measured immediately before CBD treatment (baseline) ranged from 37.5 to 38.3 °C. On 3 dpi, the average body temperature was reduced by 3.4 °C from the baseline at 2 h post-CBD treatment and that could be considered mildly hypothermic, however, the temperature quickly recovered by 4 h post-CBD treatment. While a reduction in average body temperature of up to 2.1 °C occurred at 2 h post-CBD treatment everyday from 4-7 dpi, that extent of a temperature reduction is not generally considered to be hypothermic (Wong et al., 1997). Further,

seizure frequency and severity were similar between CBD (180 mg/kg)-treated mice and vehicle-treated mice on 3 dpi, but significantly reduced during 4-7 dpi (Figure 4.2b). Therefore, these data suggest that hypothermia likely did not contribute to the observed decrease in acute seizures. Mechanism(s) for the antiseizure effects of the high dose of CBD (180 mg/kg) are currently unknown and should be investigated in future studies.

In an additional set of experiments, we tested the efficacy of 135, 150, and 165 mg/kg CBD in reducing TMEV-induced acute seizures. None of these additional three doses had any effect on either the average number of seizures or the average cumulative seizure burden when compared to the TMEV-infected vehicle treatment group (Figure 4.4a, 4.4b).

CBD (150 mg/kg) reduces TMEV-induced acute seizures at 4 h, but not at 9 h, posttreatment

Acute seizure monitoring was conducted at 4 and 9 h post-CBD treatment in all the experiments described above. If the time to peak effect (TPE) of CBD in this model is less than 4 h posttreatment, we might not have detected any potential antiseizure effects of CBD with doses less than 180 mg/kg. Therefore, the TPE of CBD was investigated in male C57BL/6J mice using the 6 Hz psychomotor seizure test as previously described (Barton et al., 2001). The TPE for CBD was found to be 2 h post-CBD treatment, with a diminished efficacy at 4 h (unpublished data, Dr. Misty D. Smith, University of Utah). Therefore, to detect any beneficial effect of CBD treatment on seizures at the 4 h posttreatment observation time point, we analyzed the data for the two daily monitoring time points separately. Seizure frequency and severity were not different at 4 h post-CBD

treatment in the groups treated with 22.5, 45, 90, 135, or 165 mg/kg of CBD compared to vehicle-treated control mice. However, mice treated with 150 mg/kg CBD had a significant reduction in the average number of seizures during the acute seizure activity period monitored at 4 h posttreatment (CBD: 0.5 ± 0.15, Vehicle: 1.45 ± 0.31, n = 20, p=0.0095; Data are presented as average seizures ± SEM.), but not at 9 h (CBD: 1.15 ± 0.25, Vehicle: 1.55 ± 0.26, n = 20, p=0.2747. Data are presented as average seizures ± SEM.) (Figure 4.5). Likewise, the average cumulative seizure burden, calculated by analyzing seizures only at the 4 h post-CBD time point was significantly reduced in 150 mg/kg CBD group at 6 and 7 dpi (Figure 4.5b). These data suggest that the doses of CBD investigated (22.5-165 mg/kg) might be effective in reducing TMEV-induced acute seizures if seizures were monitored at the TPE of CBD.

Discussion

The experiments conducted here demonstrate that CBD (180 mg/kg) consistently reduced both the frequency and severity of acute behavioral seizures following TMEV infection, but the lower doses of CBD (ranging from 22.5 to 165 mg/kg) did not improve seizure outcome during the acute infection period. However, we found a significant reduction in frequency and severity of acute seizures monitored at 4 h post-CBD (150 mg/kg) treatment, whereas these beneficial effects were not observed when the seizures were monitored at the 9 h post-CBD treatment. Based on this finding, and data suggesting that the TPE for C57BL/6J is 2 h in acute seizure models, future studies should evaluate seizure incidence in the TMEV model at or before the TPE. Other pharmacokinetic parameters such as half-life and bioavailability of CBD in TMEV-infected mice are

unknown and the detailed understanding of these parameters will be helpful in determining an optimum dosing paradigm of CBD for the treatment of TMEV-induced acute seizures.

Acute seizures due to CNS infection greatly increase the probability for the development of chronic spontaneous seizures (Berg, 2008; Hesdorffer et al., 1998). It will be of utmost importance to investigate whether suppression of TMEV-induced acute behavioral seizures by CBD treatment (180 mg/kg) provides disease-modifying effects and can prevent the development of epilepsy in this model. Acute TMEV infection causes a robust increase in the levels of proinflammatory cytokines and chemokines as well as oxidative stress markers (Bhuyan et al., 2015; Kirkman et al., 2010), and CBD exerts antiinflammatory and antioxidant actions (Rosenberg et al., 2015). Therefore, the changes in the levels of the proinflammatory cytokines and oxidative stress markers, coincident with the changes in acute seizures due to CBD treatment, should be measured in future studies to assess the contribution of inflammation and oxidative stress in driving seizures in this model and also to assess the mechanism of action of CBD.

The present study highlights the importance of the TMEV model of limbic epilepsy as a drug screening tool for the development of novel therapeutic approaches for the treatment of acute seizures as well as for the prevention of epileptogenesis. The efficacy of carbamazepine and valproate has been assessed in this model (Barker-Haliski et al., 2015). Valproate (200 mg/kg) and carbamazepine (20 mg/kg) given twice daily during the first week of TMEV infection did not decrease numbers of TMEV-infected mice developing acute seizures; however, valproate reduced the seizure severity (Barker-Haliski et al., 2015). In contrast, carbamazepine treatment increased the numbers of mice

developing seizures and the concomitant seizure burden, and decreased the latency to first seizure (Barker-Haliski et al., 2015). Thus, this model is refractory to at least one commonly used ASD. Given intense scientific and public interest in cannabinoid-based therapies for intractable epilepsies, thorough animal studies evaluating the safety and efficacy of CBD either alone or in combination with available ASDs in a battery of epilepsy models are highly desirable. In line with that goal, Dr. Misty D. Smith recently conducted an isobolographic analysis of CBD in combination with five mechanistically different ASDs (carbamazepine, clonazepam, levetiracetam, valproate, and lacosamide) in their ED_{50} combinations of 3:1, 1:1 and 1:3 to investigate their efficacy in preventing seizures in the 6 Hz model in CF1 mice. Only the 1:1 combination of CBD:levetiracetam showed synergistic effects in suppressing seizures among all the other combinations tested. Therefore, polytherapy using CBD and levetiracetam may provide superior control of seizures with minimal adverse effects because 1) there are diverse mechanisms of antiseizure actions of CBD and levetiracetam and 2) their complementary actions in reducing distinct sets of cytokines as levetiracetam reduces the levels of IL-1β (Kim et al., 2010) and CBD decreases expression of TNFα, IL-6, IL-2, IFNγ, IL-12p40, and IL-17 (Burstein, 2015). Consistency of these findings should be evaluated using other models of epilepsy including the TMEV model.

In conclusion, CBD (180 mg/kg) given twice daily intraperitoneally consistently reduces acute behavioral seizures induced by TMEV infection. The pharmacology of CBD in the TMEV model will be studied in detail by determining the pharmacokinetic parameters which will better inform future study design and by investigating mechanism(s) of antiseizure actions.

References

Barker-Haliski, M.L., Dahle, E.J., Heck, T.D., Pruess, T.H., Vanegas, F., Wilcox, K.S., White, H.S., 2015. Evaluating an etiologically relevant platform for therapy development for temporal lobe epilepsy: effects of carbamazepine and valproic acid on acute seizures and chronic behavioral comorbidities in the Theiler's murine encephalomyelitis virus mouse model. J. Pharmacol. Exp. Ther. 353, 318-329.

Barton, M.E., Klein, B.D., Wolf, H.H., White, H.S., 2001. Pharmacological characterization of the 6 Hz psychomotor seizure model of partial epilepsy. Epilepsy Res. 47, 217-227.

Berg, A.T., 2008. Risk of recurrence after a first unprovoked seizure. Epilepsia 49 Suppl 1, 13-18.

Bhuyan, P., Patel, D.C., Wilcox, K.S., Patel, M., 2015. Oxidative stress in murine Theiler's virus-induced temporal lobe epilepsy. Exp. Neurol. 271, 329-334.

Boison, D., 2012. Adenosine dysfunction in epilepsy. Glia 60, 1234-1243.

Burstein, S., 2015. Cannabidiol (CBD) and its analogs: a review of their effects on inflammation. Bioorg. Med. Chem. 23, 1377-1385.

Carrier, E.J., Auchampach, J.A., Hillard, C.J., 2006. Inhibition of an equilibrative nucleoside transporter by cannabidiol: a mechanism of cannabinoid immunosuppression. Proc. Natl. Acad. Sci. U. S. A. 103, 7895-7900.

Cusick, M.F., Libbey, J.E., Patel, D.C., Doty, D.J., Fujinami, R.S., 2013. Infiltrating macrophages are key to the development of seizures following virus infection. J. Virol. 87, 1849-1860.

Friedman, D., Devinsky, O., 2015. Cannabinoids in the Treatment of Epilepsy. N. Engl. J. Med. 373, 1048-1058.

Guilliams, K., Rosen, M., Buttram, S., Zempel, J., Pineda, J., Miller, B., Shoykhet, M., 2013. Hypothermia for pediatric refractory status epilepticus. Epilepsia 54, 1586-1594.

Hasko, G., Cronstein, B.N., 2004. Adenosine: an endogenous regulator of innate immunity. Trends Immunol. 25, 33-39.

Hegde, V.L., Nagarkatti, P.S., Nagarkatti, M., 2011. Role of myeloid-derived suppressor cells in amelioration of experimental autoimmune hepatitis following activation of TRPV1 receptors by cannabidiol. PLoS One 6, e18281.

Hesdorffer, D.C., Logroscino, G., Cascino, G., Annegers, J.F., Hauser, W.A., 1998. Risk of unprovoked seizure after acute symptomatic seizure: effect of status epilepticus. Ann. Neurol. 44, 908-912.

Kim, J.E., Choi, H.C., Song, H.K., Jo, S.M., Kim, D.S., Choi, S.Y., Kim, Y.I., Kang, T.C., 2010. Levetiracetam inhibits interleukin-1 beta inflammatory responses in the hippocampus and piriform cortex of epileptic rats. Neurosci. Lett. 471, 94-99.

Kirkman, N.J., Libbey, J.E., Wilcox, K.S., White, H.S., Fujinami, R.S., 2010. Innate but not adaptive immune responses contribute to behavioral seizures following viral infection. Epilepsia 51, 454-464.

Kozela, E., Lev, N., Kaushansky, N., Eilam, R., Rimmerman, N., Levy, R., Ben-Nun, A., Juknat, A., Vogel, Z., 2011. Cannabidiol inhibits pathogenic T cells, decreases spinal microglial activation and ameliorates multiple sclerosis-like disease in C57BL/6 mice. Br. J. Pharmacol. 163, 1507-1519.

Libbey, J.E., Kennett, N.J., Wilcox, K.S., White, H.S., Fujinami, R.S., 2011. Interleukin-6, produced by resident cells of the central nervous system and infiltrating cells, contributes to the development of seizures following viral infection. J. Virol. 85, 6913-6922.

Liou, G.I., Auchampach, J.A., Hillard, C.J., Zhu, G., Yousufzai, B., Mian, S., Khan, S., Khalifa, Y., 2008. Mediation of cannabidiol anti-inflammation in the retina by equilibrative nucleoside transporter and A2A adenosine receptor. Invest. Ophthalmol. Vis. Sci. 49, 5526-5531.

Loewen, J.L., Barker-Haliski, M.L., Dahle, E.J., White, H.S., Wilcox, K.S., 2016. Neuronal injury, gliosis, and glial proliferation in two models of temporal lobe epilepsy. J. Neuropathol. Exp. Neurol. 75, 366-378.

Mecha, M., Feliu, A., Inigo, P.M., Mestre, L., Carrillo-Salinas, F.J., Guaza, C., 2013. Cannabidiol provides long-lasting protection against the deleterious effects of inflammation in a viral model of multiple sclerosis: a role for A2A receptors. Neurobiol. Dis. 59, 141-150.

Rosenberg, E.C., Tsien, R.W., Whalley, B.J., Devinsky, O., 2015. Cannabinoids and Epilepsy. Neurotherapeutics 12, 747-768.

Scheirer, C.J., Ray, W.S., Hare, N., 1976. The analysis of ranked data derived from completely randomized factorial designs. Biometrics 32, 429-434.

Smith, M.D., Wilcox, K.S., White, H.S., 2015. Abstract 1.215: Analysis of cannabidiol interactions with antiseizure drugs, 69th Annual Meeting of American Epilespy Society, Philadelphia.

Stewart, K.A., Wilcox, K.S., Fujinami, R.S., White, H.S., 2010. Development of postinfection epilepsy after Theiler's virus infection of C57BL/6 mice. J. Neuropathol. Exp. Neurol. 69, 1210-1219.

Sylantyev, S., Jensen, T.P., Ross, R.A., Rusakov, D.A., 2013. Cannabinoid- and lysophosphatidylinositol-sensitive receptor GPR55 boosts neurotransmitter release at central synapses. Proc. Natl. Acad. Sci. U. S. A. 110, 5193-5198.

Vezzani, A., French, J., Bartfai, T., Baram, T.Z., 2011. The role of inflammation in epilepsy. Nat. Rev. Neurol. 7, 31-40.

Wang, Y., Liu, P.P., Li, L.Y., Zhang, H.M., Li, T., 2011. Hypothermia reduces brain edema, spontaneous recurrent seizure attack, and learning memory deficits in the kainic acid treated rats. CNS Neurosci. Ther. 17, 271-280.

Wong, J.P., Saravolac, E.G., Clement, J.G., Nagata, L.P., 1997. Development of a murine hypothermia model for study of respiratory tract influenza virus infection. Lab. Anim. Sci. 47, 143-147.

Figure 4.1 Prophylactic treatment with 180 mg/kg CBD reduces average frequency and severity of TMEV-induced acute seizures. (a) Outline of prophylactic CBD treatment regimen. (b) Acute seizures were induced by handling the mice four times a day – during CBD/vehicle injections (7:00 AM, 7:00 PM) and during seizure monitoring (11:00 AM, 4:00 PM). Seizure severity was video-monitored with the experimenter blinded to the treatment groups, scored based on a modified Racine scale ranging from stage 3 to 6, and depicted as a heat map using green, yellow, orange, and red colors corresponding to seizure scores in increasing order (DI, during injection; dpi, days postinfection). (c, d) Prophylactic CBD treatment significantly reduces seizure frequency (c) plotted as total numbers of seizures per mouse and seizure severity (d) as measured by average cumulative seizure burden during acute seizure period (3-8 dpi) in TMEV-infected mice. Each circle represents an individual mouse and the horizontal line indicates the average number of seizures per group. (e) Development of the first acute seizure is significantly delayed in CBD-treated mice compared to vehicle-treated mice. Statistics: unpaired t-test (frequency), Scheirer-Ray-Hare test (severity), **$p<0.01$, ***$p<0.001$.

a.

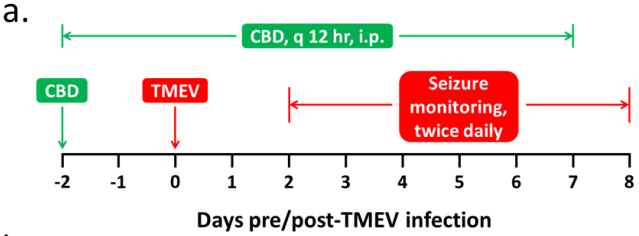
CBD, q 12 hr, i.p.
CBD
TMEV
Seizure monitoring, twice daily
-2 -1 0 1 2 3 4 5 6 7 8
Days pre/post-TMEV infection

b.

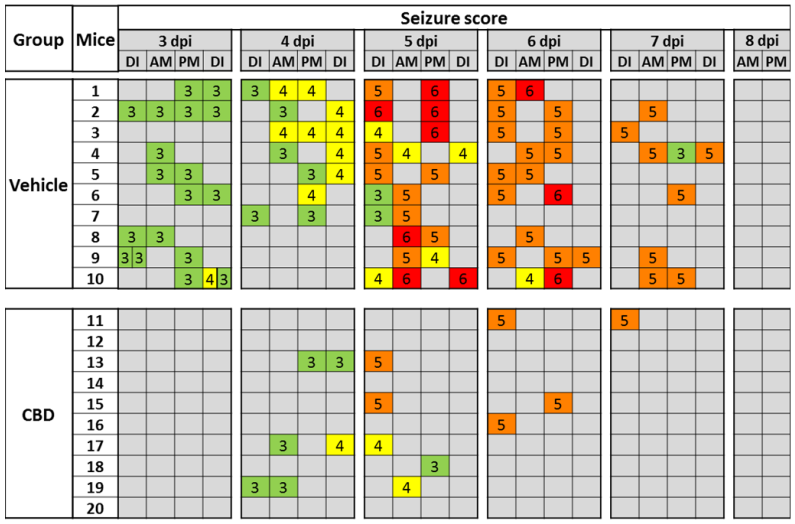
Group
Mice
Seizure score
3 dpi
4 dpi
5 dpi
6 dpi
7 dpi
8 dpi
DI AM PM DI
Vehicle
CBD

c.

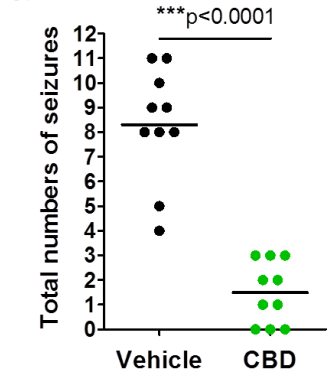
***p<0.0001
Total numbers of seizures
Vehicle
CBD

d.

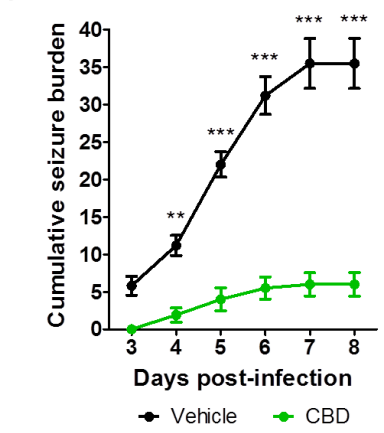
Cumulative seizure burden
Days post-infection
Vehicle
CBD

e.

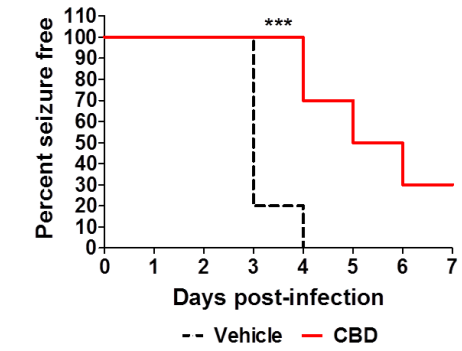
Percent seizure free
Days post-infection
Vehicle
CBD

Figure 4.2 Therapeutic treatment with CBD (180 mg/kg) reduces average frequency and severity of TMEV-induced acute seizures. (a) Outline of therapeutic CBD treatment regimen. (b) Acute seizures were induced by handling the mice four times a day – during CBD/vehicle injections (7:00 AM, 7:00 PM) and during seizure monitoring (11:00 AM, 4:00 PM). Seizure severity was video-monitored with the experimenter blinded to the treatment groups, categorized based on modified Racine scale ranging from stage 3 to 6, and data depicted as a heat map using green, yellow, orange, and red colors corresponding to seizure scores in increasing order (DI, during injection; dpi, days postinfection). (c, d) Therapeutic CBD treatment significantly reduces seizure frequency (c) plotted as total numbers of seizures per mouse and seizure severity (d) as measured by average cumulative seizure burden during acute seizure period (3-8 dpi) compared to vehicle-treated TMEV-infected mice. Each circle represents an individual mouse and the horizontal line indicates the average number of seizures per group. (e) Development of the first seizure is not significantly different between treatment groups. Statistics: unpaired t-test (frequency), Scheirer-Ray-Hare test (severity), **$p<0.01$, ***$p<0.001$.

a.

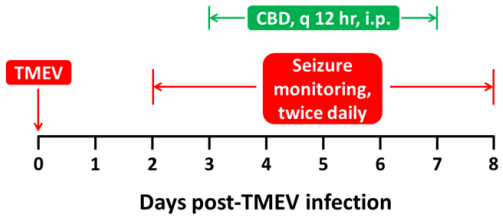
CBD, q 12 hr, i.p.
TMEV
Seizure monitoring, twice daily
0 1 2 3 4 5 6 7 8
Days post-TMEV infection

b.

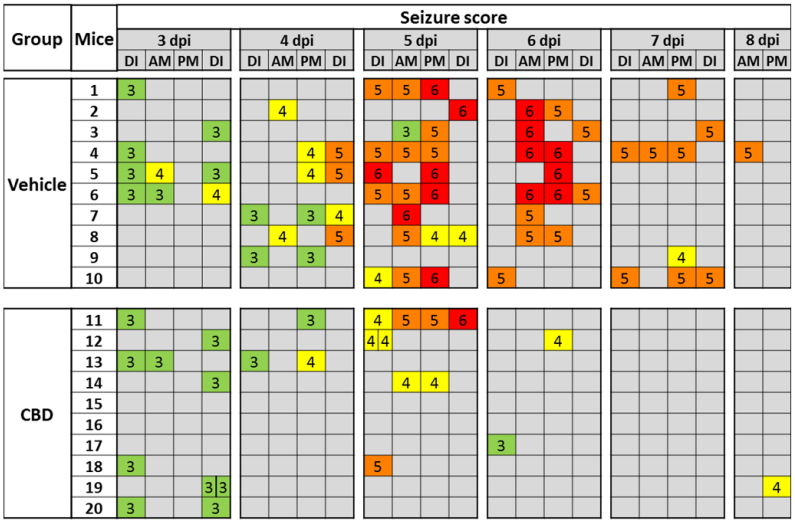
Group
Mice
Seizure score
3 dpi
4 dpi
5 dpi
6 dpi
7 dpi
8 dpi
DI AM PM DI
Vehicle
CBD

c.

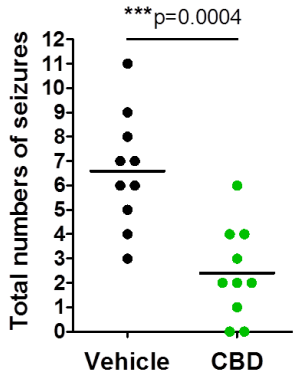
***p=0.0004
Total numbers of seizures
Vehicle
CBD

d.

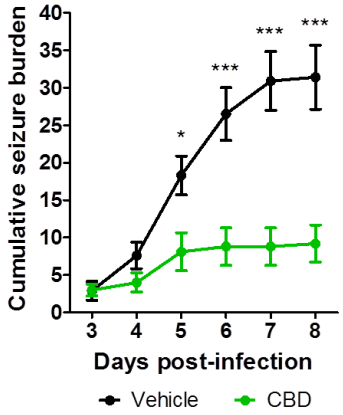
Cumulative seizure burden
Days post-infection
Vehicle
CBD

e.

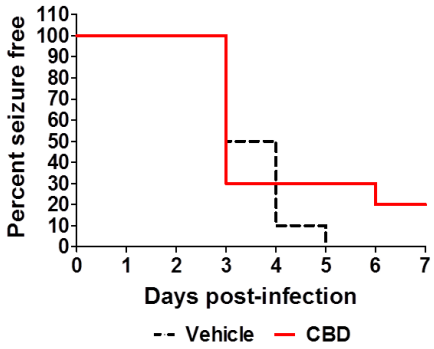
Percent seizure free
Days post-infection
Vehicle
CBD

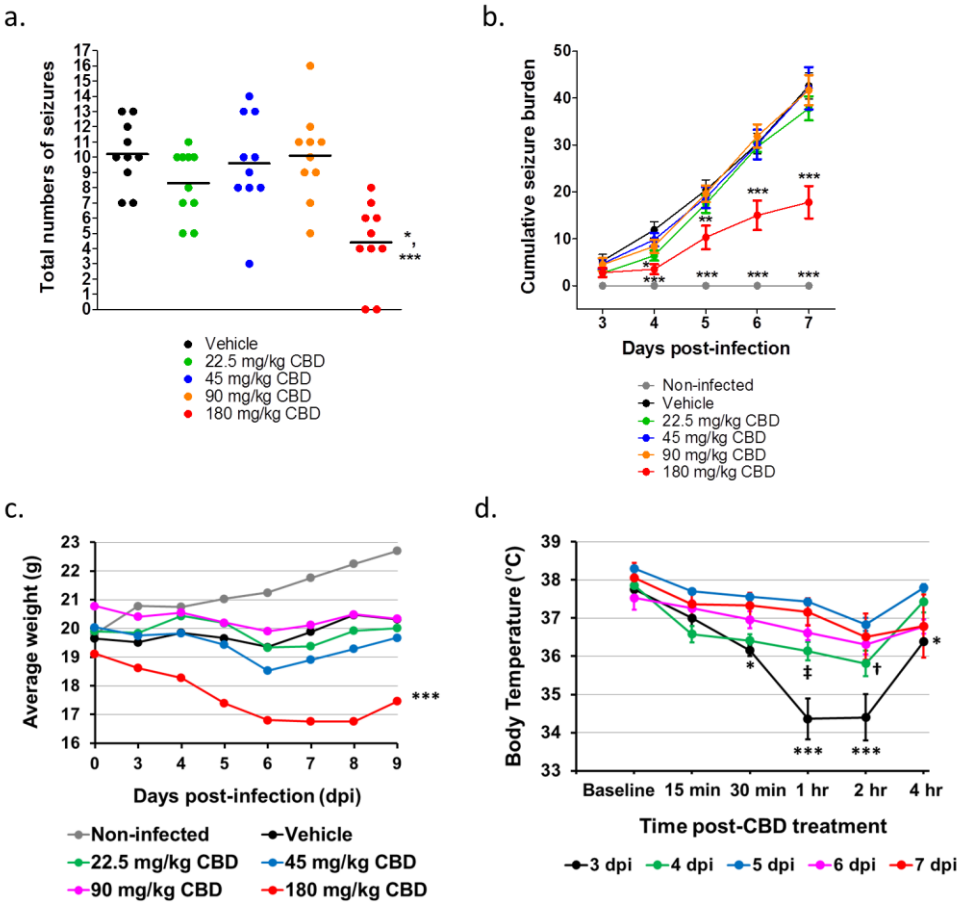

Figure 4.3 Only one dose of CBD (180 mg/kg; range of 22.5 to 180 mg/kg) reduces frequency and severity of TMEV-induced acute seizures. Five groups of mice (n = 10 per group) were infected with TMEV ($2x10^5$ PFU/mouse) and treated with either vehicle or different doses of CBD (22.5, 45, 90, and 180 mg/kg) i.p. every 12 h for 5 days starting at 3 dpi. (a) CBD (180 mg/kg) treatment, but not the other doses, significantly reduces seizure frequency plotted as total numbers of seizures per mouse compared to vehicle as well as 22.5, 45, and 90 mg/kg CBD groups. Each circle indicates individual mouse and the horizontal line indicates average number of seizures per group. (b) Similarly, only 180 mg/kg CBD reduces seizure severity as measured by average cumulative seizure burden compared to all the other treatment groups, but the treatment with the lower doses of CBD does not affect seizure severity. (c) Changes in the average weight of mice in each treatment group over acute infection period shows a significant reduction in 180 mg/kg CBD treated mice compared to other treatment groups between 5-9 dpi. (d) Core body temperature of 180 mg/kg CBD-treated mice as measured immediately before CBD treatment (baseline) and at 15 min, 30 min, 1, 2, and 4 h posttreatment each day during 3-7 dpi shows a significant reduction on 3 dpi compared to other days. Statistics: unpaired t-test (frequency), Scheirer-Ray-Hare test (severity), two-way ANOVA, (weight and body temperature) *p<0.05, **p<0.01, ***p<0.001, †p<0.05, ‡p<0.01.

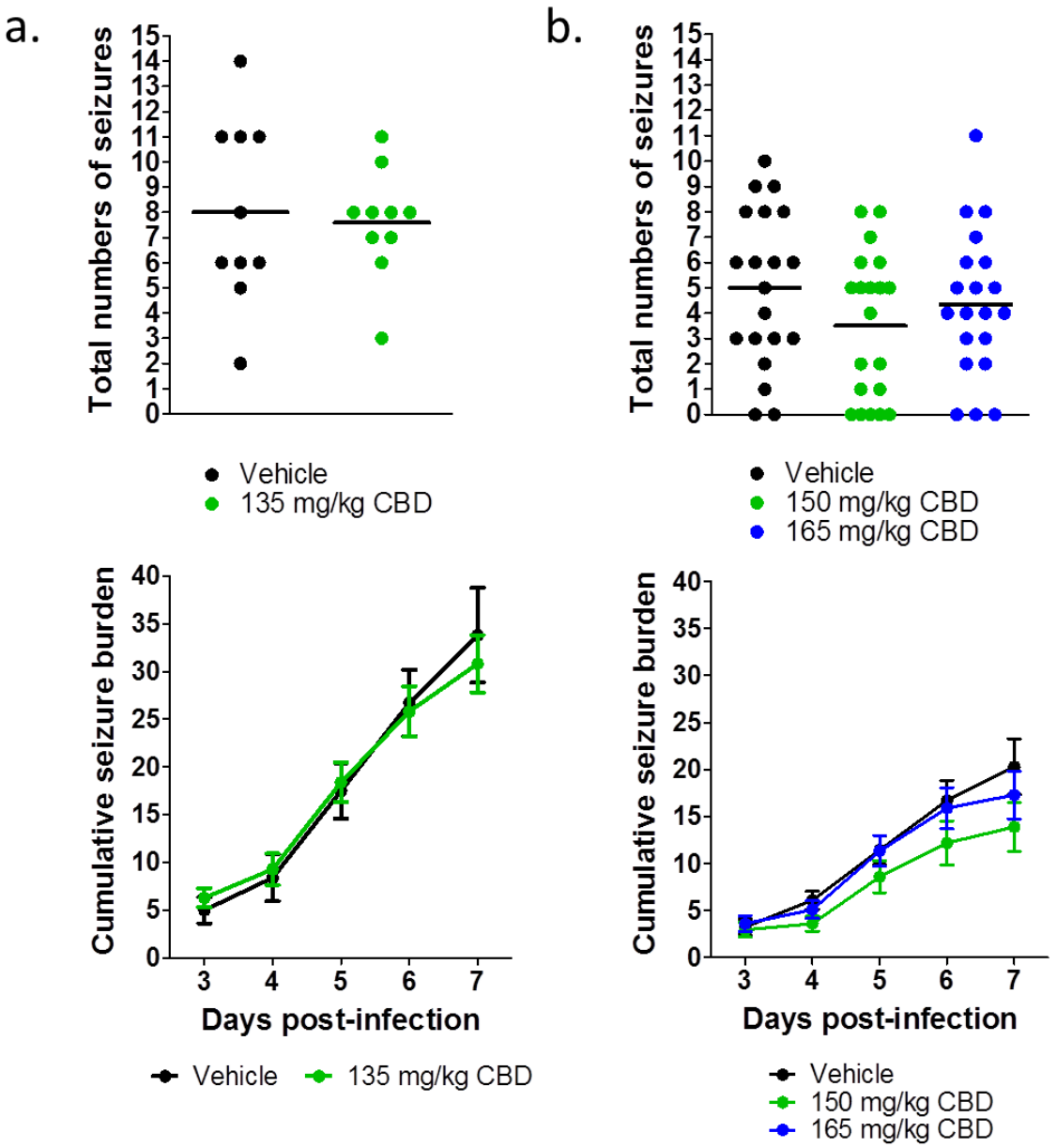

Figure 4.4 Low doses of CBD have no effect on TMEV-induced acute seizures. Mice were infected with TMEV ($2x10^5$ PFU/mouse) and treated with either vehicle or CBD (135, 150, and 165 mg/kg) i.p. every 12 h for 5 days starting at 3 dpi. 135 mg/kg (a) as well as 150 and 165 mg/kg (b) CBD treatment does not reduce average frequency (upper panels) and intensity (lower panels) of TMEV-induced seizures. Data from two separate experiments testing 150 and 165 mg/kg CBD (n = 10/group) were pooled for seizure analysis.

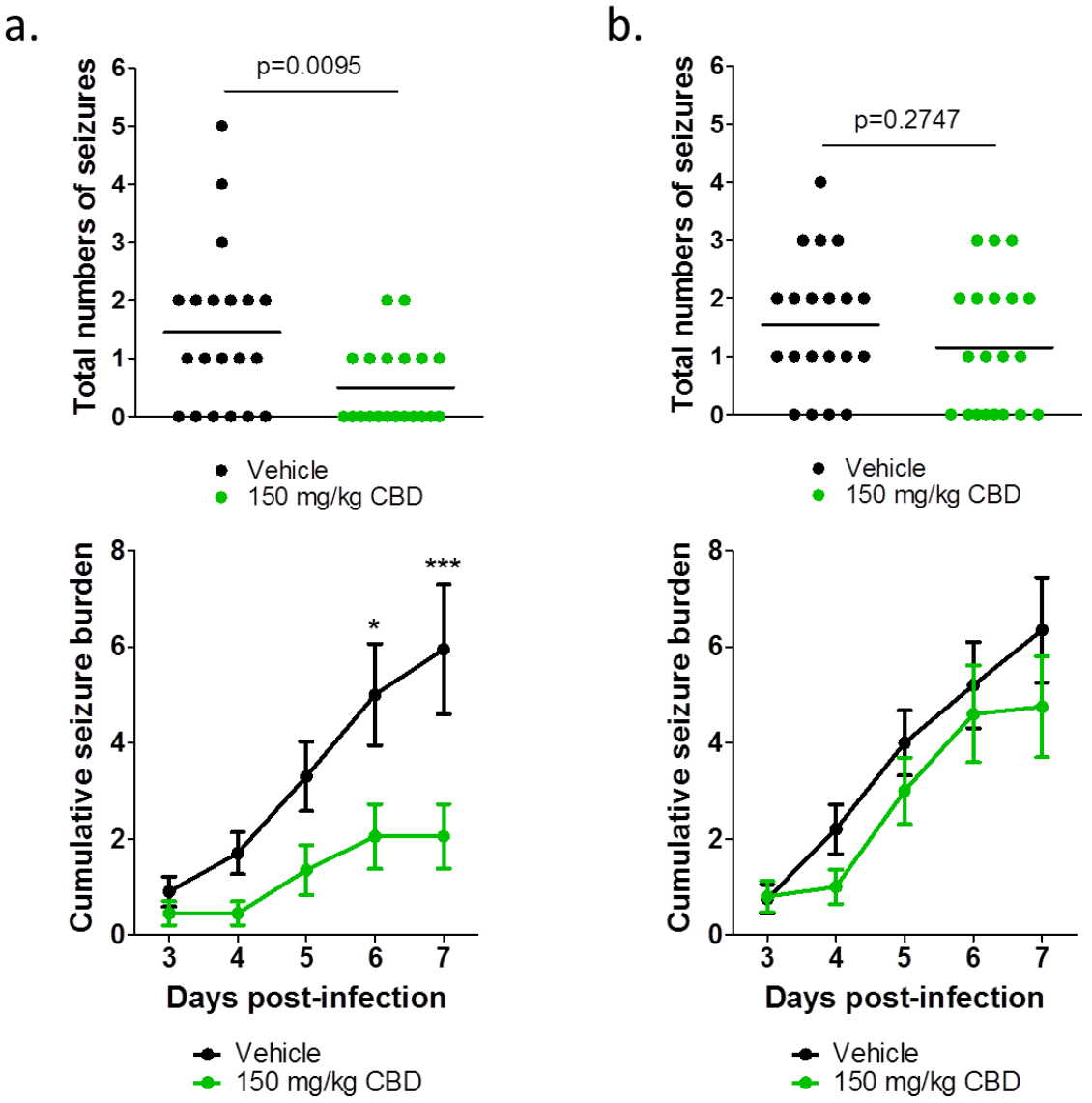

Figure 4.5 CBD (150 mg/kg) administration decreases TMEV-induced seizures monitored at 4 h post-CBD treatment but not at 9 h post-CBD treatment. (a) Analysis of seizures monitored at 4 h post-CBD treatment shows a significant reduction in the average number of seizures (upper panel) and the average cumulative seizure burden at 6 and 7 dpi (lower panel) compared to the vehicle group. (b) CBD (150 mg/kg) treatment does not affect seizure endpoints measured at 9 h posttreatment. Statistics: unpaired t-test (frequency), Scheirer-Ray-Hare test (severity), *p<0.05, ***p<0.001.

CHAPTER 5

SUMMARY, FUTURE DIRECTIONS, AND PERSPECTIVES

The Theiler's Murine Encephalitis Virus (TMEV) model is a recently developed CNS infection-induced animal model of temporal lobe epilepsy (TLE) crucial to our ability to investigate the cellular, molecular, and network level mechanisms implicated in seizure generation, propagation and transforming homeostatic neural circuits into epileptic circuits. The TMEV model also provides an important platform to test next-generation therapeutics aimed at symptomatic seizure control (antiseizure) as well as for disease modification (antiepileptogenic). Previous studies have discovered that innate immune responses, mainly driven by the cytokines TNFα, IL-6 and complement protein C3, cause inflammatory reactions in the brains of TMEV-infected mice concurrently with acute behavioral seizures (Kirkman et al., 2010). Inflammation is known to contribute to oxidative stress and mitochondrial dysfunction (Morris and Berk, 2015), whereas the latter can cause injury by inducing inflammation, contributing to neurodegeneration, and inducing hyperexcitability (Naik and Dixit, 2011). Both inflammation and oxidative stress could therefore be both a cause and/or a consequence of brain damage and seizure activity. Further, CNS infections and mitochondrial disorders are associated with increased incidence of seizures and epilepsy in patients (Vezzani et al., 2016; Waldbaum and Patel, 2010). Thus, a cross-talk can occur between inflammation, oxidative stress,

neuronal injury and seizures; however, the details of the relationship between these factors have not been studied during TMEV infection-induced seizures and epilepsy. Therefore, the present studies investigated the occurrence of oxidative stress and inflammation in the hippocampus, a brain region known to generate limbic seizures, during the TMEV-induced acute seizure period and how inflammation could modulate acute seizures.

Summary and implications of findings

Our data show a strong correlation between impairment of redox status, a robust increase in proinflammatory markers, and acute behavioral seizures following TMEV infection. Among the numbers of cytokines elevated in the hippocampus during acute seizures, we studied TNFα and its receptors in depth for their contribution to hyperexcitability and seizures. TNFR1-mediated signaling of TNFα predominantly drives hyperexcitatory synaptic changes and contributes to seizure occurrence, since $TNFR1^{-/-}$ and $TNFR1^{-/-}TNFR2^{-/-}$ mice are markedly resistant to developing TMEV-induced acute seizures. In contrast, TNFR2-mediated signaling of TNFα could be a part of an endogenous antiseizure mechanism, as the numbers and severity of seizures are worse in $TNFR2^{-/-}$ mice than in WT. Given the changes in other cytokines and oxidative stress markers, the mechanisms of seizure generation in this model are most likely multifactorial and interactions between additional underlying factors should be investigated further. Also, due to the observed increases in the levels of multiple proinflammatory cytokines, we also tested the efficacy of cannabidiol (CBD) which exhibits broad spectrum antiinflammatory and antiseizure activities (Burstein, 2015;

Rosenberg et al., 2015). CBD (180 mg/kg) effectively suppressed TMEV-induced acute seizures, however, the pharmacokinetic and pharmacodynamic properties of CBD in this model require further investigation.

The present research has strong translational implications by targeting TNFRs in the brain for the treatment of acute seizures during infections and possibly for the prevention of epilepsies caused by infection and CNS inflammation. The mechanism by which TNFα causes hippocampal hyperexcitability through TNFR1 is not just limited to the TMEV model of epilepsy. Indeed, a proictogenic role of TNFR1-mediated signaling and an antiictogenic role of TNFR2-mediated signaling have also been reported in the kainic acid-induced model of epilepsy (Balosso et al., 2005; Weinberg et al., 2013). TNFRs have been proven to be successful targets for treating many peripheral inflammatory diseases, and several biologics targeting the TNF system in the CNS are under development (Fischer et al., 2015; McCoy and Tansey, 2008) which might be helpful to treat inflammation-induced TLE. Inhibition of other inflammatory pathways mediated by IL-1 receptor and Toll-like receptors also provides antiseizure effects in various seizure models, and therefore, suggests that targeting inflammation could be an important strategy to treat pharmacoresistant epilepsies (Vezzani et al., 2011b). In line with previous findings, our results further substantiate the role of inflammation in causing seizures. The present research also demonstrates the utilization of an animal model of infection-induced epilepsy in testing novel compounds that have antiinflammatory as well as antiseizure activities. CBD-based drugs are currently under clinical trials for the treatment of Dravet syndrome, Lennox-Gastaut syndrome and other intractable forms of epilepsies (Friedman and Devinsky, 2015). Further CBD studies should build upon the

results presented here by evaluating safety and antiseizure mechanisms of CBD that will be beneficial in future clinical trial design.

Future directions

Future experiments will be directed toward site-specific and conditional deletion of TNFR1 in excitatory neurons and other cell types using a $TNFR1^{fl/fl}$ mouse to investigate a causal link between enhanced TNFR1 signaling and network hyperexcitability. $TNFR1^{fl/fl}$ mice were obtained from Dr. George Kollias' group (Van Hauwermeiren et al., 2013). The effects of TNFα on neural circuit functions depend on various factors, including the relative expression levels of TNFRs (TNFR1 and 2) in the tissue and the cell types expressing them. For example, astrocyte dysfunction occurs in many acquired epilepsies (Robel and Sontheimer, 2016; Steinhauser and Seifert, 2012) and TNFα signaling through activation of TNFR1 has been shown to decrease expression of the astrocyte glutamate transporter (GLT-1) (Carmen et al., 2009) and connexin-43 (Morioka et al., 2015). Pathogenic levels of TNFα also induce lasting synaptic alterations and cognitive impairment through astrocytic TNFR1-mediated signaling (Habbas et al., 2015). Thus, the role of TNFR1 signaling in astrocytes should be investigated and the use of the $TNFR1^{fl/fl}$ mouse will be instrumental for such studies. TMEV-infected mice have widespread astrogliosis in the hippocampus during the acute infection period (Loewen et al., 2016). In addition, TMEV-infected mice exhibit anxiety-like behavior and cognitive impairment (Umpierre et al., 2014). Whether signaling through the TNFR1 pathway in astrocytes contributes to such tripartite synaptic alterations should be explored. On the other hand, activation of TNFR2 may provide protection against seizures and neuronal

damage. Although the studies on TNFR2 agonists are limited, activation of signaling through TNFR2 has been shown to ameliorate oxidative stress-induced cell death in cultured dopaminergic neurons (Fischer et al., 2011). Thus, a combination of a TNFR1 antagonist and TNFR2 agonist might be an effective strategy for preventing TMEV-induced seizures. In addition, since the protein expression of TNFR2 decreases in the hippocampus during acute seizures following TMEV infection, the molecular mechanisms that regulate synthesis and cell surface expression of TNFR2 could be exploited to increase the level of TNFR2.

Considering the intracortical method of TMEV infection used and the observed infiltration of macrophages into the brain (Cusick et al., 2013), the blood-brain barrier (BBB) of TMEV-infected mice could be compromised. BBB injury is a contributing factor to the development of epilepsy (van Vliet et al., 2007). Extravasation of albumin from plasma into the brain occurs following BBB damage and albumin activation of TGFβ receptors on astrocytes can cause astrocyte dysfunction by impairing the functions of glutamate transporters, gap junction proteins, and inwardly-rectifying potassium channel currents, thus leading to hyperexcitation (Ivens et al., 2007). Interestingly, TGFβ expression in the hippocampus correlates with TMEV-associated seizure activity (Libbey et al., 2008). Future studies should evaluate BBB damage and TGFβ signaling in regulating astrocyte-neuronal functions following TMEV infection. In addition, numerous other cytokines such as IL-6, IFNγ, and IL-1β are also upregulated in the hippocampus during TMEV-induced acute seizures. Given the involvement of IL-6, IFNγ, and IL-1β in neuronal excitability in other models of epilepsy (Getts et al., 2007; Samland et al., 2003; Vezzani et al., 2011b), the contributions of these cytokines and

their interactions with TNFα following TMEV infection should be characterized. Such studies would better inform antiinflammatory therapy for the treatment of seizures.

Perspectives

A large body of clinical evidence suggests that inflammation could be one of the driving factors in precipitating seizures and mediating epileptogenesis (Vezzani et al., 2011a). For example: 1) autoimmune diseases such as lupus and celiac disease increase the risk for seizures (Devinsky et al., 2013), 2) febrile seizures, which can lead to epilepsy, are correlated with immunological changes and inflammation (Choy et al., 2014), 3) epileptic conditions with a strong inflammatory component, such as Rasmussen's encephalitis and paraneoplastic autoimmune encephalitis, are associated with seizures that are often resistant to antiseizure drugs (Davis and Dalmau, 2013), 4) CNS developmental conditions such as cortical dysplasia and tuberous sclerosis are also associated with brain inflammation and increased seizure susceptibility (Aronica and Crino, 2014), and 5) antiinflammatory therapies, for example, steroids, can prevent seizures in several intractable epilepsies (Vincent et al., 2010). Confirmative clinical studies linking specific inflammatory components with elevated seizure probability are required. Thus, animal models mimicking clinical aspects of inflammation-associated epilepsies, such as the TMEV model of limbic epilepsy, must be leveraged to identify molecular mechanisms that could be targeted for future pharmacotherapies.

Several caveats must be considered before applying antiinflammatory treatment for the treatment of seizures and for intervening in the process of epileptogenesis. First, the diagnosis of infectious and/or the inflammatory origin of seizures could be very

challenging, particularly under latent CNS infections. Chronic mild to moderate neuroinflammatory conditions may not reveal clinical symptoms for several years, as observed in neurodegenerative diseases (Frank-Cannon et al., 2009). Therefore, studies directed toward the development of biomarkers for CNS inflammation should be prioritized, as such biomarkers will be highly useful for a timely pharmacological intervention to prevent seizures and the development of subsequent epilepsy. Second, timing for the initiation of antiinflammatory therapies will require a detailed understanding of the purpose of inflammation under CNS pathologies associated with seizures. Inflammation can be a double-edged sword, as it is necessary for the resolution of the CNS insult and the clearance of infectious agents from the brain. It is not advisable to resort to the use of broad-spectrum antiinflammatory drugs for a prolonged period as that may also interfere with the beneficial functions of inflammatory mechanisms and may cause collateral CNS damage. The ideal strategy should be to reestablish homeostatic equilibrium between endogenous inflammatory and antiinflammatory mechanisms and future research should help to determine the factors crucial in maintaining the equilibrium between inflammatory processes. Finally, many antiseizure drugs can affect innate and adaptive immune functions (Marchi et al., 2014). Therefore, thorough animal studies must be conducted to evaluate interactions between antiseizure and antiinflammatory drugs before initiating a combination therapy in the clinic for the treatment of acute seizures and the prevention of epilepsy following infection. No doubt the TMEV model of TLE, which has greatly contributed to our understanding of infection-induced epilepsy, will be useful in the preclinical development of such novel therapies for those patients at risk for developing epilepsy following a CNS infection.

References

Aronica, E., Crino, P.B., 2014. Epilepsy related to developmental tumors and malformations of cortical development. Neurotherapeutics 11, 251-268.

Balosso, S., Ravizza, T., Perego, C., Peschon, J., Campbell, I.L., De Simoni, M.G., Vezzani, A., 2005. Tumor necrosis factor-alpha inhibits seizures in mice via p75 receptors. Ann. Neurol. 57, 804-812.

Burstein, S., 2015. Cannabidiol (CBD) and its analogs: a review of their effects on inflammation. Bioorg. Med. Chem. 23, 1377-1385.

Carmen, J., Rothstein, J.D., Kerr, D.A., 2009. Tumor necrosis factor-alpha modulates glutamate transport in the CNS and is a critical determinant of outcome from viral encephalomyelitis. Brain Res. 1263, 143-154.

Choy, M., Dube, C.M., Ehrengruber, M., Baram, T.Z., 2014. Inflammatory processes, febrile seizures, and subsequent epileptogenesis. Epilepsy Curr. 14, 15-22.

Cusick, M.F., Libbey, J.E., Patel, D.C., Doty, D.J., Fujinami, R.S., 2013. Infiltrating macrophages are key to the development of seizures following virus infection. J. Virol. 87, 1849-1860.

Davis, R., Dalmau, J., 2013. Autoimmunity, seizures, and status epilepticus. Epilepsia 54 Suppl 6, 46-49.

Devinsky, O., Schein, A., Najjar, S., 2013. Epilepsy associated with systemic autoimmune disorders. Epilepsy Curr. 13, 62-68.

Fischer, R., Kontermann, R., Maier, O., 2015. Targeting sTNF/TNFR1 signaling as a new therapeutic strategy. Antibodies 4, 48-70.

Fischer, R., Maier, O., Siegemund, M., Wajant, H., Scheurich, P., Pfizenmaier, K., 2011. A TNF receptor 2 selective agonist rescues human neurons from oxidative stress-induced cell death. PLoS One 6, e27621.

Frank-Cannon, T.C., Alto, L.T., McAlpine, F.E., Tansey, M.G., 2009. Does neuroinflammation fan the flame in neurodegenerative diseases? Mol. Neurodegener. 4, 47.

Friedman, D., Devinsky, O., 2015. Cannabinoids in the Treatment of Epilepsy. N. Engl. J. Med. 373, 1048-1058.

Getts, D.R., Matsumoto, I., Muller, M., Getts, M.T., Radford, J., Shrestha, B., Campbell, I.L., King, N.J., 2007. Role of IFN-gamma in an experimental murine model of West Nile virus-induced seizures. J. Neurochem. 103, 1019-1030.

Habbas, S., Santello, M., Becker, D., Stubbe, H., Zappia, G., Liaudet, N., Klaus, F.R., Kollias, G., Fontana, A., Pryce, C.R., Suter, T., Volterra, A., 2015. Neuroinflammatory TNFalpha Impairs Memory via Astrocyte Signaling. Cell 163, 1730-1741.

Ivens, S., Kaufer, D., Flores, L.P., Bechmann, I., Zumsteg, D., Tomkins, O., Seiffert, E., Heinemann, U., Friedman, A., 2007. TGF-beta receptor-mediated albumin uptake into astrocytes is involved in neocortical epileptogenesis. Brain 130, 535-547.

Kirkman, N.J., Libbey, J.E., Wilcox, K.S., White, H.S., Fujinami, R.S., 2010. Innate but not adaptive immune responses contribute to behavioral seizures following viral infection. Epilepsia 51, 454-464.

Libbey, J.E., Kirkman, N.J., Smith, M.C., Tanaka, T., Wilcox, K.S., White, H.S., Fujinami, R.S., 2008. Seizures following picornavirus infection. Epilepsia 49, 1066-1074.

Loewen, J.L., Barker-Haliski, M.L., Dahle, E.J., White, H.S., Wilcox, K.S., 2016. Neuronal injury, gliosis, and glial proliferation in two models of temporal lobe epilepsy. J. Neuropathol. Exp. Neurol. 75, 366-378.

Marchi, N., Granata, T., Janigro, D., 2014. Inflammatory pathways of seizure disorders. Trends Neurosci. 37, 55-65.

McCoy, M.K., Tansey, M.G., 2008. TNF signaling inhibition in the CNS: implications for normal brain function and neurodegenerative disease. J. Neuroinflammation 5, 45.

Morioka, N., Zhang, F.F., Nakamura, Y., Kitamura, T., Hisaoka-Nakashima, K., Nakata, Y., 2015. Tumor necrosis factor-mediated downregulation of spinal astrocytic connexin43 leads to increased glutamatergic neurotransmission and neuropathic pain in mice. Brain. Behav. Immun. 49, 293-310.

Morris, G., Berk, M., 2015. The many roads to mitochondrial dysfunction in neuroimmune and neuropsychiatric disorders. BMC Med. 13, 68.

Naik, E., Dixit, V.M., 2011. Mitochondrial reactive oxygen species drive proinflammatory cytokine production. J. Exp. Med. 208, 417-420.

Robel, S., Sontheimer, H., 2016. Glia as drivers of abnormal neuronal activity. Nat. Neurosci. 19, 28-33.

Rosenberg, E.C., Tsien, R.W., Whalley, B.J., Devinsky, O., 2015. Cannabinoids and Epilepsy. Neurotherapeutics 12, 747-768.

Samland, H., Huitron-Resendiz, S., Masliah, E., Criado, J., Henriksen, S.J., Campbell,

I.L., 2003. Profound increase in sensitivity to glutamatergic- but not cholinergic agonist-induced seizures in transgenic mice with astrocyte production of IL-6. J. Neurosci. Res. 73, 176-187.

Steinhauser, C., Seifert, G., 2012. Astrocyte dysfunction in epilepsy, in: Noebels, J.L., Avoli, M., Rogawski, M.A., Olsen, R.W., Delgado-Escueta, A.V. (Eds.), Jasper's Basic Mechanisms of the Epilepsies, 4th ed, Bethesda (MD).

Umpierre, A.D., Remigio, G.J., Dahle, E.J., Bradford, K., Alex, A.B., Smith, M.D., West, P.J., White, H.S., Wilcox, K.S., 2014. Impaired cognitive ability and anxiety-like behavior following acute seizures in the Theiler's virus model of temporal lobe epilepsy. Neurobiol. Dis. 64, 98-106.

Van Hauwermeiren, F., Armaka, M., Karagianni, N., Kranidioti, K., Vandenbroucke, R.E., Loges, S., Van Roy, M., Staelens, J., Puimege, L., Palagani, A., Berghe, W.V., Victoratos, P., Carmeliet, P., Libert, C., Kollias, G., 2013. Safe TNF-based antitumor therapy following p55TNFR reduction in intestinal epithelium. J. Clin. Invest. 123, 2590-2603.

van Vliet, E.A., da Costa Araujo, S., Redeker, S., van Schaik, R., Aronica, E., Gorter, J.A., 2007. Blood-brain barrier leakage may lead to progression of temporal lobe epilepsy. Brain 130, 521-534.

Vezzani, A., French, J., Bartfai, T., Baram, T.Z., 2011a. The role of inflammation in epilepsy. Nat. Rev. Neurol. 7, 31-40.

Vezzani, A., Fujinami, R.S., White, H.S., Preux, P.M., Blumcke, I., Sander, J.W., Loscher, W., 2016. Infections, inflammation and epilepsy. Acta Neuropathol. 131, 211-234.

Vezzani, A., Maroso, M., Balosso, S., Sanchez, M.A., Bartfai, T., 2011b. IL-1 receptor/Toll-like receptor signaling in infection, inflammation, stress and neurodegeneration couples hyperexcitability and seizures. Brain. Behav. Immun. 25, 1281-1289.

Vincent, A., Irani, S.R., Lang, B., 2010. The growing recognition of immunotherapy-responsive seizure disorders with autoantibodies to specific neuronal proteins. Curr. Opin. Neurol. 23, 144-150.

Waldbaum, S., Patel, M., 2010. Mitochondria, oxidative stress, and temporal lobe epilepsy. Epilepsy Res. 88, 23-45.

Weinberg, M.S., Blake, B.L., McCown, T.J., 2013. Opposing actions of hippocampus TNFalpha receptors on limbic seizure susceptibility. Exp. Neurol. 247, 429-437.